UC Berkeley

UC Berkeley Electronic Theses and Dissertations

Title

Functional Characterization of the DEAD-box ATPase Dhh1 - a regulator of cytoplasmic mRNA fate

Permalink

https://escholarship.org/uc/item/25q230wv

Author

Mugler, Christopher Frederick

Publication Date

2014

Peer reviewed|Thesis/dissertation

eScholarship.org Powered by the California Digital Library
University of California

Functional characterization of the DEAD-box ATPase Dhh1 – a regulator of cytoplasmic mRNA fate

By

Christopher Frederick Mugler

A dissertation submitted in partial satisfaction of the

requirements for the degree of

Doctor of Philosophy

in

Molecular and Cell Biology

in the

Graduate Division

of the

University of California, Berkeley

Committee in charge:

Professor Karsten Weis, Chair
Professor Kathleen Collins
Professor Britt Glaunsinger
Professor Steven E. Brenner

Fall 2014

Functional characterization of the DEAD-box ATPase Dhh1 – a regulator of cytoplasmic mRNA fate

© 2014 Christopher Frederick Mugler
All rights reserved

Abstract:

Functional characterization of the DEAD-box ATPase Dhh1 – a regulator of cytoplasmic mRNA fate

by

Christopher Frederick Mugler

Doctor of Philosophy in Molecular and Cell Biology
University of California, Berkeley
Professor Karsten Weis, Chair

Rapid modulation of gene expression is critical for cells to respond to environmental challenges and initiate developmental programs. Cells employ a large number of mechanisms to achieve tight regulation of gene expression, including post-transcriptional control of active messenger RNA (mRNA) levels by inhibition of translation or by mRNA degradation. While mRNA production via transcription has been extensively characterized, our understanding of how mRNAs are partitioned between an actively translating state and an inactive state is limited. In this thesis I examine the role of a highly evolutionarily conserved protein, the DEAD-box ATPase Dhh1, in mRNA inactivation and turnover in *S. cerevisiae*.

Previous work from our lab puts Dhh1 at the crossroads of mRNA fate. For example, artificially tethering Dhh1 to an mRNA is sufficient to trigger its degradation. In contrast, in cells compromised in the 5'-3' decay pathway, tethered Dhh1 can no longer direct degradation of the message, yet still possesses the ability to repress its translation. Moreover, ATPase activity of Dhh1 is critical for mRNA localization in the cell, as ATPase-deficient mutants of Dhh1 induce the constitutive formation of mRNA-protein (mRNP) foci known as Processing Bodies (PBs) – enigmatic cellular structures that can direct storage or degradation of mRNAs. However, mechanistically how Dhh1 functions in translation repression and mRNA decay, as well as its role in PB assembly has remained elusive.

In the following dissertation, I further characterize Dhh1 activities in translation repression, mRNA degradation, and PB formation. Using the previously established tethering assay, I identified protein factors that are distinctly required for translational repression or mRNA decay by Dhh1. Furthermore, I discovered that a mutant of Dhh1 that cannot bind to ATP is unable to interact with the Ccr4-NOT deadenylase complex – a major intracellular machine involved in transcriptional regulation and mRNA turnover. Finally, I show that Not1, the major scaffold of the Ccr4-NOT complex, controls Dhh1 localization to PB foci. In summary, my work suggests that the ATPase activity of Dhh1 is regulated *in vivo*, and this regulation may ultimately determine the fate of an mRNA – whether it is actively translated in the cytoplasm, or delivered to Processing Bodies for degradation or storage.

Dedication:

To my grandparents, Frederick R. Mugler and Barbara Mugler, and Edwin S. Smith and Lois Smith. My love for science and education comes from you.

Acknowledgements:

Without question, I must first acknowledge my advisor, Karsten Weis. Throughout my time in your lab you have always been incredibly supportive, both scientifically and on a personal level, and I cannot thank you enough for all you've done for me. Your scientific curiosity is infectious, and it's not a surprise our lab has been a great environment for budding scientists. There are not many other people I would be willing to follow across the world. I was also fortunate to secure three excellent scientists for my thesis committee – Steven Brenner, Kathy Collins, and Britt Glaunsinger – thank you all for your insight and input.

The Weis lab has had its share of talented scientists over the years, and I'm very thankful for all my labmates, past and present, who have helped me along the way – both from the Berkeley contingent (Adriana, Ben, Brett, Christiane, Evgeny, Elisa, Johanna, Leon, Leslie, Naoki, Ryan, Sarah, Steve, Ying, and Zain) and the ETH group (Carina, Carmen, Jeff, Maria, Ruchika, Roberta, Sarah, Sasi, Stephanie, and Yohei). I am especially grateful for our RNA decay team: Adriana, Johanna, Naoki, Brett, Leon, Ruchika, and Maria – you all taught me how to approach problems from a different perspective, and I can't overstate how valuable our meetings were to my development as a scientist. No doubt, research science is a challenging pursuit, but part of what has made my experience so wonderful is that I have been surrounded by creative and intelligent people who are genuinely invested in my success.

There are a number of people that I want to recognize, in particular, who have had a tremendous impact on my graduate school experience:

To Leon and Ryan – not only are you both absurdly good scientists, you are also absurdly good friends. I can't overstate how grateful I am to have you in my corner.

To Gloria and Elcin, and the Br-Un labs – for welcoming our Weis lab satellite into your space. I'm still not quite sure how we ended up in Barker, but man, I am thankful that we did.

To Kevin, Joe, and Ben – for afternoon beer lunches, causing some serious late night ruckus, and for giving me so many awesome Berkeley memories.

To my Parker bro, Thomas – unequivocally, my experience at Berkeley would not have been the same without you.

To Pat and Josh, who helped me keep my sanity throughout grad school – and being an outlet when I needed one.

To Danielle, your love and support has shaped me into who I am today, and I can't express how much that has meant to me. I will never take that for granted.

And to my parents, Rick and Alice, and my sister Sarah – for your incredible positivity and encouragement. There is no way I can pay you back, but the plan is to show that I understand.

Table of Contents

List of Figures:

List of Tables:

Chapter I: Introduction

Summary

Precise control of gene expression is critical for how cells rapidly adapt to internal and external challenges. The contribution of post-transcriptional regulation to gene expression is critical, as mRNA levels are determined not only by synthesis (transcription) but also by degradation. However, in contrast to transcriptional control, the regulation of mRNA turnover remains poorly understood. The work in this thesis seeks to characterize the regulation of mRNA turnover, with a particular emphasis on the function of Dhh1, a member of the highly conserved DEAD-box protein family of ATPase/RNA helicases, and a key regulator of cytoplasmic mRNA fate in *Saccharomyces cerevisiae*.

In yeast, cytoplasmic mRNA turnover occurs primarily in a deadenylation-dependent manner. First, the poly(A) tail of mature mRNA is removed by the Pan2/3 heterodimer or the Ccr4-NOT deadenylase complex. The deadenylated mRNA can then be degraded by the exosome, a multi-subunit 3'-5' exonuclease, or alternatively, and more commonly, the 5' methylguanosine cap is removed by the Dcp1-Dcp2 coenzyme complex and the message is degraded in a 5'-3' direction by the exonuclease Xrn1.

While the major enzymatic activities contributing to mRNA decay have been identified, their regulation and contribution to the control of gene expression are unclear. Furthermore, there are several additional factors that have been implicated in mRNA turnover whose functional roles are poorly understood. This includes the Lsm1-7 complex, a heptameric ring that can recognize oligoadenylated mRNAs *in vivo*, and Pat1, a factor that binds directly to the decapping enzyme. Dhh1, which is the focus of this dissertation, is a highly conserved protein factor and member of the DEAD-box family of ATPases that is thought not only to stimulate mRNA decay, but also to repress mRNA translation.

One other common feature of these mRNA turnover proteins is that yeast lacking any of these genes show an accumulation of capped, deadenylated mRNAs. Moreover, these factors form a highly plastic protein-protein interaction network along with the decapping enzyme and exonuclease Xrn1, and can assemble into a class of cytoplasmic mRNA-protein (mRNP) structures called Processing Bodies (PBs), which are postulated sites of mRNA decay and translational repression that form following stress.

In this introduction, I will largely focus on general aspects of post-transcriptional gene regulation, beginning with mechanisms of bulk mRNA turnover in the cytoplasm. During my thesis work I uncovered a previously unknown connection between Dhh1 and the Ccr4-NOT complex, thus, special attention is given to the role of the deadenylase complex in initiating mRNA decay. Second, the role of quality control and clearance of aberrant transcripts are discussed. Third, I examine the assembly and functional role of mRNA-protein complexes like Processing Bodies (PBs) and Stress Granules (SGs) in post-transcriptional gene regulation. Finally, an overview of the role of DEAD-box in RNA metabolism is presented, with a larger discussion on Dhh1 as a critical regulator of cytoplasmic mRNA fate.

Cytoplasmic bulk mRNA decay of mature mRNAs

As an mRNA is synthesized in the nucleus, a 7-methylguanosine cap is co-transcriptionally added to its 5' end and a poly(A) tail is added at its 3' end. Both of these modifications stabilize the mRNA and protect it from degradation both in the nucleus and the cytoplasm. Once properly capped and polyadenylated, a mature mRNA is exported into the cytoplasm, where it can undergo rounds of translation or can be targeted for storage or degradation. General turnover of properly matured cytoplasmic mRNA is completed by a conserved set of enzymes whose catalytic activities are well-established – namely deadenylation of the poly(A) tail by Pan2/3 and the Ccr4-NOT complex, removal of the 7-methylguanosine cap by the Dcp1-Dcp2 decapping complex, and exonucleolytic degradation by either the 5'-3' exonuclease Xrn1 or the 3'-5' exosome complex **(Fig 1.1)**. Although in some cases mRNAs contain *cis* elements that can recruit decapping and exonuclease factors in a deadenylation-independent manner, a majority of current data supports deadenylation-dependent turnover as the primary mechanism of cytoplasmic mRNA decay (Cao and Parker, 2001; Miller et al., 2011; Munchel et al., 2011). The half-life of the vast majority of mRNAs in the transcriptome can be fitted to a single-exponential decay curve, indicating a single rate-limiting step controls the turnover of most genes (Munchel et al., 2011), but whether deadenylation or other steps in decay limit the process remains unknown. An extensive discussion of deadenylation-dependent mechanisms that govern bulk mRNA turnover are described below, followed by a brief overview of established examples of deadenylation-independent decay.

Fig 1.1

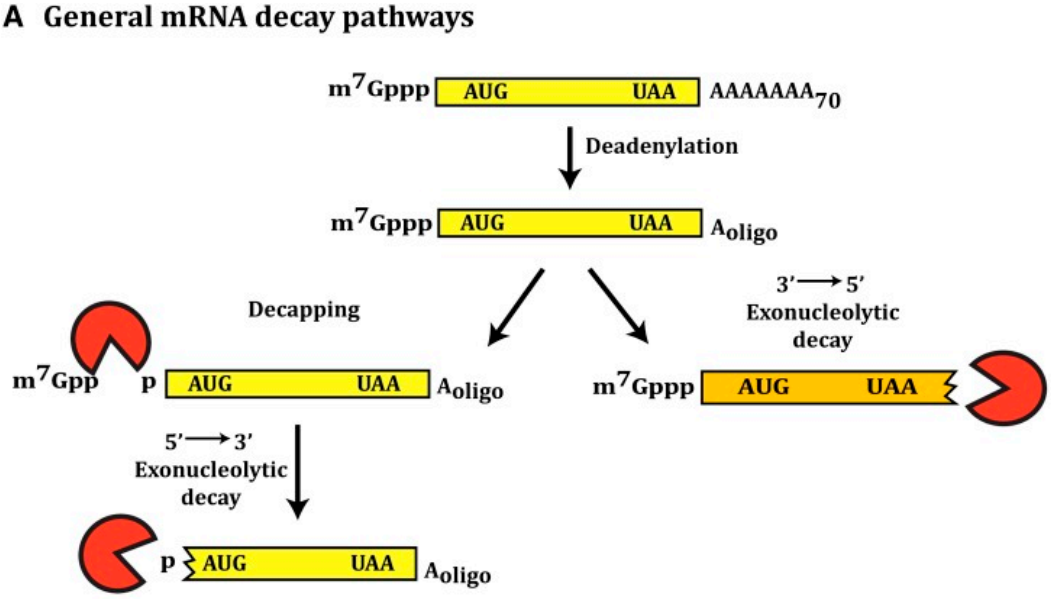

Figure 1.1: General schematic of bulk mRNA turnover mechanisms in yeast
Bulk mRNA turnover occurs by two main pathways in yeast, both of which are deadenylation-dependent. After removal of the poly(A) tail, an mRNA can be degraded from the 3' end by the exosome complex, or alternatively, the 7'methylguanosine cap at the 5' end can be removed by the Dcp1-Dcp2 decapping enzyme, followed by degradation from the 5' end by Xrn1. Reprinted with permission from (Parker, 2012).

Deadenylation-dependent mRNA turnover

Initial poly(A) trimming by the Pan2/3 exonucleases

In *Saccharomyces cerevisiae,* evidence suggests that yeast mRNAs possess poly(A) tails of roughly 50-100 nucleotides that are added to the message co-transcriptionally. The poly(A) tails of translationally competent mRNAs are bound by the poly(A)-binding protein – Pab1 –which facilitates recruitment of the 48S ribosome. In the transition of an mRNA from a translationally active state towards degradation, one of two distinct deadenylase complexes, either Pan2/3 or the Ccr4-NOT complex, can be recruited to the message to trigger deadenylation. Pan2/3 is a heterodimeric deadenylase complex that is stimulated by Pab1 (Siddiqui et al., 2007). Pan3 forms a homodimer through a coiled-coil region, which binds to a conserved C-terminal knob domain in Pan2, thus allowing the formation of an asymmetric heterodimer that is catalytically active (Christie et al., 2013; Jonas et al., 2014). Importantly, Pan2 has low affinity for mRNA in the absence of Pan3, suggesting both proteins are required for efficient deadenylation (Wolf et al., 2014). In humans, Pan2/3 is thought to initially trim poly(A) tails from their full length down to a shorter form, which is then removed by Ccr4-NOT. However, this does not appear to be the mechanism of deadenylation in budding yeast (Wolf and Passmore, 2014; Wolf et al., 2014). Recently, global analysis identified that the Pan2/3 complex has substrate mRNA preferences in yeast, and that these substrates do not overlap significantly with those of the Ccr4-NOT complex (Sun et al., 2013). Moreover, deletion of Ccr4-NOT complex subunits had strong mRNA degradation defects, while loss of *PAN2* or *PAN3* showed only a mild effects (Sun et al., 2013; Tucker et al., 2001), suggesting that in yeast, the Ccr4-NOT complex is more likely the major mRNA deadenylase.

Ccr4-NOT: the major deadenylase complex

The Ccr4-NOT complex (in *S. cerevisiae*) is a nine subunit complex that is held together by a major scaffolding protein, Not1 **(Fig 1.2)**. Not1 coordinates binding of the additional eight factors, which includes two deadenylases - Pop2 (Caf1) and Ccr4 – and six additional factors, Caf130 and Not1-Not5 (Collart and Panasenko, 2012; Wahle and Winkler, 2013).

Fig 1.2

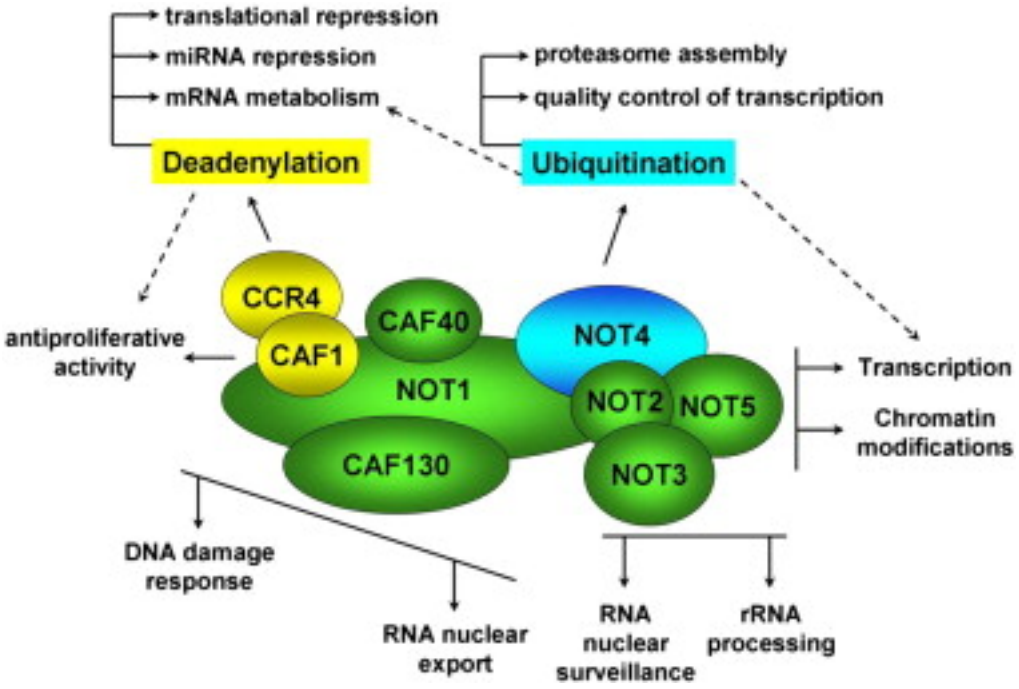

Figure 1.2: Schematic of the 1 MDa Ccr4-NOT complex
The Ccr4-NOT complex, which can be purified as a 1 MDa particle, consists of nine subunits that are color coded according to their functional role. Not1, a 240-kDa scaffold protein coordinates the binding of the eight remaining subunits. Reprinted with permission from (Collart and Panasenko, 2012).

A Ccr4 and Pop2-containing module can be biochemically isolated from Not2, 4, and 5 and the two modules show distinct activities, demonstrating the Ccr4-NOT complex may exist in more than one organization (Bai et al., 1999), with the Ccr4-Pop2 module being important for deadenylation. Recent work has elucidated the structural interactions between Not1, Ccr4, and Pop2. Not1 provides a scaffolding surface for Pop2 through a middle domain of initiation factor 4G-like (MIF4G) motif that is largely alpha helical (Basquin et al., 2012; Petit et al., 2012). Ccr4 is not directly bound to Not1, but instead is effectively tethered to Not1 through its interaction with Pop2 (Basquin et al., 2012). The structural regions of Not1 that facilitate this binding are highly conserved. For example, human CNOT1 and CAF1 (Pop2) interact using these conserved residues, demonstrating the functional importance of the interaction between Not1 and Pop2 (Petit et al., 2012). Interestingly, although Ccr4 and Pop2 both contain catalytic domains, there is disagreement about which of the two enzymes is the predominant catalytic subunit *in vivo*. Purification of Ccr4 from yeast lacking *POP2* did not show a defect in deadenylation rates when assayed *in vitro*, whereas disruption of Ccr4 catalytic activity by mutations in residues of the catalytic pocket showed a dramatic reduction of deadenylation *in vitro* (Tucker et al., 2002). Similarly, yeast lacking

POP2, which have a severe growth defect, can be complemented by expression of a catalytically inactive Pop2. In contrast, unlike *POP2*, loss of *CCR4* does not show a strong growth phenotype. This suggests either Pop2, the Pan2/3 complex, or an unidentified factor can still stimulate deadenylation in the absence of *CCR4*. Moreover, the residues that comprise the catalytic site of Pop2 are highly conserved across the eukaryotic kingdom (Bianchin et al., 2005), suggesting that catalytic activity of Pop2 may also be conserved.

Ccr4-NOT recruitment by miRNAs and translational repression of mRNA in higher eukaryotes

While the major enzymatic activities that govern bulk mRNA turnover in the cytoplasm are well established, the signals and mechanisms that serve to recruit degradation machinery to mRNAs are poorly understood. In addition to its role as the major cytoplasmic deadenylase, the Ccr4-NOT complex is also of interest because it has been shown to be recruited to mRNAs by other effector proteins. For example, Ccr4-NOT can be recruited to targets of the miRNA pathway through interaction with the miRNA-induced silencing complex (miRISC) (Fabian et al., 2011). In the miRNA pathway, a miRNA bound to complementary sequences in the 3'UTR of a target mRNA can recruit argonaute family proteins (AGOs) to the message that in turn can recruit GW182 proteins (also known as TNRC6A-C in mammals), forming a mature miRISC complex (Fabian et al., 2010a, 2010b). In mammals, TNRC6 binds to CNOT1 through a series of conserved phenylalanine (W)-containing motifs (Chekulaeva et al., 2011), and through additional coordination with a mammalian-specific Ccr4-NOT subunit, CNOT9 (Mathys et al., 2014). Recent structural work provided insight into the mechanism for integrating miRNA-mediated repression with both deadenylation and subsequently mRNA decay **(Fig 1.3)** (Chen et al., 2014).

Fig 1.3

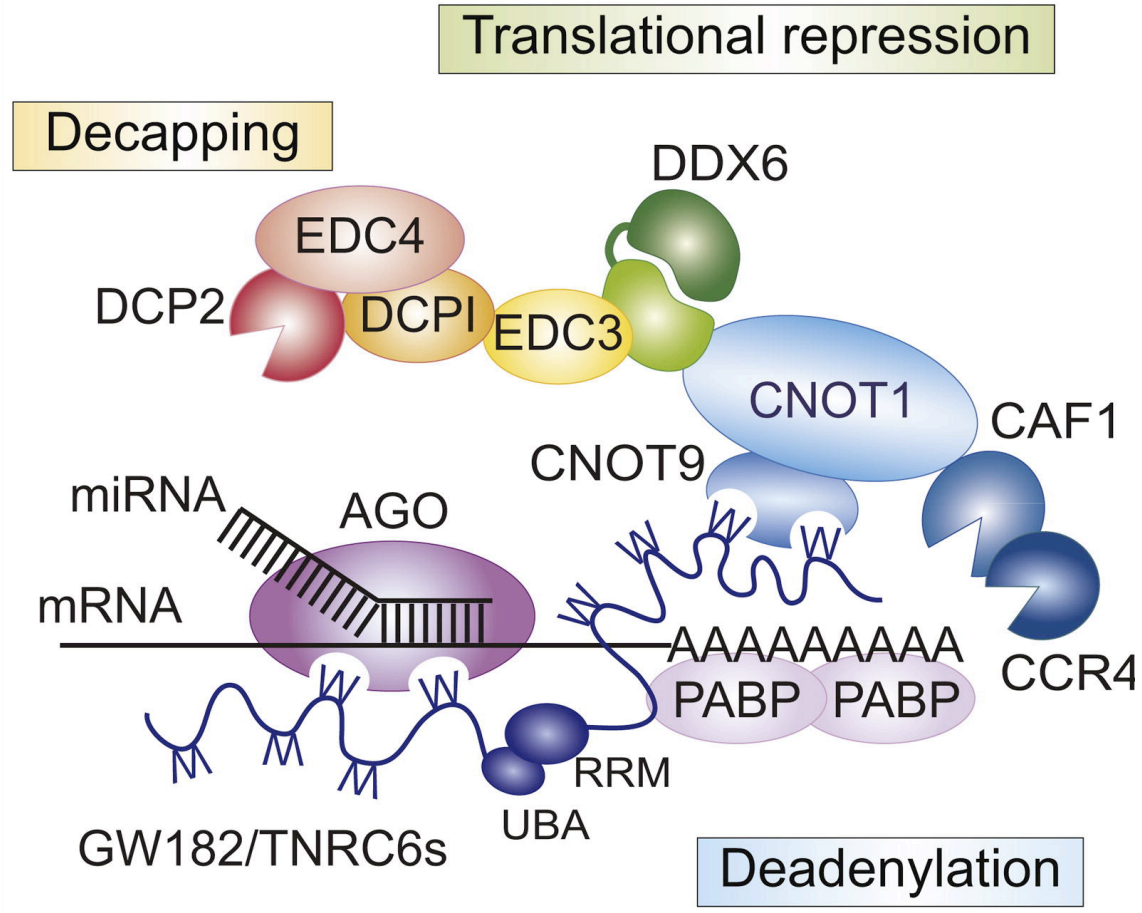

Figure 1.3: Integration of miRNA, translational repression, deadenylation and decapping machinery
Schematic representing protein-protein interactions between miRNA, translational repression, deadenylation, and decapping machinery. In mammalian cells, the miRISC complex recruits GW182-family proteins, which interface with the Ccr4-NOT complex through the mammalian CNOT9 protein. CNOT1 directly interacts with Caf1 (Pop2) and Ccr4 to stimulate deadenylation, as well as DDX6, which in turn binds to the decapping enzyme as well as decapping associated factors. Reprinted with permission from (Chen, Y., Boland, A., Kuzuoğlu-Öztürk, D., Bawankar, P., Loh, B., Chang, C.-T., Weichenrieder, O., and Izaurralde, E., 2014).

Ccr4-NOT recruitment by Puf-family proteins: RNA binding proteins as regulators of mRNA fate

In addition to the miRNA machinery, specific sequence elements in the 3'UTR of certain classes of mRNAs can also stimulate mRNA inactivation by recruiting the deadenylation machinery. This includes AU-rich elements (AREs), which are

recognized by specific RNA binding proteins, ultimately leading to mRNA destabilization and/or degradation (Gingerich et al., 2004). The Pumilio family of proteins is one such example of RNA binding proteins thought to destabilize mRNAs by recruitment of the Ccr4-NOT complex (Quenault et al., 2011). Puf family proteins contain variable numbers of 36 amino acid Puf repeats that are responsible for binding to unique sequence features in the 3'UTR of individual transcripts, particularly for transcripts that are highly regulated during development (Miller and Olivas, 2011). In yeast, Mpt5, a Puf family protein, recruits Ccr4-NOT to post-transcriptionally control mRNA levels for *HO* endonuclease – the DNA endonuclease responsible for orchestrating mating-type switching (Goldstrohm et al., 2006). However, instead of recruiting Ccr4-NOT through a direct interaction with Not1, Mpt5 appears to bind directly to Pop2 through a highly conserved interaction (Goldstrohm et al., 2006). Similar to Mpt5, the Smg5-Smg7 heterodimer, which, along with Smg6 is responsible for targeting substrates of nonsense-mediated decay (NMD) – an mRNA quality control pathway discussed below – can also directly interact with Pop2 to recruit the Ccr4-NOT complex (Loh et al., 2013). The shared mechanism of Mpt5 and Smg5-Smg7 binding directly to Pop2 may be another common mode of recruitment of the Ccr4-NOT complex that can trigger degradation of transcripts in a regulated fashion.

The cytoplasmic exosome and 3'-5' degradation

The exosome is a ten-subunit exonuclease protein complex that has distinct nuclear and cytoplasmic activities. In the nucleus, the exosome is responsible for proper RNA maturation: mediating the processing of small nuclear RNAs (snRNAs), small nucleolar RNAs (snoRNAs), and some non-coding RNAs (ncRNAs), and degrading transcripts that are improperly spliced, processed or assembled (Vanacova and Stefl, 2007). In the cytoplasm, the exosome appears to exclusively function as a processive exonuclease, degrading deadenylated mRNAs in a 3'-5' direction (Garneau et al., 2007). The scavenger decapping enzyme DcpS can then hydrolyze the cap structure at the 5' end of exosome-degraded mRNAs to prevent accumulation of toxic capped mRNA fragments (Milac et al., 2014).

The exosome structure consists of three parts, the first two of which are utilized by both nuclear and cytoplasmic complexes: 1) a hexameric ring, 2) a trimeric cap that participates in substrate recognition and RNA binding, and 3) an exonuclease subunit that is responsible for degrading the message. The exonuclease Rrp44 is present in both the nucleus and the cytoplasm, while Rrp6 degrades unstructured RNAs and localizes exclusively to the nucleus (Januszyk and Lima, 2011, 2014).The trimeric cap proteins facilitate the threading of RNAs through the central pore of the exosome, and orient the message for processive degradation by Rrp44 (Liu et al., 2006).

Recruitment of the exosome to cytoplasmic mRNA is typically accomplished by interaction with the superkiller (SKI) complex, a heterotetramer that consists of Ski2, Ski3, and Ski8 in a 1:1:2 stoichiometry (Synowsky and Heck, 2008). An additional SKI protein, Ski7 physically links the exosome and the SKI complex. The SKI complex is required for exosomal degradation as part of several cytoplasmic

surveillance pathways (Halbach et al., 2013). Interestingly, the docking of the SKI complex with the exosome is conceptually similar to the function of the 20S proteasome, where a substrate is threaded through a channel towards a degradative enzyme **(Fig. 1.4)** (Halbach et al., 2013).

Fig 1.4

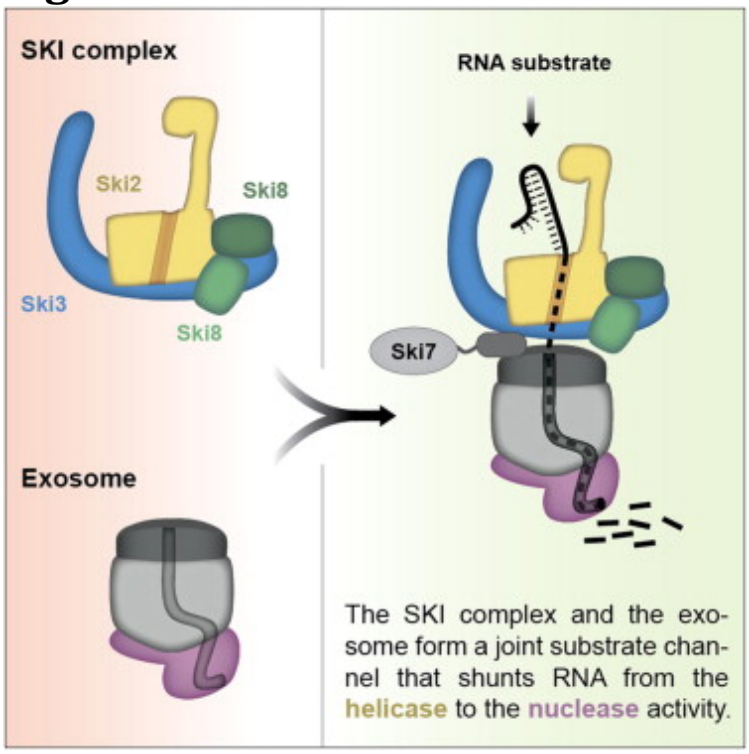

Figure 1.4: Docking of the SKI adaptor complex with the cytoplasmic exosome
The hetero-tetrameric SKI complex, upon binding to the Ski7 adaptor protein, can interface with the cytoplasmic exosome. RNAs are threaded through an additional channel in the Ski2 complex towards the processive exonuclease subunit Rrp44 at the base of the exosome. Reprinted with permission from (Halbach, F., Reichelt, P., Rode, M., and Conti, E., 2013).

Assembly of the decapping complex

Loss of a transcript's poly(A) tail through deadenylation by Pan2/3 and Ccr4-NOT decreases the mRNA's translational competency, which is presumed to increase the accessibility of an mRNA by the cytoplasmic turnover machinery (Parker and Sheth, 2007). However, degradation of the message from the 5' end first requires the removal of the 7-methylguanosine cap by the major cytoplasmic decapping enzyme Dcp2. Although Dcp2 is thought to be the major yeast cytoplasmic decapping enzyme, its activity is highly dependent on its cofactor Dcp1. For example, loss of *DCP1* causes such a dramatic loss of *in vivo* decapping activity that it was mistakenly identified as the decapping enzyme (LaGrandeur and Parker,

1998). Catalysis by Dcp2 is decreased roughly 1000-fold *in vitro* in the absence of Dcp1, which is consistent with the observation that efficient decapping activity by Dcp2 requires Dcp1 *in vivo* (Beelman et al., 1996; Borja et al., 2011). Structural data of the Dcp1-Dcp2 coenzyme in *Schizosaccharomyces pombe* demonstrates that the complex exists in both a closed and an open conformation (She et al., 2006, 2008). Although the exact nature of the cap removal remains elusive, NMR data suggests that the closed conformation is likely the catalytically active structure of Dcp2 (Arribas-Layton et al., 2013). Dcp1 and the N-terminal domain (NTD) of Dcp2 appear to stabilize the closed state to facilitate decapping, as mutations in these peptides not only prevent the formation of the closed conformation, but also block decapping activity (She et al., 2008).

Enhancers of decapping

Although the Dcp1-Dcp2 complex serves as that catalytic unit of decapping activity in yeast, and is conserved among eukaryotes, several additional proteins have been postulated to influence decapping activity. These factors were identified either as high copy suppressors of *dcp1Δ* and *dcp2Δ* mutants or because their loss leads to the accumulation of capped, but deadenylated transcripts (Arribas-Layton et al., 2013). However, the number of – and nature of – activators of decapping activity differs between various species. In *S. cerevisiae,* the most prominent activators of decapping are Edc3, Pat1, the Lsm1-7 complex, and Dhh1, although their exact role in promoting decapping is unclear. The evidence for these factors participating in decapping is discussed below.

Edc3, an important decay mRNA-protein oligomerization factor

While Edc3 was initially identified in an *in silico* screen as an "enhancer of decapping", loss of *EDC3* alone does not significantly affect decapping rate (Kshirsagar and Parker, 2004). However, Edc3 can directly bind to Dcp1, Dcp2, Dhh1, and Pat1, and is targeted to Processing Bodies (PBs) – large mRNA-protein (mRNP) granules that are postulated sites of mRNA decay and storage (Decker et al., 2007; Harigaya et al., 2010; Nissan et al., 2010; Tritschler et al., 2007, 2008, 2009). Increasing evidence suggests that the primary functional role of Edc3 is to facilitate formation of PBs and higher order oligomerization of mRNPs. Edc3 contains a Yjef-N domain that facilitates self-dimerization, and an Lsm domain that can interact with one of several helical leucine motifs (HLMs) in Dcp2 (Fromm et al., 2012; Harigaya et al., 2010) For example, in *Schizosaccharomyces pombe* purified Edc3, Dcp1, Dcp2, and the *S. pombe*-specific Pdc1 can reversibly form PB-like aggregates *in vitro* (Fromm et al., 2014). Furthermore, loss of Edc3, along with a poly-glutamine (poly(Q)) repeat sequence in the C-terminus of the Lsm1-7 complex protein Lsm4, causes nearly a complete loss of PB formation (Decker et al., 2007). Thus, Edc3 may enhance decapping by strengthening protein-protein interactions between other mRNA decay factors and by seeding formation of larger decay mRNPs.

The Lsm1-7 complex and *in vivo* detection of oligo(A) tails

The Lsm protein motif (so-called because of its similarity to the Sm protein fold) is commonly found among factors involved in mRNA turnover. Many of these proteins can oligomerize to form hexameric or heptameric ring complexes (Jonas and Izaurralde, 2013; Wu et al., 2014; Zhou et al., 2014). Lsm2-7 forms a hexameric complex that achieves nuclear or cytoplasmic localization by interaction with one of two additional factors; Lsm8 targets the ring to function in the nucleus to facilitate splicing, while Lsm1 binding recruits the complex into the cytoplasm (Chowdhury et al., 2007; Spiller et al., 2007). While structures of Lsm1-7 have been recently solved (Jonas and Izaurralde, 2013; Wu et al., 2014; Zhou et al., 2014) the exact function of the Lsm1-7 complex in mRNA turnover remains unclear. The Lsm1-7 heptameric ring complex has well characterized affinity for oligo(A) versus poly(A) mRNA *in vitro* and *in vivo* (Chowdhury et al., 2007), which is facilitated by the presence of a poly(U) tract in the 3'UTR that stimulates Lsm1-7 recruitment (Chowdhury and Tharun, 2008). These observations suggest that the Lsm1-7 complex may function at – or immediately after the deadenylation step. However, *lsm1Δ* yeast accumulates capped, but deadenylated mRNAs, similar to *dhh1Δ* and *pat1Δ*, consistent with a block in decapping (Bouveret et al., 2000). Moreover, some *lsm1* mutant alleles can still bind mRNA but yet can not stimulate robust decapping (Chowdhury and Tharun, 2009). More work is needed to further define how exactly the Lsm1-7 complex facilitates post-binding steps of decapping.

Pat1, a decay factor scaffold, a translational repressor, or both?

Pat1 was characterized as an important regulator of mRNA fate, with described functions in both decay and translation repression. Several mRNAs are stabilized by loss of *PAT1* (Bonnerot et al., 2000; Luo et al., 2011). Furthermore, Pat1 can repress translation by inhibiting the formation of the 48S preinitiation complex (Nissan et al., 2010). Similar to several other factors involved in mRNA decay, Pat1 is also a well known PB component, and binds directly to several of the factors involved in mRNA turnover, including Lsm1-7, Dcp1, Dcp2, Edc3, and Dhh1 (Nissan et al., 2010). Pat1 and Dhh1 also have additive affects on mRNA decay and translation repression, suggesting they function in independent, yet related pathways (Coller and Parker, 2005). However, because several other mRNA decay factors also bind directly to one another and can localize to PBs, how exactly Pat1 stimulates decay and represses translation remains unknown. Furthermore, whether or not these two functions are distinct or occur as part of the same path is also unclear.

Recently, Pat1 was identified as a target of protein kinase A (PKA), a major glucose sensor in yeast (Ramachandran et al., 2011). Upon PKA inactivation, or shift to glucose-free media, Pat1 is dephosphorylated. Interestingly, ectopic expression of a phosphomimetic Pat1 variant during glucose starvation prevented PB formation, suggesting that Pat1 dephosphorylation may be an important prerequisite for PB assembly (Ramachandran et al., 2011). Phosphomimetic Pat1 not only showed a decrease in PB formation, but also a decreased interaction with Dhh1, which is an extremely interesting observation with respect to the work presented in this thesis.

However, numerous attempts to recapitulate some of the observations from this study were unsuccessful. More work is needed to identify the role of Pat1 phosphorylation in promoting mRNA decay and translation repression.

5'-3' degradation by Xrn1

After removal of the 5'cap by the decapping coenzyme complex, the exonuclease Xrn1 degrades messages in a 5'-3' direction. Importantly, the specificity for messages with an exposed 5' monophosphate is explained by the crystal structure of mammalian XRN1, which showed that the 7-methylguanosine cap does not fit into the catalytic pocket (Jinek et al., 2011). Similarly, triphosphorylated mRNA species, as well as double-stranded RNA duplexes are also too large to fit in the basic pocket, helping make Xrn1 specific for monophosphorylated substrates (Jinek et al., 2011). In addition to its role in bulk turnover of cytoplasmic mRNA, Xrn1 can also facilitate degradation of NMD substrates, as well as a unique class of long non-coding RNAs (lncRNAs) called Xrn1-sensitive unstable transcripts (XUTs), a class of antisense regulatory RNA in yeast (van Dijk et al., 2011; Geisler et al., 2012).

Deadenylation-independent mRNA turnover

There are a few described instances of mRNA turnover in the absence of deadenylation by either the Pan2/3 or Ccr4-NOT complexes. In the yeast *EDC1* mRNA, a poly(U) tract in its 3'UTR loops over the poly(A) tail, thus preventing deadenylation (Muhlrad and Parker, 2005). While it is unknown how decapping activators are recruited to the *EDC1* mRNA, trapping of decay intermediates by inserting a poly-guanine (poly(G)) tract in the 3'UTR, which forms a strong secondary structure that can block exonucleolytic cleavage, leads to an accumulation of mRNA fragments that still have an intact poly(A) tail. Much like *EDC1,* the ribosomal protein mRNA *RPS28B* also forms an autoregulatory loop that is bound by the Rps28B protein. Rps28B binding in turn recruits Edc3, which triggers degradation of the *RPS28B* message (Badis et al., 2004; He et al., 2014). These unique cases of decapping-without-deadenylation raise the possibility that there are other unidentified *cis and trans* mechanisms of mRNA decay that feed into the canonical 5'-3' decay pathway.

Cytoplasmic degradation of aberrant transcripts: mechanisms that regulate mRNA fidelity in the cytoplasm

Although the nucleus employs quality control mechanisms to prevent the export of inappropriately processed mRNAs, there are also cytoplasmic surveillance mechanisms that can detect improperly matured mRNAs, ensuring that all cytoplasmic transcripts are competent for translation. Three major cytoplasmic

quality control pathways, which use translational fidelity to identify aberrant messages, are discussed below.

No-Go decay (NGD): destruction of mRNAs that cannot properly initiate translation

mRNAs with strong stalls in translation are effectively cleared by the cell, not only to free the ribosome to return to the cytoplasmic pool, but also to prevent inefficient or faulty translation. One such example of mRNA surveillance is the so-called no-go decay (NGD) pathway, which detects stalled ribosomes and initiates endonucleolytic cleavage (Garneau et al., 2007). The mechanism of NGD has not been well characterized, but one hypothesis is that during translation a strong secondary structure within the sequence of the mRNA may cause ribosome stalling during elongation. Subsequently, the A site of the ribosome is not efficiently occupied by a cognate amino-acyl tRNA. If the A site remains empty for a prolonged period, Dom34 and Hbs1 – evolutionarily conserved protein factors that structurally resemble translation termination factors eRF1 and eRF3 (Doma and Parker, 2006) – will bind to the empty A site to stimulate peptidyl-tRNA hydrolysis and endonucleolytic cleavage and degradation of the fragmented mRNA by Xrn1 and the exosome (Harigaya and Parker, 2010).

Non-stop decay (NSD): destruction of mRNAs lacking a proper stop codon

Messages that have lost a proper stop codon, due to a frameshift mutation for example, erroneously translate along the poly(A) tail (Shoemaker and Green, 2012), and are recognized by a surveillance process called non-stop decay (NSD). One proposed mechanism is that the exosome and the SKI complex could mediate both ribosome release and mRNA degradation. The C-terminus of Ski7, which is structurally similar to the GTPase domain of eRF3, could bind to the A-site of the ribosome and facilitates its release (Frischmeyer et al., 2002; Inada and Aiba, 2005). Loss of the ribosome from the mRNA presumably shifts the mRNA toward a decay fate, which is stimulated by Ski7 recruitment of the exosome to deadenylate and degrade the transcript.

Nonsense-mediated decay (NMD): destruction of mRNAs containing premature stop codons (PTCs)

Nonsense-mediated decay (NMD) – one of the most well-studied mRNA surveillance pathways – is a process by which mRNAs encoding a premature stop codon (PTC) are arrested during translation and subsequently destabilized and endonucleolytically cleaved. This surveillance pathway prevents translation of aberrant protein products that might significantly interfere with normal protein function. This includes improperly spliced mRNAs containing intronic sequences that have escaped nuclear degradation (Garneau et al., 2007). Moreover, NMD can also be used to as an alternatively way to regulate gene expression, as alternative

splicing produces mRNA isoforms that contain premature stop codons that are cleared by the NMD pathway in *Drosophila melanogaster* (Hansen et al., 2009).

The strategies that trigger NMD differ among various species. In higher eukaryotes, the exon junction protein complex (EJC), which serves as a mark of splicing, is deposited upstream of every exon junction and is displaced by the ribosome during translation (Le Hir et al., 2000). However, in PTC-containing mRNAs, the EJC remains associated with the mRNA downstream of the PTC, which is then detected by the surveillance machinery (Garneau et al., 2007). In contrast, the EJC is not required for NMD in *S. cerevisiae.* Instead, the presence of a PTC increases the distance between the terminating ribosome and the poly(A) tail, which appears to disrupt efficient ribosome release from the mRNA (Amrani et al., 2004; Leeds et al., 1991, 1992). The activation of NMD in all currently characterized pathways requires the ATPase activity of Upf1, a principle regulator of NMD that is discussed in more detail below.

Processing Bodies and the role of messenger ribonucleoprotein (mRNP) granules in silencing mRNAs

Diversity of mRNP complexes: Processing Bodies (PBs), Stress Granules (SGs), and other large mRNA-protein complexes

Not only are mRNAs influenced by the proteins to which they are bound, the localization of mRNA-protein complexes may also be an important determinant of mRNA fate. A variety of different mRNP structures have been identified in yeast and other cell types, many of which seem to play distinct, but related, roles in mRNA metabolism. Perhaps the most studied types of mRNP granules are Processing Bodies (PBs) and Stress Granules (SGs), which form in yeast following a variety of different stresses, such as carbon starvation, oxidative stress, and osmotic shock (Decker and Parker, 2012). These foci are postulated to function as sites of mRNA decay and storage because they contain many important factors involved in mRNA decay and translation initiation (Kedersha and Anderson, 2009). However, the functional importance of these foci is debated. For example, PBs are not formed under normal growth conditions in yeast, and deletion of *EDC3* and *PAT1*, which prevent the formation of PBs, does not appear to have a functional defect in the turnover of most genes (Buchan et al., 2008; Decker et al., 2007; Eulalio et al., 2007). Still, recent evidence has shown that *edc3Δ pat1Δ* yeast appear to be unable to recover from oxidative stress as well as enter into quiescence (Lavut and Raveh, 2012; Shah et al., 2013)). Moreover, ectopic expression of highly expressed mRNAs in cells that cannot form PBs showed a loss of viability, demonstrating that PBs indeed are important under certain conditions (Lavut and Raveh, 2012).

In addition to a role in the yeast stress response, PBs and SGs appear to be found in virtually all eukaryotic cell types (Anderson and Kedersha, 2009). Furthermore, a variety of other cell types form large mRNP granules, such as P Granules in *Caenorhabtidis elegans,* Germ Granules in germ-line cells, and Neuronal

Granules that are specific to neurons (Buchan, 2014). Many of these granules have been shown to localize with components of PBs and SGs (Buchan, 2014).

Functional definition (or lack thereof) and structural composition of Processing Bodies

Despite their discovery almost two decades ago, an accepted functional definition for PBs has yet to be established. Most often the presence of PB foci is defined by punctate localization of either Dcp2 or Edc3 by fluorescent light microscopy (Decker and Parker, 2012). The ambiguity surrounding a functional definition is in part because PB structures have been shown to function both as sites of translational repression and storage, and also as sites of mRNA decay. In yeast, visualization of a reporter mRNA using MS2-CP-YFP, which binds to mRNAs with MS2-stem loops engineered into the 3'UTR of the message, shows that mRNAs accumulate in *xrn1Δ* strains that are blocked for mRNA decay (Sheth and Parker, 2003). In contrast, *UFO1*, an mRNA that is rapidly transcribed – but not translated – following oxidative stress, accumulates in PBs until cells adapt and begin *UFO1* translation (Lavut and Raveh, 2012).

PBs are thought to be accumulations of all the major proteins involved in 5'-3' mRNA decay (Franks and Lykke-Andersen, 2008). For example, Dcp1/2, Xrn1, Dhh1, Pat1, Edc3, Ccr4, Scd6, and the Lsm1-7 heptameric ring complex all colocalize in PBs (Teixeira and Parker, 2007). Recently an atlas of PB and SG-localizing factors was established by observing the location of proteins from the yeast GFP-tagged library (Mitchell et al., 2013). However, factors were only defined as "PB localizing" or "SG localizing" according to their percentage of overlap with Edc3-mCherry (a PB marker) or Pub1-mCherry (a SG marker), rather than by a more stringent functional or structural definition. Again, this demonstrates the difficulty in defining what proteins truly define a PB structure.

Assembly and Disassembly of Processing Bodies

Several observations suggest that the formation of PB structures is dependent on the translational status of the mRNA and having a large pool of non-translating mRNA. For example, blocking translation initiation using a temperature-sensitive *prt1-63* allele, a component of the eIF3 complex, causes an increase in PB size (Teixeira et al., 2005). In contrast, treatment of cells with cycloheximide, which locks polysomes on translating mRNAs, causes a decrease in PB formation (Brengues et al., 2005; Teixeira et al., 2005). The prevailing hypothesis of PB assembly is that non-translating mRNAs are bound by factors that trigger inactivation and/or degradation of the message. After accumulation of factors on the transcript, these translationally repressed mRNPs can accumulate into larger structures through both protein-protein and protein-RNA interactions. PB assembly appears to rely on redundant mechanisms based on two main observations: First, deletion of a single gene does not appear to be sufficient to block PB assembly, and second, many of the factors involved in PB assembly can directly bind to one another (Nissan et al., 2010; Teixeira and Parker, 2007).

Many of the known PB components also have protein domains that are either common among, and in some cases unique to, factors involved in mRNA turnover. These motifs facilitate the formation of higher-order mRNP structures. For example, Dcp2 orthologs contain variable amounts of helical-leucine motifs (HLMs) that serve as binding sites for a C-terminal like-sm (LSm) domain of Edc3 in *S. pombe* (Fromm et al., 2012) **(Fig 1.5)**. Alternatively, Edc3 and Lsm4 are both capable of self-dimerization through distinct domains. Edc3 contains an N-terminal Yjef-N motif, while Lsm4 contains a C-terminal glutamine/asparagine (Q/N)-rich prion-like domain – both of which facilitate self-dimerization (Decker et al., 2007). Furthermore, several mRNA decay factors, such as Edc3, Scd6, Pat1, and Dhh1, also possess phenylalanine-aspartate-phenylalanine (FDF)-motifs that appear to be uniquely found in factors involved in mRNA turnover (Anantharaman and Aravind, 2004). Dhh1 possesses a known FDF-binding pocket in its C-terminus (Sharif et al., 2013; Tritschler et al., 2009). Because Dhh1 is in significant molecular excess compared with both mRNA and other decay factors (Ernoult-Lange et al., 2012; Gygi et al., 1999), the FDF-binding pocket may contribute to the formation of a continuum of PB structures. Different Dhh1-containing sub-complexes can form by Edc3, Pat1, and Scd6 and other associated factors that compete for binding to this hydrophobic pocket (Jonas and Izaurralde, 2013).

In addition to protein-protein interactions, there is evidence that PBs also require RNA to form. PBs that were partially purified by differential centrifugation were disrupted by treatment with RNase A (Teixeira et al., 2005). Moreover, *dcp1Δ* and *xrn1Δ* mutants, which trap mRNAs at the decapping and degradation steps respectively, show an increase in PB size and number in the absence of stress (Sheth and Parker, 2003). An ectopically expressed reporter mRNA containing a poly(G) tract, which blocks degradation by Xrn1, also accumulates in PBs (Decker and Parker, 1993; Parker and Sheth, 2007)

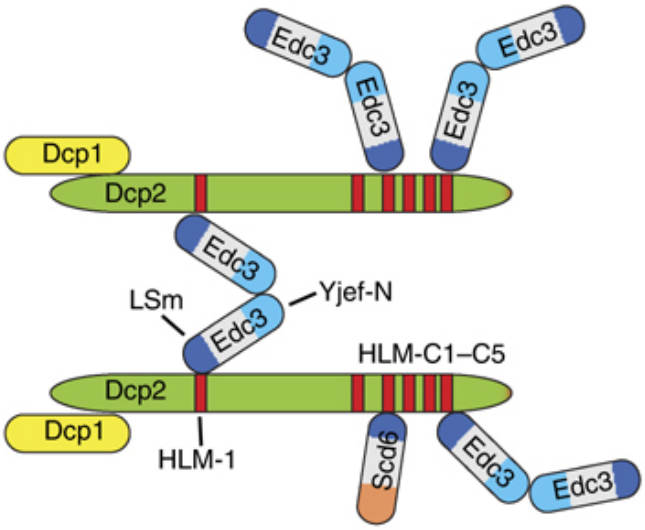

Figure 1.5: Multivalency of Processing Body Assembly
Many mRNA decay factors possess multivalent domains that can facilitate protein-protein interactions that may lead to assembly of PB foci. For example, several helical-leucine repeat motifs (HLMs) of Dcp2 can be bound by the C-terminal Like Sm (LSm) motif of Edc3. Edc3 also contains an N-terminal Yjef-N motif that promotes self-dimerization. Furthermore, several mRNA decay factors, such as Lsm4, possess poly(Q) domains that can contribute to aggregation. In combination, these mechanisms provide plasticity in the formation of larger PB assemblies. Reprinted with permission from (Fromm, S.A., Truffault, V., Kamenz, J., Braun, J.E., Hoffmann, N.A., Izaurralde, E., and Sprangers, R., 2012).

mRNP aggregates have also recently been shown to possess liquid droplet-like features, that imply PBs and the surrounding cytoplasm follow classical liquid-liquid phase separation (Brangwynne et al., 2009). Interestingly, purified mRNA decay factors from *Schizosaccharomyces pombe* can reversibly form a droplet that resembles a phase-transition *in vitro,* with only four protein factors required for assembly (Fromm et al., 2014). In addition, many mRNA binding proteins possess low complexity sequences (LCS) that can form hydrogels *in vitro,* much like purified FG-repeat nucleoporin proteins (Frey et al., 2006; Kato et al., 2012).

Although lipid-droplet like particles composed of PB proteins can form in a reversible manner *in vitro* (Fromm et al., 2014), it is unclear if large mRNP complexes possess this property *in vivo*. Current evidence demonstrates that certain classes of granules need chaperones to properly disassemble. In yeast, stress granules are cleared through an autophagy pathway, and are targeted for dissolution in the lysosome in a *CDC48*-dependent manner (Buchan et al., 2013). Similarly, loss of *ATG15* – a vacuolar lipase that is responsible for normal autophagic vesicle breakdown – causes an accumulation of PBs in the vacuole (Buchan et al., 2013). Still, this mechanism appears to more prevalently target SGs, as only a few PB marker proteins localized modestly to vacuoles in *atg15Δ* yeast.

Interestingly, the RNA-binding protein TDP-43 forms cytoplasmic inclusions aggregates when mutated, and is hallmark of ALS and other neurodegenerative diseases (Ramaswami et al., 2013). Because RNA-binding proteins that can become pathogenic, like TDP-43, can colocalize with stress granule components (Dormann et al., 2010), it is possible that proper formation and clearance of large mRNP aggregates in the cell may be necessary to prevent the creation of pathological inclusions that may contribute to disease **(Fig 1.6)**. In this case, autophagy may function as a "fail-safe" mechanism that clears mRNP aggregates that are either insensitive to normal disassembly mechanisms or are too large to be efficiently cleared (Ramaswami et al., 2013). Additional studies will be needed to elucidate whether aberrant mRNP disassembly is a driver of neurodegenerative disease.

Fig 1.6

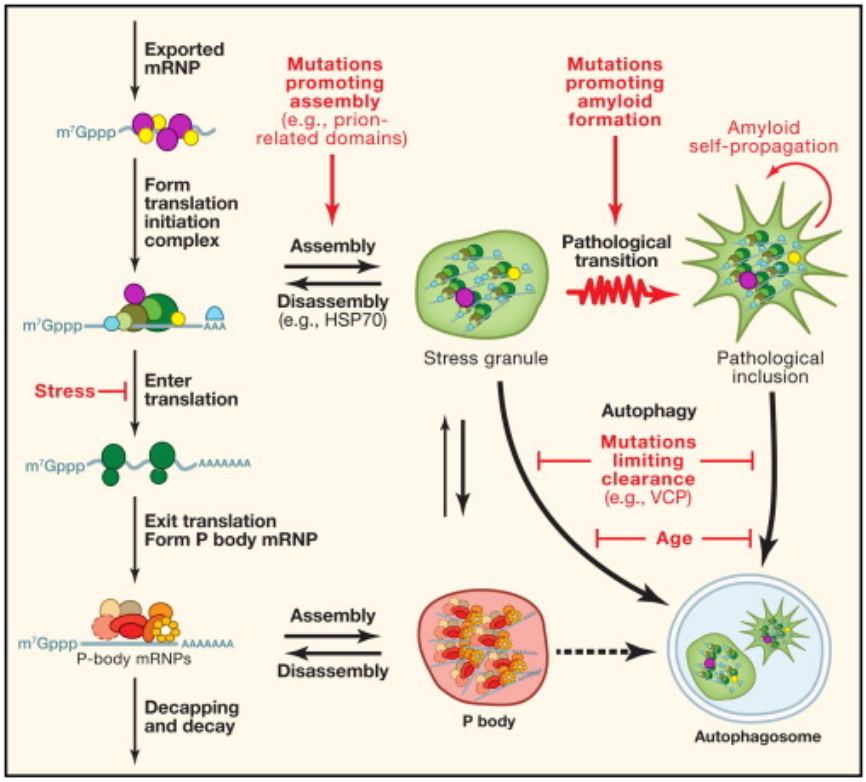

Fig 1.6: Model of pathological mRNP aggregation
mRNP granules are normally formed when nontranslating mRNAs are sequestered with translation initiation factors in stress granules (SGs) or with mRNA degradation machinery in processing bodies (PBs). The recent observation that SGs are targeted for degradation by autophagy, and that several factors involved in mRNA turnover possess prion-like domains, suggests that normal disassembly and clearance of large mRNPs like SGs and PBs may prevent pathological aggregation in higher eukaryotes. Reprinted with permission from (Ramaswami et al., 2013).

DEAD-box proteins as regulators of RNA metabolism

Classification and structural composition

DEAD-box enzymes are members of the SF2 super family of helicases traditionally named after the presence of the canonical Asp-Glu-Ala-Asp (DEAD) motif. They are critical regulators of a virtually every aspect of mRNA metabolism, including but not limited to: splicing, export, translation and degradation (Russell et al., 2013) **(Fig 1.7)**. Further highlighting their significant role in cellular function,

there are 37 known DEAD-box proteins in humans and 25 in budding yeast (Iost et al., 2013; Linder and Jankowsky, 2011), and they are found in all three kingdoms of life (Fairman-Williams et al., 2010).

Fig 1.7

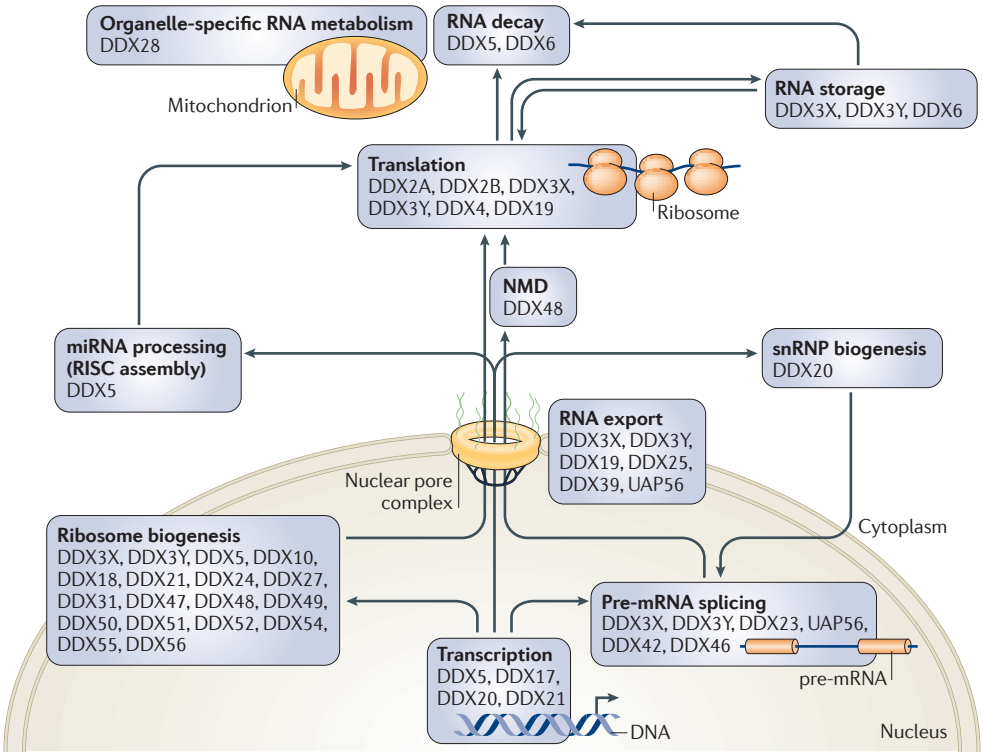

Figure 1.7: DEAD-box proteins control virtually all steps of RNA metabolism, DEAD-box proteins have been identified as participating in a vast array of RNA processing functions, from ribosome biogenesis to mRNA decay. Above are the known human DEAD-box proteins and the process they participate in. Reprinted with permission from (Linder and Jankowsky, 2011).

The core of DEAD-box proteins is comprised of two RecA-like domains connected by a short flexible linker sequence **(Fig 1.8)**. There are 10-12 canonical protein motifs, most notably the Walker A - also known as the Q-motif - and Walker B motifs, which facilitate binding to the adenine base of ATP, and the DEAD motif which is essential for ATP hydrolysis (Cordin et al., 2006). ATP binding is shared by motifs present on both N and C-terminal RecA domains. The general hypothesis of DEAD-box activation is that upon ATP-binding by the two RecA domains, a basic groove is formed, allowing for sequence-independent binding to the phosphate backbone of RNA or DNA species.

Fig 1.8

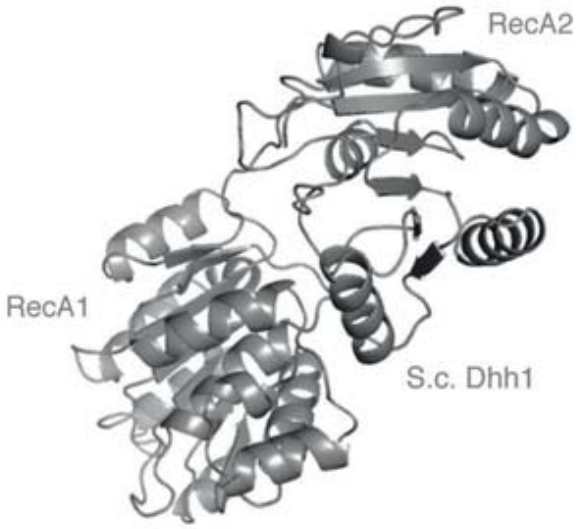

Fig 1.8: Crystal structure of *S. cerevisiae* Dhh1$^{30\text{-}425}$
The crystal structure of Dhh1 depicts the conserved structure of DEAD-box proteins, which contain a well-conserved core domain composed of two globular RecA-like domains (RecA1 and RecA2) connected by a short flexible linker. This structure lacks the N and C-terminal extensions, which are unstructured regions of varying length among DEAD box proteins that confer additional functionality or specificity. Reprinted with permission from (Mathys et al., 2014).

Many DEAD-box proteins possess long, flexible regions at their N and C-termini, and the length of these regions often differs among orthologs. Because of the difficulty in crystallizing DEAD-box proteins with these unstructured extensions, the functional roles of these regions are in many cases unknown. However, there are a few instances where these extension regions have been crystalized separately from the DEAD-box core. For example, the C-terminus of the ribosome biogenesis factor YxiN – an ortholog of *E. coli* DbpA – was shown to possess an RNA recognition motif (RRM) that gives YxiN processive helicase activity (Hardin et al., 2010). Alternatively, the C-terminal extension of Dhh1 crosslinks to RNA, suggesting that DEAD-box unstructured tails may also participate in RNA binding and ATPase function (Sharif et al., 2013). Thus, while the core region of the DEAD-box protein is responsible for canonical protein family activities, the adaptor extension regions may enhance DEAD-box activity or serve as platforms for additional protein factor binding.

Postulated mechanisms of DEAD box protein function

In general, DEAD-box proteins bind RNA with high affinity in an ATP-dependent manner. However, despite their initial classification as “RNA helicases”,

recent evidence demonstrates that many known DEAD-box proteins do not possess helicase activity *in vitro* – at least not in the absence of additional co-factors (Ballut et al., 2005; Fairman et al., 2004; Parvatiyar et al., 2012; Putnam and Jankowsky, 2013). As a result, several other mechanisms of DEAD-box protein function have surfaced, suggesting that these proteins can use their conserved catalytic ATP and RNA-binding core to co-opt a variety of other functions. For example, these proteins may function as so-called "RNPases" by using ATP binding and hydrolysis to facilitate binding or dissociation of factors bound to the RNA, therefore remodeling the mRNP complex. Alternatively, ATPase activity may be inhibited by additional factors, thus turning the protein into a RNA binding clamp. Therefore, a more general description of this protein family is that they utilize ATP hydrolysis to perform work on an RNA substrate. Some examples of the hypothesized mechanisms of DEAD-box protein function are described below.

eIF4A, the helicase: melting RNA duplexes in 5'UTRs

Eukaryotic initiation factor 4A, or eIF4A, was one of the first DEAD-box protein characterized (Ray et al., 1985). eIF4A was shown to have ATP-dependent RNA helicase activity *in vitro*, thus leading to the description of DEAD box proteins as RNA helicases (Ray et al., 1985; Rogers et al., 1999). Unlike other DEAD-box proteins, eIF4A contains only small extensions outside of its conserved core, suggesting that it is a minimal helicase that is co-opted by additional protein factors, such as eIF4G and eIF4E – other members of the eIF4F ternary translation initiation complex (Andreou and Klostermeier, 2013). Consistent with this hypothesis, eIF4A alone is a weak RNA helicase, but its activity is enhanced by eIF4B, eIF4H,eIF4E, and eIF4G (Andreou and Klostermeier, 2014; Rogers et al., 2001; Schütz et al., 2008). The eIF4A complex is required for translation of mRNAs with stable secondary structures in their 5' untranslated regions (UTRs) (Svitkin et al., 2001). Still, there are likely to be other contexts outside of unwinding where eIF4A functions, such as the displacement of proteins bound to the 5'UTR of mRNAs.

Dbp5 and Gle1: MIF4G-like proteins as activators of DEAD-box activity

Dbp5 is a DEAD-box ATPase that plays a critical role in directing the export of mRNA from the nucleus to the cytoplasm. Recently, work from our lab demonstrated that Gle1, a largely alpha helical protein of the nuclear pore complex that specifically localizes to the cytoplasmic surface of the NPC, activates the Dbp5 ATPase cycle, triggering RNA release from Dbp5 (Montpetit et al., 2011). Interestingly, there is a high degree of structural similarity between Dbp5-Gle1 and eIF4A-eIF4G (Linder and Jankowsky, 2011; Montpetit et al., 2011). The interactions between these protein pairs rely on a stable contact between the activator and the C-terminal RecA domain of the ATPase, and a more transient interaction between the activator and the N-terminal RecA domain. Unlike other known DEAD-box activator pairs, the interaction between Dbp5 and Gle1 is strengthened by the presence of the small soluble molecule inositolhexakisphopshate (IP6) (Miller et al., 2004; Montpetit et al., 2011; Weirich et al., 2006).

eIF4AIII, the scaffold: coordinating protein factors at the Exon Junction Complex

In addition to postulated functions as non-processive helicases and RNPases, DEAD-box proteins may also function as scaffolds that facilitate the formation of mRNPs. For example, eIF4AIII is involved in the formation of the exon-junction complex – a stable protein complex that is deposited around 25 nucleotides upstream of the exon-exon junction on spliced mRNAs (Le Hir and Andersen, 2008). EJCs serve as critical beacons for other RNA binding factors involved in mRNA export, localization, translation, and nonsense mediated decay. The stability of this protein complex is accomplished by inhibition of the ATPase activity of the DEAD-box eIF4AIII by MAGOH and Y14 (Ballut et al., 2005). Interestingly, an additional protein factor, CWC22, which also possesses a MIF4G domain, was shown to regulate eIF4AIII activity in human cells by inhibiting ATP and RNA binding (Buchwald et al., 2013). Moreover, CWC22 is required for recruitment of eIF4AIII to RNA (Buchwald et al., 2013), suggesting that its function is to prevent eIF4AIII ATP hydrolysis in order to allow the EJC to assemble. The interaction between CWC22 and eIF4AIII illustrates how DEAD-box ATPase activity can be inhibited by additional protein factors.

Functional similarity between SF1 and SF2 family helicases

Upf1, a member of the SF1 family of ATPase/RNA helicases that is required for nonsense-mediated decay (NMD), contains two RecA-like domains connected by a flexible linker region and is structurally similar to members of the SF2 family – including Dhh1, a DEAD-box ATPase that is the focus of this work. Interestingly, Upf1 interacts with Upf2, a protein that contains multiple MIF4G (middle portion of eIF4G-like) domains, much like Gle1, eIF4G, and Not1 – proteins shown to interact with and potentially activate the ATPase cycle of Dbp5, eIF4A, and Dhh1 respectively (He and Jacobson, 1995; Mathys et al., 2014; Mendell et al., 2000; Montpetit et al., 2011; Schütz et al., 2008). In addition, Upf2 and Upf3 are required for ATPase activation of Upf1 *in vitro* (Franks et al., 2010). When unbound by Upf2, Upf1 exists in a closed conformation, with its cysteine-histidine rich motif (CH) acting as an autoinhibitory mechanism that increases RNA binding activity, but disrupts efficient ATPase and RNA helicase activity (Chakrabarti et al., 2011) that is critical for interaction with Upf2. Similarly, Dhh1 adopts an unusually closed conformation compared with other DEAD-box proteins, due to the presence of interdomain contacts between its N and C-terminal RecA domains, giving it a significantly lower ATPase activity compared to other DEAD-box family proteins (Dutta et al., 2011; Montpetit et al., 2011). Although the mechanisms employed by Upf1 and Dhh1 are not identical, their similarities suggest that there are both *cis* and *trans* regulators of the ATPase cycle of SF1 and SF2 family helicases that are critical for proper regulation of mRNA metabolism. In addition, the presence of MIF4G-like protein folds in known activators of SF1 and SF2 proteins suggests that this may be a common mechanism for stimulating the ATPase cycle of these helicase families.

Dhh1 – a DEAD-box ATPase as a regulator of cytoplasmic mRNA fate

Dhh1 is a critical regulator of mRNA fate, and has been described as both a translational repressor and a stimulator of decapping. Although *DHH1* is not essential in budding yeast, *dhh1Δ* cells have a significant growth defect. Dhh1 is a highly conserved protein, with 68% identity and 82% similarity to its human homolog, p54/RCK/DDX6 (Bergkessel and Reese, 2004; Westmoreland et al., 2003). The conservation of function is demonstrated by heterologous expression of *H. sapiens* DDX6 in *dhh1Δ* cells, which can rescue growth defects and temperature sensitivity (Bergkessel and Reese, 2004). Furthermore, *dhh1Δ* cells are hypersensitive to DNA damage and are unable to reenter the cell cycle following activation of the G1/S DNA damage checkpoint. Similarly, Me31B and CGH-1, the *D. melanogaster* and *C. elegans* orthologs of Dhh1 are required for proper execution of meiosis (Navarro and Blackwell, 2005; Navarro et al., 2001). Yeast lacking *DHH1* also show defects in budding, mating, and sporulation (Moriya and Isono, 1999; unpublished data). Thus, while *DHH1* is not an essential gene, its functionality is important for several major developmental programs in yeast (Weston and Sommerville, 2006). Below, I describe the three well-known functions of Dhh1 and provide evidence for each function: 1) as a stimulator of mRNA decay, 2) as a translational repressor, and 3) as a critical processing body (PB) component.

Evidence for a role in mRNA decay

Dhh1 was initially identified as a multicopy suppressor of the Ccr4-NOT deadenylase enzyme Pop2 (Hata et al., 1998). In addition, Dhh1 co-precipitates with members of both the deadenylation and decapping machinery (Coller et al., 2001), suggesting it plays an important role in mRNA decay. Deletion of *DHH1* causes an increase in mRNA half-life for several known transcripts, as well as the accumulation of deadenylated, capped mRNAs (Chang and Lee, 2012; Dutta et al., 2011; Fischer and Weis, 2002; Haimovich et al., 2013; Talarek et al., 2010). Dhh1 is a highly abundant protein, and binds mRNA in a sequence-independent manner through interactions with the phosphate backbone, and thus, is postulated to function globally in mRNA turnover (Cheng et al., 2005; Ernoult-Lange et al., 2012). More recently, we have shown that tethering Dhh1 to an mRNA using the high affinity interaction between the bacteriophage coat protein PP7 and its RNA recognition stem loop is sufficient to trigger mRNA of the bound mRNA (Carroll et al., 2011).

Evidence for a role in translational repression

In addition to playing a role in mRNA turnover, recent work by our lab and others has shown that Dhh1 also has a role in repressing mRNA translation.

Overexpression of Dhh1 leads to a bulk loss of polysomes, as well as a decrease in protein synthesis (Coller and Parker, 2005). Furthermore, Dhh1 association to mRNA causes an accumulation of heavy sedimenting mRNPs by sucrose gradient fractionation. These higher sedimenting fractions contain ribosomal subunits, suggesting that Dhh1 association on mRNA leads to ribosome slowing (Sweet et al., 2012). Several orthologs of Dhh1 also have been shown to function in translation repression. For example, the *D. melanogaster* ortholog of Dhh1, Me31B, is also a well known translational repressor of *oskar* and *bicoid* mRNA in nurse cells during *Drosophila* oocyte development (Nakamura et al., 2001).

Our recent tethering experiments also demonstrate a role for Dhh1 in translation repression. Tethering Dhh1 to an mRNA reporter in the absence of functional decapping activity (i.e. *dcp1Δ*) leads to a stabilization of the bound mRNA reporter (Carroll et al., 2011; Sweet et al., 2012). Interestingly, although Dhh1 cannot stimulate degradation of the bound mRNA in the absence of decapping activity, it nonetheless represses its protein translation (Carroll et al., 2011). This result provides a particularly appealing framework for addressing a functional role for Dhh1 in translation repression because it allows us to uncouple translation repression and decay *in vivo*.

Evidence as a major Processing Body factor

Dhh1 is a well-established component of PBs and is present in *S. cerevisiae* in large complexes, as evidenced by microscopy and by fractionation (Carroll et al., 2011; Cougot et al., 2004; Dutta et al., 2011; Teixeira and Parker, 2007; Tseng-Rogenski et al., 2003). Not only does Dhh1 colocalize with and bind to several factors involved in mRNA turnover (Nissan et al., 2010; Tritschler et al., 2009), loss of *DHH1* causes a dramatic loss in both the number and size of PB foci (Buchan et al., 2008; Coller and Parker, 2005; Teixeira and Parker, 2007; unpublished data). In addition, Dhh1 nucleotide and RNA-binding activities are required for localization of Dhh1 to PBs, as loss of either function disrupts PB formation (Dutta et al., 2011, data presented below).

Outstanding questions regarding Dhh1 function in mRNA turnover

Where does Dhh1 function in the 5'-3' mRNA turnover pathway?

Although a role for Dhh1 as a stimulator of mRNA turnover is well established, there are many questions surrounding both its mechanism and timing of action. Deletion of *DHH1* causes an accumulation of deadenylated, capped mRNAs (Coller et al., 2001; Fischer and Weis, 2002) leading to the hypothesis that Dhh1 functions at a step between decapping and deadenylation. However, Dhh1 has also been shown to block translation by distinct mechanisms, thus complicating identification of a precise point in the mRNA turnover pathway for Dhh1 function.

What role do RNA binding and ATPase activity have in Dhh1 function?

Recent work from our lab has demonstrated that Dhh1 ATPase activity controls its localization to PBs. An ATPase-deficient allele, Dhh1^{DQAD} mislocalizes to PBs constitutively and cannot recycle efficiently from these foci (Carroll et al., 2011). Despite its classification as a member of the DEAD-box ATPase protein family, Dhh1 has very low intrinsic ATPase activity *in vitro* (Dutta et al., 2011; Tritschler et al., 2009) compared to other DEAD-box proteins. Furthermore, Dhh1 also adopts different conformations when ATP-bound and nucleotide free (Cheng et al., 2005; Sharif et al., 2013). The *apo* conformation of Dhh1 has roughly 1000 fold lower RNA binding affinity than ATP-bound Dhh1, suggesting that a shift from an *apo* to ATP-bound conformation may be a point of regulation for Dhh1 function (Cheng et al., 2005; Dutta et al., 2011; Sharif et al., 2013).

Is Dhh1 ATPase activity regulated *in vivo*?

Recently, CNOT1, the human ortholog of Not1 and the main scaffold of the Ccr4-NOT complex, was shown to bind directly to DDX6 – the human ortholog of Dhh1 – *in vitro* (Chen et al., 2014; Mathys et al., 2014; Rouya et al., 2014). The three patches of CNOT1 that interact with DDX6 are outlined in **Fig 1.9**. Interactions between these proteins appear to be highly conserved in yeast (Rouya et al., 2014; data not shown). Interestingly, the MIF4G-like motif is found in other DEAD-box (and SF1 family) helicase activators like eIF4G, Gle1, and Upf1. In addition, Not1 can stimulate Dhh1 ATPase activity *in vitro* (Chen et al., 2014; Mathys et al., 2014; Rouya et al., 2014). However, the functional relevance of the Dhh1-Not1 interaction *in vivo* is unclear.

Fig 1.9

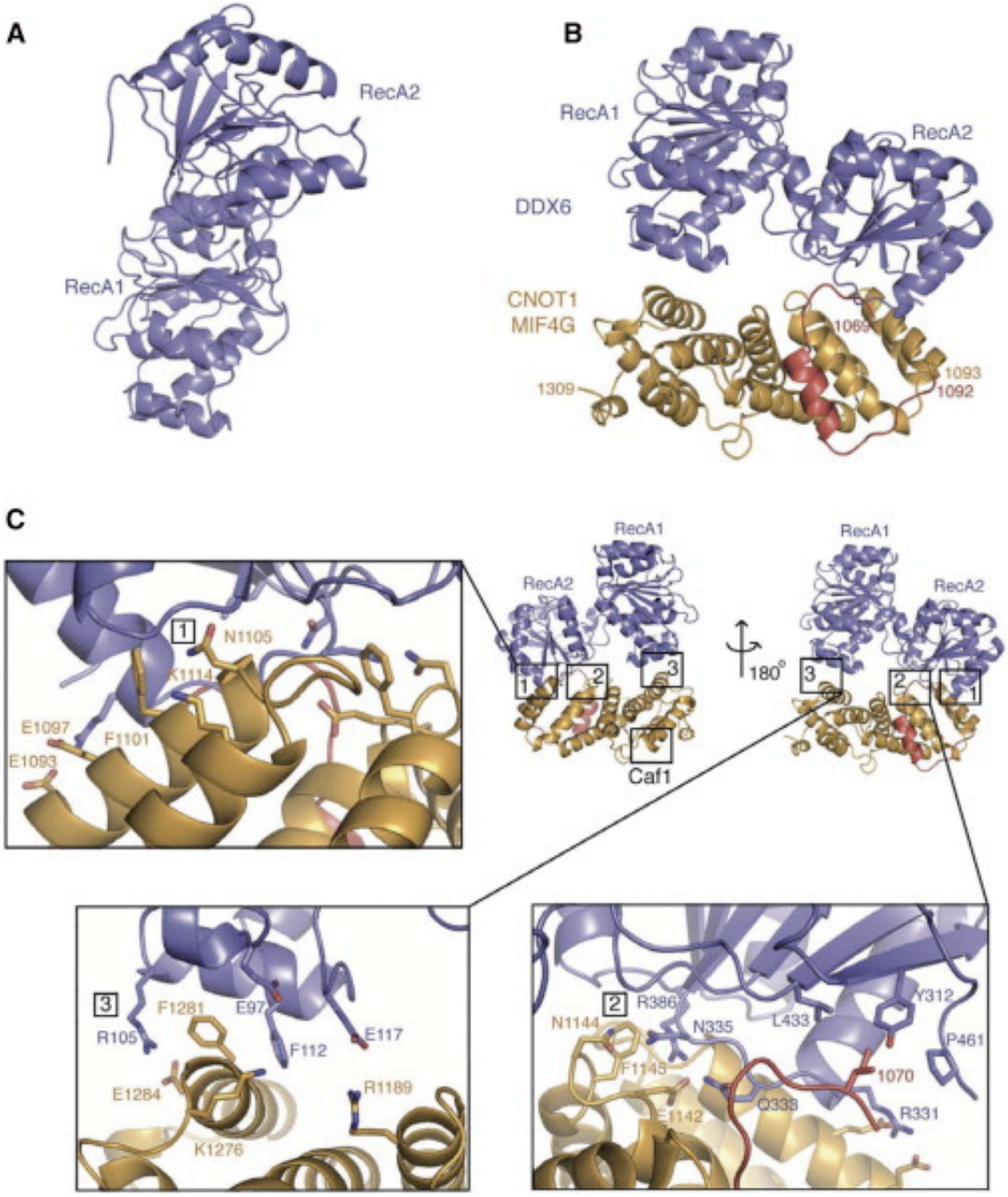

Fig 1.9: Crystal structure of CNOT1 binding to DDX6.
(A) Crystal structure of human DDX6 in blue. Similar to *S.c.* Dhh1, DDX6 possesses two globular RecA domains that are connected by a flexible linker sequence. (B) Co-crystal of DDX6 bound to the MIF4G domain of CNOT1. The five HEAT repeats of the CNOT1 MIF4G are in yellow, while the N-terminal extension is in red. (C) Hot spots of interaction between DDX6 and CNOT1 at three distinct patches (with each zoomed-in box demonstrating key residues for each patch). Reprinted with permission from (Mathys, H., Basquin, J., Ozgur, S., Czarnocki-Cieciura, M., Bonneau, F., Aartse, A., Dziembowski, A., Nowotny, M., Conti, E., and Filipowicz, W., 2014).

Findings of the work presented in this thesis dissertation:

This thesis presents three main findings: First, I show that the ATP bound conformation of Dhh1 is required to efficiently interact with members of the Ccr4-NOT deadenylase complex *in vivo*, most notably Not1 and Ccr4. Second, I show that loss of binding to Not1 by Dhh1 disrupts Dhh1 localization, leading to aberrant PB formation and recycling – similar to the phenotypes caused by the ATPase-deficient $Dhh1^{DQAD}$ allele. Finally, I demonstrate that Dhh1 requires distinct protein factors to independently mediate key functions in both mRNA decay and translation repression. Specifically, Dhh1 requires Pat1 to repress translation of a bound mRNA, while the Lsm1-7 complex is needed for Dhh1-mediated mRNA turnover.

References:

Amrani, N., Ganesan, R., Kervestin, S., Mangus, D.A., Ghosh, S., and Jacobson, A. (2004). A faux 3'-UTR promotes aberrant termination and triggers nonsense-mediated mRNA decay. Nature *432*, 112–118.

Anantharaman, V., and Aravind, L. (2004). Novel conserved domains in proteins with predicted roles in eukaryotic cell-cycle regulation, decapping and RNA stability. BMC Genomics *5*, 45.

Anderson, P., and Kedersha, N. (2009). RNA granules: post-transcriptional and epigenetic modulators of gene expression. Nat. Rev. Mol. Cell Biol. *10*, 430–436.

Andreou, A.Z., and Klostermeier, D. (2013). The DEAD-box helicase eIF4A: paradigm or the odd one out? RNA Biol. *10*, 19–32.

Andreou, A.Z., and Klostermeier, D. (2014). eIF4B and eIF4G jointly stimulate eIF4A ATPase and unwinding activities by modulation of the eIF4A conformational cycle. J. Mol. Biol. *426*, 51–61.

Arribas-Layton, M., Wu, D., Lykke-Andersen, J., and Song, H. (2013). Structural and functional control of the eukaryotic mRNA decapping machinery. Biochim. Biophys. Acta *1829*, 580–589.

Badis, G., Saveanu, C., Fromont-Racine, M., and Jacquier, A. (2004). Targeted mRNA degradation by deadenylation-independent decapping. Mol. Cell *15*, 5–15.

Bai, Y., Salvadore, C., Chiang, Y.C., Collart, M.A., Liu, H.Y., and Denis, C.L. (1999). The CCR4 and CAF1 proteins of the CCR4-NOT complex are physically and functionally separated from NOT2, NOT4, and NOT5. Mol. Cell. Biol. *19*, 6642–6651.

Ballut, L., Marchadier, B., Baguet, A., Tomasetto, C., Séraphin, B., and Le Hir, H. (2005). The exon junction core complex is locked onto RNA by inhibition of eIF4AIII ATPase activity. Nat. Struct. Mol. Biol. *12*, 861–869.

Basquin, J., Roudko, V.V., Rode, M., Basquin, C., Séraphin, B., and Conti, E. (2012). Architecture of the nuclease module of the yeast Ccr4-not complex: the Not1-Caf1-Ccr4 interaction. Mol. Cell *48*, 207–218.

Beelman, C.A., Stevens, A., Caponigro, G., LaGrandeur, T.E., Hatfield, L., Fortner, D.M., and Parker, R. (1996). An essential component of the decapping enzyme required for normal rates of mRNA turnover. Nature *382*, 642–646.

Bergkessel, M., and Reese, J.C. (2004). An essential role for the Saccharomyces cerevisiae DEAD-box helicase DHH1 in G1/S DNA-damage checkpoint recovery. Genetics *167*, 21–33.

Bianchin, C., Mauxion, F., Sentis, S., Séraphin, B., and Corbo, L. (2005). Conservation of the deadenylase activity of proteins of the Caf1 family in human. RNA N. Y. N *11*, 487–494.

Bonnerot, C., Boeck, R., and Lapeyre, B. (2000). The two proteins Pat1p (Mrt1p) and Spb8p interact in vivo, are required for mRNA decay, and are functionally linked to Pab1p. Mol. Cell. Biol. *20*, 5939–5946.

Borja, M.S., Piotukh, K., Freund, C., and Gross, J.D. (2011). Dcp1 links coactivators of mRNA decapping to Dcp2 by proline recognition. RNA N. Y. N *17*, 278–290.

Bouveret, E., Rigaut, G., Shevchenko, A., Wilm, M., and Séraphin, B. (2000). A Sm-like protein complex that participates in mRNA degradation. EMBO J. *19*, 1661–1671.

Brangwynne, C.P., Eckmann, C.R., Courson, D.S., Rybarska, A., Hoege, C., Gharakhani, J., Jülicher, F., and Hyman, A.A. (2009). Germline P granules are liquid droplets that localize by controlled dissolution/condensation. Science *324*, 1729–1732.

Brengues, M., Teixeira, D., and Parker, R. (2005). Movement of eukaryotic mRNAs between polysomes and cytoplasmic processing bodies. Science *310*, 486–489.

Buchan, J.R. (2014). mRNP granules: Assembly, function, and connections with disease. RNA Biol. *11*.

Buchan, J.R., Muhlrad, D., and Parker, R. (2008). P bodies promote stress granule assembly in Saccharomyces cerevisiae. J. Cell Biol. *183*, 441–455.

Buchan, J.R., Kolaitis, R.-M., Taylor, J.P., and Parker, R. (2013). Eukaryotic stress granules are cleared by autophagy and Cdc48/VCP function. Cell *153*, 1461–1474.

Buchwald, G., Schüssler, S., Basquin, C., Le Hir, H., and Conti, E. (2013). Crystal structure of the human eIF4AIII-CWC22 complex shows how a DEAD-box protein is inhibited by a MIF4G domain. Proc. Natl. Acad. Sci. U. S. A. *110*, E4611–E4618.

Cao, D., and Parker, R. (2001). Computational modeling of eukaryotic mRNA turnover. RNA N. Y. N *7*, 1192–1212.

Carroll, J.S., Munchel, S.E., and Weis, K. (2011). The DExD/H box ATPase Dhh1 functions in translational repression, mRNA decay, and processing body dynamics. J. Cell Biol. *194*, 527–537.

Chakrabarti, S., Jayachandran, U., Bonneau, F., Fiorini, F., Basquin, C., Domcke, S., Le Hir, H., and Conti, E. (2011). Molecular mechanisms for the RNA-dependent ATPase activity of Upf1 and its regulation by Upf2. Mol. Cell *41*, 693–703.

Chang, L.-C., and Lee, F.-J.S. (2012). The RNA helicase Dhh1p cooperates with Rbp1p to promote porin mRNA decay via its non-conserved C-terminal domain. Nucleic Acids Res. *40*, 1331–1344.

Chekulaeva, M., Mathys, H., Zipprich, J.T., Attig, J., Colic, M., Parker, R., and Filipowicz, W. (2011). miRNA repression involves GW182-mediated recruitment of CCR4-NOT through conserved W-containing motifs. Nat. Struct. Mol. Biol. *18*, 1218–1226.

Chen, Y., Boland, A., Kuzuoğlu-Öztürk, D., Bawankar, P., Loh, B., Chang, C.-T., Weichenrieder, O., and Izaurralde, E. (2014). A DDX6-CNOT1 complex and W-binding pockets in CNOT9 reveal direct links between miRNA target recognition and silencing. Mol. Cell *54*, 737–750.

Cheng, Z., Coller, J., Parker, R., and Song, H. (2005). Crystal structure and functional analysis of DEAD-box protein Dhh1p. RNA N. Y. N *11*, 1258–1270.

Chowdhury, A., and Tharun, S. (2008). lsm1 mutations impairing the ability of the Lsm1p-7p-Pat1p complex to preferentially bind to oligoadenylated RNA affect mRNA decay in vivo. RNA N. Y. N *14*, 2149–2158.

Chowdhury, A., and Tharun, S. (2009). Activation of decapping involves binding of the mRNA and facilitation of the post-binding steps by the Lsm1-7-Pat1 complex. RNA N. Y. N *15*, 1837–1848.

Chowdhury, A., Mukhopadhyay, J., and Tharun, S. (2007). The decapping activator Lsm1p-7p-Pat1p complex has the intrinsic ability to distinguish between oligoadenylated and polyadenylated RNAs. RNA N. Y. N *13*, 998–1016.

Christie, M., Boland, A., Huntzinger, E., Weichenrieder, O., and Izaurralde, E. (2013). Structure of the PAN3 pseudokinase reveals the basis for interactions with the PAN2 deadenylase and the GW182 proteins. Mol. Cell *51*, 360–373.

Collart, M.A., and Panasenko, O.O. (2012). The Ccr4--not complex. Gene *492*, 42–53.

Coller, J., and Parker, R. (2005). General translational repression by activators of mRNA decapping. Cell *122*, 875–886.

Coller, J.M., Tucker, M., Sheth, U., Valencia-Sanchez, M.A., and Parker, R. (2001). The DEAD box helicase, Dhh1p, functions in mRNA decapping and interacts with both the decapping and deadenylase complexes. RNA N. Y. N *7*, 1717–1727.

Cordin, O., Banroques, J., Tanner, N.K., and Linder, P. (2006). The DEAD-box protein family of RNA helicases. Gene *367*, 17–37.

Cougot, N., Babajko, S., and Séraphin, B. (2004). Cytoplasmic foci are sites of mRNA decay in human cells. J. Cell Biol. *165*, 31–40.

Decker, C.J., and Parker, R. (1993). A turnover pathway for both stable and unstable mRNAs in yeast: evidence for a requirement for deadenylation. Genes Dev. *7*, 1632–1643.

Decker, C.J., and Parker, R. (2012). P-bodies and stress granules: possible roles in the control of translation and mRNA degradation. Cold Spring Harb. Perspect. Biol. *4*, a012286.

Decker, C.J., Teixeira, D., and Parker, R. (2007). Edc3p and a glutamine/asparagine-rich domain of Lsm4p function in processing body assembly in Saccharomyces cerevisiae. J. Cell Biol. *179*, 437–449.

Van Dijk, E.L., Chen, C.L., d' Aubenton-Carafa, Y., Gourvennec, S., Kwapisz, M., Roche, V., Bertrand, C., Silvain, M., Legoix-Né, P., Loeillet, S., et al. (2011). XUTs are a class of Xrn1-sensitive antisense regulatory non-coding RNA in yeast. Nature *475*, 114–117.

Doma, M.K., and Parker, R. (2006). Endonucleolytic cleavage of eukaryotic mRNAs with stalls in translation elongation. Nature *440*, 561–564.

Dormann, D., Rodde, R., Edbauer, D., Bentmann, E., Fischer, I., Hruscha, A., Than, M.E., Mackenzie, I.R.A., Capell, A., Schmid, B., et al. (2010). ALS-associated fused in sarcoma (FUS) mutations disrupt Transportin-mediated nuclear import. EMBO J. *29*, 2841–2857.

Dutta, A., Zheng, S., Jain, D., Cameron, C.E., and Reese, J.C. (2011). Intermolecular interactions within the abundant DEAD-box protein Dhh1 regulate its activity in vivo. J. Biol. Chem. *286*, 27454–27470.

Ernoult-Lange, M., Baconnais, S., Harper, M., Minshall, N., Souquere, S., Boudier, T., Bénard, M., Andrey, P., Pierron, G., Kress, M., et al. (2012). Multiple binding of repressed mRNAs by the P-body protein Rck/p54. RNA N. Y. N *18*, 1702–1715.

Eulalio, A., Behm-Ansmant, I., Schweizer, D., and Izaurralde, E. (2007). P-body formation is a consequence, not the cause, of RNA-mediated gene silencing. Mol. Cell. Biol. *27*, 3970–3981.

Fabian, M.R., Sonenberg, N., and Filipowicz, W. (2010a). Regulation of mRNA translation and stability by microRNAs. Annu. Rev. Biochem. *79*, 351–379.

Fabian, M.R., Sundermeier, T.R., and Sonenberg, N. (2010b). Understanding how miRNAs post-transcriptionally regulate gene expression. Prog. Mol. Subcell. Biol. *50*, 1–20.

Fabian, M.R., Cieplak, M.K., Frank, F., Morita, M., Green, J., Srikumar, T., Nagar, B., Yamamoto, T., Raught, B., Duchaine, T.F., et al. (2011). miRNA-mediated deadenylation is orchestrated by GW182 through two conserved motifs that interact with CCR4-NOT. Nat. Struct. Mol. Biol. *18*, 1211–1217.

Fairman, M.E., Maroney, P.A., Wang, W., Bowers, H.A., Gollnick, P., Nilsen, T.W., and Jankowsky, E. (2004). Protein displacement by DExH/D "RNA helicases" without duplex unwinding. Science *304*, 730–734.

Fairman-Williams, M.E., Guenther, U.-P., and Jankowsky, E. (2010). SF1 and SF2 helicases: family matters. Curr. Opin. Struct. Biol. *20*, 313–324.

Fischer, N., and Weis, K. (2002). The DEAD box protein Dhh1 stimulates the decapping enzyme Dcp1. EMBO J. *21*, 2788–2797.

Franks, T.M., and Lykke-Andersen, J. (2008). The control of mRNA decapping and P-body formation. Mol. Cell *32*, 605–615.

Franks, T.M., Singh, G., and Lykke-Andersen, J. (2010). Upf1 ATPase-dependent mRNP disassembly is required for completion of nonsense- mediated mRNA decay. Cell *143*, 938–950.

Frey, S., Richter, R.P., and Görlich, D. (2006). FG-rich repeats of nuclear pore proteins form a three-dimensional meshwork with hydrogel-like properties. Science *314*, 815–817.

Frischmeyer, P.A., van Hoof, A., O'Donnell, K., Guerrerio, A.L., Parker, R., and Dietz, H.C. (2002). An mRNA surveillance mechanism that eliminates transcripts lacking termination codons. Science *295*, 2258–2261.

Fromm, S.A., Truffault, V., Kamenz, J., Braun, J.E., Hoffmann, N.A., Izaurralde, E., and Sprangers, R. (2012). The structural basis of Edc3- and Scd6-mediated activation of the Dcp1:Dcp2 mRNA decapping complex. EMBO J. *31*, 279–290.

Fromm, S.A., Kamenz, J., Nöldeke, E.R., Neu, A., Zocher, G., and Sprangers, R. (2014). In vitro reconstitution of a cellular phase-transition process that involves the mRNA decapping machinery. Angew. Chem. Int. Ed Engl. *53*, 7354–7359.

Garneau, N.L., Wilusz, J., and Wilusz, C.J. (2007). The highways and byways of mRNA decay. Nat. Rev. Mol. Cell Biol. *8*, 113–126.

Geisler, S., Lojek, L., Khalil, A.M., Baker, K.E., and Coller, J. (2012). Decapping of long noncoding RNAs regulates inducible genes. Mol. Cell *45*, 279–291.

Gingerich, T.J., Feige, J.-J., and LaMarre, J. (2004). AU-rich elements and the control of gene expression through regulated mRNA stability. Anim. Health Res. Rev. Conf. Res. Work. Anim. Dis. *5*, 49–63.

Goldstrohm, A.C., Hook, B.A., Seay, D.J., and Wickens, M. (2006). PUF proteins bind Pop2p to regulate messenger RNAs. Nat. Struct. Mol. Biol. *13*, 533–539.

Gygi, S.P., Rochon, Y., Franza, B.R., and Aebersold, R. (1999). Correlation between protein and mRNA abundance in yeast. Mol. Cell. Biol. *19*, 1720–1730.

Haimovich, G., Medina, D.A., Causse, S.Z., Garber, M., Millán-Zambrano, G., Barkai, O., Chávez, S., Pérez-Ortín, J.E., Darzacq, X., and Choder, M. (2013). Gene expression is

circular: factors for mRNA degradation also foster mRNA synthesis. Cell *153*, 1000–1011.

Halbach, F., Reichelt, P., Rode, M., and Conti, E. (2013). The yeast ski complex: crystal structure and RNA channeling to the exosome complex. Cell *154*, 814–826.

Hansen, K.D., Lareau, L.F., Blanchette, M., Green, R.E., Meng, Q., Rehwinkel, J., Gallusser, F.L., Izaurralde, E., Rio, D.C., Dudoit, S., et al. (2009). Genome-wide identification of alternative splice forms down-regulated by nonsense-mediated mRNA decay in Drosophila. PLoS Genet. *5*, e1000525.

Hardin, J.W., Hu, Y.X., and McKay, D.B. (2010). Structure of the RNA binding domain of a DEAD-box helicase bound to its ribosomal RNA target reveals a novel mode of recognition by an RNA recognition motif. J. Mol. Biol. *402*, 412–427.

Harigaya, Y., and Parker, R. (2010). No-go decay: a quality control mechanism for RNA in translation. Wiley Interdiscip. Rev. RNA *1*, 132–141.

Harigaya, Y., Jones, B.N., Muhlrad, D., Gross, J.D., and Parker, R. (2010). Identification and analysis of the interaction between Edc3 and Dcp2 in Saccharomyces cerevisiae. Mol. Cell. Biol. *30*, 1446–1456.

Hata, H., Mitsui, H., Liu, H., Bai, Y., Denis, C.L., Shimizu, Y., and Sakai, A. (1998). Dhh1p, a putative RNA helicase, associates with the general transcription factors Pop2p and Ccr4p from Saccharomyces cerevisiae. Genetics *148*, 571–579.

He, F., and Jacobson, A. (1995). Identification of a novel component of the nonsense-mediated mRNA decay pathway by use of an interacting protein screen. Genes Dev. *9*, 437–454.

He, F., Li, C., Roy, B., and Jacobson, A. (2014). Yeast Edc3 targets RPS28B mRNA for decapping by binding to a 3’ untranslated region decay-inducing regulatory element. Mol. Cell. Biol. *34*, 1438–1451.

Le Hir, H., and Andersen, G.R. (2008). Structural insights into the exon junction complex. Curr. Opin. Struct. Biol. *18*, 112–119.

Le Hir, H., Izaurralde, E., Maquat, L.E., and Moore, M.J. (2000). The spliceosome deposits multiple proteins 20-24 nucleotides upstream of mRNA exon-exon junctions. EMBO J. *19*, 6860–6869.

Inada, T., and Aiba, H. (2005). Translation of aberrant mRNAs lacking a termination codon or with a shortened 3’-UTR is repressed after initiation in yeast. EMBO J. *24*, 1584–1595.

Iost, I., Bizebard, T., and Dreyfus, M. (2013). Functions of DEAD-box proteins in bacteria: current knowledge and pending questions. Biochim. Biophys. Acta *1829*, 866–877.

Januszyk, K., and Lima, C.D. (2011). Structural components and architectures of RNA exosomes. Adv. Exp. Med. Biol. *702*, 9–28.

Januszyk, K., and Lima, C.D. (2014). The eukaryotic RNA exosome. Curr. Opin. Struct. Biol. *24*, 132–140.

Jinek, M., Coyle, S.M., and Doudna, J.A. (2011). Coupled 5' nucleotide recognition and processivity in Xrn1-mediated mRNA decay. Mol. Cell *41*, 600–608.

Jonas, S., and Izaurralde, E. (2013). The role of disordered protein regions in the assembly of decapping complexes and RNP granules. Genes Dev. *27*, 2628–2641.

Jonas, S., Christie, M., Peter, D., Bhandari, D., Loh, B., Huntzinger, E., Weichenrieder, O., and Izaurralde, E. (2014). An asymmetric PAN3 dimer recruits a single PAN2 exonuclease to mediate mRNA deadenylation and decay. Nat. Struct. Mol. Biol. *21*, 599–608.

Kato, M., Han, T.W., Xie, S., Shi, K., Du, X., Wu, L.C., Mirzaei, H., Goldsmith, E.J., Longgood, J., Pei, J., et al. (2012). Cell-free formation of RNA granules: low complexity sequence domains form dynamic fibers within hydrogels. Cell *149*, 753–767.

Kedersha, N., and Anderson, P. (2009). Regulation of translation by stress granules and processing bodies. Prog. Mol. Biol. Transl. Sci. *90*, 155–185.

Kshirsagar, M., and Parker, R. (2004). Identification of Edc3p as an enhancer of mRNA decapping in Saccharomyces cerevisiae. Genetics *166*, 729–739.

LaGrandeur, T.E., and Parker, R. (1998). Isolation and characterization of Dcp1p, the yeast mRNA decapping enzyme. EMBO J. *17*, 1487–1496.

Lavut, A., and Raveh, D. (2012). Sequestration of highly expressed mRNAs in cytoplasmic granules, P-bodies, and stress granules enhances cell viability. PLoS Genet. *8*, e1002527.

Leeds, P., Peltz, S.W., Jacobson, A., and Culbertson, M.R. (1991). The product of the yeast UPF1 gene is required for rapid turnover of mRNAs containing a premature translational termination codon. Genes Dev. *5*, 2303–2314.

Leeds, P., Wood, J.M., Lee, B.S., and Culbertson, M.R. (1992). Gene products that promote mRNA turnover in Saccharomyces cerevisiae. Mol. Cell. Biol. *12*, 2165–2177.

Linder, P., and Jankowsky, E. (2011). From unwinding to clamping - the DEAD box RNA helicase family. Nat. Rev. Mol. Cell Biol. *12*, 505–516.

Liu, Q., Greimann, J.C., and Lima, C.D. (2006). Reconstitution, activities, and structure of the eukaryotic RNA exosome. Cell *127*, 1223–1237.

Loh, B., Jonas, S., and Izaurralde, E. (2013). The SMG5-SMG7 heterodimer directly recruits the CCR4-NOT deadenylase complex to mRNAs containing nonsense codons via interaction with POP2. Genes Dev. *27*, 2125–2138.

Luo, X., Talarek, N., and De Virgilio, C. (2011). Initiation of the yeast G0 program requires Igo1 and Igo2, which antagonize activation of decapping of specific nutrient-regulated mRNAs. RNA Biol. *8*, 14–17.

Mathys, H., Basquin, J., Ozgur, S., Czarnocki-Cieciura, M., Bonneau, F., Aartse, A., Dziembowski, A., Nowotny, M., Conti, E., and Filipowicz, W. (2014). Structural and biochemical insights to the role of the CCR4-NOT complex and DDX6 ATPase in microRNA repression. Mol. Cell *54*, 751–765.

Mendell, J.T., Medghalchi, S.M., Lake, R.G., Noensie, E.N., and Dietz, H.C. (2000). Novel Upf2p orthologues suggest a functional link between translation initiation and nonsense surveillance complexes. Mol. Cell. Biol. *20*, 8944–8957.

Milac, A.L., Bojarska, E., and Wypijewska del Nogal, A. (2014). Decapping Scavenger (DcpS) enzyme: advances in its structure, activity and roles in the cap-dependent mRNA metabolism. Biochim. Biophys. Acta *1839*, 452–462.

Miller, M.A., and Olivas, W.M. (2011). Roles of Puf proteins in mRNA degradation and translation. Wiley Interdiscip. Rev. RNA *2*, 471–492.

Miller, A.L., Suntharalingam, M., Johnson, S.L., Audhya, A., Emr, S.D., and Wente, S.R. (2004). Cytoplasmic inositol hexakisphosphate production is sufficient for mediating the Gle1-mRNA export pathway. J. Biol. Chem. *279*, 51022–51032.

Miller, C., Schwalb, B., Maier, K., Schulz, D., Dümcke, S., Zacher, B., Mayer, A., Sydow, J., Marcinowski, L., Dölken, L., et al. (2011). Dynamic transcriptome analysis measures rates of mRNA synthesis and decay in yeast. Mol. Syst. Biol. *7*, 458.

Mitchell, S.F., Jain, S., She, M., and Parker, R. (2013). Global analysis of yeast mRNPs. Nat. Struct. Mol. Biol. *20*, 127–133.

Montpetit, B., Thomsen, N.D., Helmke, K.J., Seeliger, M.A., Berger, J.M., and Weis, K. (2011). A conserved mechanism of DEAD-box ATPase activation by nucleoporins and InsP6 in mRNA export. Nature *472*, 238–242.

Moriya, H., and Isono, K. (1999). Analysis of genetic interactions between DHH1, SSD1 and ELM1 indicates their involvement in cellular morphology determination in Saccharomyces cerevisiae. Yeast Chichester Engl. *15*, 481–496.

Muhlrad, D., and Parker, R. (2005). The yeast EDC1 mRNA undergoes deadenylation-independent decapping stimulated by Not2p, Not4p, and Not5p. EMBO J. *24*, 1033–1045.

Munchel, S.E., Shultzaberger, R.K., Takizawa, N., and Weis, K. (2011). Dynamic profiling of mRNA turnover reveals gene-specific and system-wide regulation of mRNA decay. Mol. Biol. Cell *22*, 2787–2795.

Nakamura, A., Amikura, R., Hanyu, K., and Kobayashi, S. (2001). Me31B silences translation of oocyte-localizing RNAs through the formation of cytoplasmic RNP complex during Drosophila oogenesis. Dev. Camb. Engl. *128*, 3233–3242.

Navarro, R.E., and Blackwell, T.K. (2005). Requirement for P granules and meiosis for accumulation of the germline RNA helicase CGH-1. Genes. N. Y. N 2000 *42*, 172–180.

Navarro, R.E., Shim, E.Y., Kohara, Y., Singson, A., and Blackwell, T.K. (2001). cgh-1, a conserved predicted RNA helicase required for gametogenesis and protection from physiological germline apoptosis in C. elegans. Dev. Camb. Engl. *128*, 3221–3232.

Nissan, T., Rajyaguru, P., She, M., Song, H., and Parker, R. (2010). Decapping activators in Saccharomyces cerevisiae act by multiple mechanisms. Mol. Cell *39*, 773–783.

Parker, R. (2012). RNA degradation in Saccharomyces cerevisae. Genetics *191*, 671–702.

Parker, R., and Sheth, U. (2007). P bodies and the control of mRNA translation and degradation. Mol. Cell *25*, 635–646.

Parvatiyar, K., Zhang, Z., Teles, R.M., Ouyang, S., Jiang, Y., Iyer, S.S., Zaver, S.A., Schenk, M., Zeng, S., Zhong, W., et al. (2012). The helicase DDX41 recognizes the bacterial secondary messengers cyclic di-GMP and cyclic di-AMP to activate a type I interferon immune response. Nat. Immunol. *13*, 1155–1161.

Petit, A.-P., Wohlbold, L., Bawankar, P., Huntzinger, E., Schmidt, S., Izaurralde, E., and Weichenrieder, O. (2012). The structural basis for the interaction between the CAF1 nuclease and the NOT1 scaffold of the human CCR4-NOT deadenylase complex. Nucleic Acids Res. *40*, 11058–11072.

Putnam, A.A., and Jankowsky, E. (2013). DEAD-box helicases as integrators of RNA, nucleotide and protein binding. Biochim. Biophys. Acta *1829*, 884–893.

Quenault, T., Lithgow, T., and Traven, A. (2011). PUF proteins: repression, activation and mRNA localization. Trends Cell Biol. *21*, 104–112.

Ramachandran, V., Shah, K.H., and Herman, P.K. (2011). The cAMP-dependent protein kinase signaling pathway is a key regulator of P body foci formation. Mol. Cell *43*, 973–981.

Ramaswami, M., Taylor, J.P., and Parker, R. (2013). Altered ribostasis: RNA-protein granules in degenerative disorders. Cell *154*, 727–736.

Ray, B.K., Lawson, T.G., Kramer, J.C., Cladaras, M.H., Grifo, J.A., Abramson, R.D., Merrick, W.C., and Thach, R.E. (1985). ATP-dependent unwinding of messenger RNA structure by eukaryotic initiation factors. J. Biol. Chem. *260*, 7651–7658.

Rogers, G.W., Richter, N.J., and Merrick, W.C. (1999). Biochemical and kinetic characterization of the RNA helicase activity of eukaryotic initiation factor 4A. J. Biol. Chem. *274*, 12236–12244.

Rogers, G.W., Richter, N.J., Lima, W.F., and Merrick, W.C. (2001). Modulation of the helicase activity of eIF4A by eIF4B, eIF4H, and eIF4F. J. Biol. Chem. *276*, 30914–30922.

Rouya, C., Siddiqui, N., Morita, M., Duchaine, T.F., Fabian, M.R., and Sonenberg, N. (2014). Human DDX6 effects miRNA-mediated gene silencing via direct binding to CNOT1. RNA N. Y. N *20*, 1398–1409.

Russell, R., Jarmoskaite, I., and Lambowitz, A.M. (2013). Toward a molecular understanding of RNA remodeling by DEAD-box proteins. RNA Biol. *10*, 44–55.

Schütz, P., Bumann, M., Oberholzer, A.E., Bieniossek, C., Trachsel, H., Altmann, M., and Baumann, U. (2008). Crystal structure of the yeast eIF4A-eIF4G complex: an RNA-helicase controlled by protein-protein interactions. Proc. Natl. Acad. Sci. U. S. A. *105*, 9564–9569.

Shah, K.H., Zhang, B., Ramachandran, V., and Herman, P.K. (2013). Processing body and stress granule assembly occur by independent and differentially regulated pathways in Saccharomyces cerevisiae. Genetics *193*, 109–123.

Sharif, H., Ozgur, S., Sharma, K., Basquin, C., Urlaub, H., and Conti, E. (2013). Structural analysis of the yeast Dhh1-Pat1 complex reveals how Dhh1 engages Pat1, Edc3 and RNA in mutually exclusive interactions. Nucleic Acids Res. *41*, 8377–8390.

She, M., Decker, C.J., Chen, N., Tumati, S., Parker, R., and Song, H. (2006). Crystal structure and functional analysis of Dcp2p from Schizosaccharomyces pombe. Nat. Struct. Mol. Biol. *13*, 63–70.

She, M., Decker, C.J., Svergun, D.I., Round, A., Chen, N., Muhlrad, D., Parker, R., and Song, H. (2008). Structural basis of dcp2 recognition and activation by dcp1. Mol. Cell *29*, 337–349.

Sheth, U., and Parker, R. (2003). Decapping and decay of messenger RNA occur in cytoplasmic processing bodies. Science *300*, 805–808.

Shoemaker, C.J., and Green, R. (2012). Translation drives mRNA quality control. Nat. Struct. Mol. Biol. *19*, 594–601.

Siddiqui, N., Mangus, D.A., Chang, T.-C., Palermino, J.-M., Shyu, A.-B., and Gehring, K. (2007). Poly(A) nuclease interacts with the C-terminal domain of polyadenylate-binding protein domain from poly(A)-binding protein. J. Biol. Chem. *282*, 25067–25075.

Spiller, M.P., Reijns, M.A.M., and Beggs, J.D. (2007). Requirements for nuclear localization of the Lsm2-8p complex and competition between nuclear and cytoplasmic Lsm complexes. J. Cell Sci. *120*, 4310–4320.

Sun, M., Schwalb, B., Pirkl, N., Maier, K.C., Schenk, A., Failmezger, H., Tresch, A., and Cramer, P. (2013). Global analysis of eukaryotic mRNA degradation reveals Xrn1-dependent buffering of transcript levels. Mol. Cell *52*, 52–62.

Svitkin, Y.V., Pause, A., Haghighat, A., Pyronnet, S., Witherell, G., Belsham, G.J., and Sonenberg, N. (2001). The requirement for eukaryotic initiation factor 4A (elF4A) in translation is in direct proportion to the degree of mRNA 5' secondary structure. RNA N. Y. N *7*, 382–394.

Sweet, T., Kovalak, C., and Coller, J. (2012). The DEAD-box protein Dhh1 promotes decapping by slowing ribosome movement. PLoS Biol. *10*, e1001342.

Synowsky, S.A., and Heck, A.J.R. (2008). The yeast Ski complex is a hetero-tetramer. Protein Sci. Publ. Protein Soc. *17*, 119–125.

Talarek, N., Cameroni, E., Jaquenoud, M., Luo, X., Bontron, S., Lippman, S., Devgan, G., Snyder, M., Broach, J.R., and De Virgilio, C. (2010). Initiation of the TORC1-regulated G0 program requires Igo1/2, which license specific mRNAs to evade degradation via the 5'-3' mRNA decay pathway. Mol. Cell *38*, 345–355.

Teixeira, D., and Parker, R. (2007). Analysis of P-body assembly in Saccharomyces cerevisiae. Mol. Biol. Cell *18*, 2274–2287.

Teixeira, D., Sheth, U., Valencia-Sanchez, M.A., Brengues, M., and Parker, R. (2005). Processing bodies require RNA for assembly and contain nontranslating mRNAs. RNA N. Y. N *11*, 371–382.

Tritschler, F., Eulalio, A., Truffault, V., Hartmann, M.D., Helms, S., Schmidt, S., Coles, M., Izaurralde, E., and Weichenrieder, O. (2007). A divergent Sm fold in EDC3 proteins mediates DCP1 binding and P-body targeting. Mol. Cell. Biol. *27*, 8600–8611.

Tritschler, F., Eulalio, A., Helms, S., Schmidt, S., Coles, M., Weichenrieder, O., Izaurralde, E., and Truffault, V. (2008). Similar modes of interaction enable Trailer Hitch and EDC3 to associate with DCP1 and Me31B in distinct protein complexes. Mol. Cell. Biol. *28*, 6695–6708.

Tritschler, F., Braun, J.E., Eulalio, A., Truffault, V., Izaurralde, E., and Weichenrieder, O. (2009). Structural basis for the mutually exclusive anchoring of P body components EDC3 and Tral to the DEAD box protein DDX6/Me31B. Mol. Cell *33*, 661–668.

Tseng-Rogenski, S.S.-I., Chong, J.-L., Thomas, C.B., Enomoto, S., Berman, J., and Chang, T.-H. (2003). Functional conservation of Dhh1p, a cytoplasmic DExD/H-box protein present in large complexes. Nucleic Acids Res. *31*, 4995–5002.

Tucker, M., Valencia-Sanchez, M.A., Staples, R.R., Chen, J., Denis, C.L., and Parker, R. (2001). The transcription factor associated Ccr4 and Caf1 proteins are components of the major cytoplasmic mRNA deadenylase in Saccharomyces cerevisiae. Cell *104*, 377–386.

Tucker, M., Staples, R.R., Valencia-Sanchez, M.A., Muhlrad, D., and Parker, R. (2002). Ccr4p is the catalytic subunit of a Ccr4p/Pop2p/Notp mRNA deadenylase complex in Saccharomyces cerevisiae. EMBO J. *21*, 1427–1436.

Vanacova, S., and Stefl, R. (2007). The exosome and RNA quality control in the nucleus. EMBO Rep. *8*, 651–657.

Wahle, E., and Winkler, G.S. (2013). RNA decay machines: deadenylation by the Ccr4-not and Pan2-Pan3 complexes. Biochim. Biophys. Acta *1829*, 561–570.

Weirich, C.S., Erzberger, J.P., Flick, J.S., Berger, J.M., Thorner, J., and Weis, K. (2006). Activation of the DExD/H-box protein Dbp5 by the nuclear-pore protein Gle1 and its coactivator InsP6 is required for mRNA export. Nat. Cell Biol. *8*, 668–676.

Westmoreland, T.J., Olson, J.A., Saito, W.Y., Huper, G., Marks, J.R., and Bennett, C.B. (2003). Dhh1 regulates the G1/S-checkpoint following DNA damage or BRCA1 expression in yeast. J. Surg. Res. *113*, 62–73.

Weston, A., and Sommerville, J. (2006). Xp54 and related (DDX6-like) RNA helicases: roles in messenger RNP assembly, translation regulation and RNA degradation. Nucleic Acids Res. *34*, 3082–3094.

Wolf, J., and Passmore, L.A. (2014). mRNA deadenylation by Pan2-Pan3. Biochem. Soc. Trans. *42*, 184–187.

Wolf, J., Valkov, E., Allen, M.D., Meineke, B., Gordiyenko, Y., McLaughlin, S.H., Olsen, T.M., Robinson, C.V., Bycroft, M., Stewart, M., et al. (2014). Structural basis for Pan3 binding to Pan2 and its function in mRNA recruitment and deadenylation. EMBO J. *33*, 1514–1526.

Wu, D., Muhlrad, D., Bowler, M.W., Jiang, S., Liu, Z., Parker, R., and Song, H. (2014). Lsm2 and Lsm3 bridge the interaction of the Lsm1-7 complex with Pat1 for decapping activation. Cell Res. *24*, 233–246.

Zhou, L., Zhou, Y., Hang, J., Wan, R., Lu, G., Yan, C., and Shi, Y. (2014). Crystal structure and biochemical analysis of the heptameric Lsm1-7 complex. Cell Res. *24*, 497–500.

Chapter II: Not1 regulates the dynamic localization of Dhh1 to Processing Bodies

Introduction

Precise control of gene expression is critical for cells to properly respond to internal and external cues. Cells employ a large number of mechanisms to achieve tight regulation of gene expression, including post-transcriptional control of active messenger RNA (mRNA) levels by inhibition of translation or by mRNA degradation. However, the events mediating the transition of an mRNA between translation and storage or decay remains poorly understood.

mRNAs are transcribed and processed in the nucleus, after which they are exported to the cytoplasm where they can either template protein synthesis by the ribosome or serve as a substrate for mRNA degradation or storage. Mature mRNAs are marked by a 7-methylguanosine cap at the 5' end and by a poly(A) tail at the 3' end. These modifications promote interaction with translation initiation factors like poly(A) binding protein (Pab1), eIF4E, and eIF4G while preventing exonucleolytic degradation (Coller and Parker, 2004). However, in response to stress or a change in translational status, the complement of proteins bound to the mRNA changes, shifting the mRNA from a translationally competent messenger ribonucleoprotein (mRNP) complex to a nontranslating mRNP that can be stored or targeted for degradation.

In budding yeast, mRNAs are degraded predominantly in a deadenylation-dependent manner, which is accomplished either by the Pan2/Pan3 heterodimer or by the Ccr4-NOT complex (Brown and Sachs, 1998; Muhlrad and Parker, 1992). Deadenylated mRNAs can be degraded from the 3' end by the 10-subunit exosome complex (Chlebowski et al., 2013), or alternatively by removal of the 5' cap by the Dcp1-Dcp2 decapping enzyme and degradation by the 5'-3' exonuclease Xrn1 (Garneau et al., 2007). Several additional factors have been identified, such as Pat1, Edc3, and the Lsm1-7 complex, that cause an accumulation of capped, deadenylated mRNAs when deleted, suggesting these genes are also involved in mRNA turnover (Parker, 2012). While removal of the 5' cap is thought to mark an irreversible step in mRNA decay, deadenylated mRNAs can exist in complex with other protein factors in a nontranslating messenger ribonucleoprotein complex (mRNPs) and can be readenylated in some circumstances (Franks and Lykke-Andersen, 2008). Furthermore, under certain stress conditions, such as glucose starvation and osmotic shock, mRNAs that are bound to protein factors involved in mRNA turnover can assemble in to larger mRNP foci, known as Processing Bodies (PBs) that are postulated sites of storage and mRNA decay (Aizer et al., 2014; Anderson and Kedersha, 2009; Decker and Parker, 2012)

Although many of the factors that localize to these mRNP granules are involved in translational repression and mRNA decay, mutants defective in the formation of microscopically visible PBs do not show defects in these activities (Buchan et al., 2008; Decker et al., 2007; Eulalio et al., 2007). As a result, the exact role these mRNP foci play in modulating gene expression remains unclear. However, there is increasing evidence that the ability to form PBs is critical under various stress conditions. For example, cells unable to form PBs show a severe loss in viability in stationary phase (Ramachandran et al., 2011; Shah et al., 2013). Furthermore, ectopic expression of highly expressed mRNAs in cells that cannot

form PBs showed a loss in viability (Lavut and Raveh, 2012). PBs and several other related types of granules, including stress granules, germ granules, and neuronal transport granules (Erickson and Lykke-Andersen, 2011; Kiebler and Bassell, 2006; Voronina, 2013) also form in a variety of cell types, suggesting these structures are functionally important for modulating gene expression.

Although many mRNA decay factors have been shown to localize PBs, the functional role of these complexes, as well as the mechanisms by which they assemble, are unknown. However, it is likely that partitioning mRNAs between translation and decay or storage, as well as seeding PB formation, may require an enzyme that can either remodel the translating mRNP complex or stimulate the formation of a decay-competent or repressed mRNP. The DEAD-box ATPase Dhh1 can stimulate mRNA decay and translation repression (Carroll et al., 2011; Coller and Parker, 2005; Fischer and Weis, 2002; Sweet et al., 2012) and is thought to function at an early step in PB formation, making it a good candidate to facilitate mRNA inactivation (Teixeira and Parker, 2007). Similar to other DEAD box proteins, Dhh1 possesses an N and C-terminal RecA-like domain connected by a short flexible linker, and can bind RNA through the phosphate backbone with high affinity (Cheng et al., 2005; Linder and Jankowsky, 2011; Russell et al., 2013). However, unlike canonical DEAD-box proteins, crystal structures of Dhh1 show that it has considerable intermolecular interactions between its N and C-terminal RecA lobes, giving Dhh1 a more closed conformation than other DEAD-box proteins (Cheng et al., 2005). These interdomain interactions are thought to negatively regulate the activity of Dhh1, which is a highly abundant enzyme (Ernoult-Lange et al., 2012; Gygi et al., 1999). Consistent with this observation, Dhh1 was shown to have significantly lower ATPase activity *in vitro* than other well characterized DEAD-box proteins like eIF4A and Ded1 (Cordin et al., 2006; Dutta et al., 2011; Pause and Sonenberg, 1992; Tritschler et al., 2009). Thus, Dhh1 is likely to require an activating protein to stimulate its ATP hydrolysis cycle in order to function properly.

Previously, our lab showed that an ATPase-deficient mutant of Dhh1, $Dhh1^{DQAD}$, induces the formation of, and localizes to, PBs in the absence of stress (Carroll et al., 2011). Based on this observation, we proposed that $Dhh1^{DQAD}$ forms constitutive PBs because its recycling from PBs is impaired. In this study, we sought to characterize how other biochemical activities of Dhh1, such as ATP binding and RNA binding, affect its functions in mRNA decay, translation repression, and PB formation. Interestingly, RNA binding activity was required for Dhh1 to stimulate mRNA decay and repress translation when artificially tethered to the mRNA, while ATP binding was expendable for these functions. However, both RNA binding and ATP binding were required for Dhh1 localization to PBs. Surprisingly, we saw that an ATP-binding mutant of Dhh1, $Dhh1^{Q\text{-}motif}$, was severely deficient in binding to proteins of the Ccr4-NOT complex, in particular Not1 and Ccr4. Recent work has shown that CNOT1 and DDX6 – mammalian orthologs of Not1 and Dhh1 – directly bind one another and that Not1 can activate Dhh1's ATPase activity *in vitro*(Chen et al., 2014; Mathys et al., 2014; Rouya et al., 2014). Sequence alignments of these proteins identified the residues that are required for Dhh1-Not1 interaction are highly conserved throughout evolution, including in *S. cerevisiae*. We generated a panel of Dhh1 mutants that were predicted to affect binding to Not1 and showed

that these mutants localized constitutively to PBs, similar to Dhh1^{DQAD}. Furthermore, the loss of interaction between Dhh1 and Not1 also disrupted the dynamic of localization of Dhh1 to PBs. In summary, our results demonstrate that Not1-Dhh1 binding is critical for proper localization and recycling of Dhh1 in PBs. This suggests a model where Dhh1 binds mRNA to deliver it to PBs, followed by Not1 activation of the Dhh1 ATPase cycle to facilitate Dhh1 release into the cytoplasm.

Results

Loss of ATP and RNA binding disrupt Dhh1 localization

In order to dissect the importance of ATP binding and RNA binding in Dhh1 function, we mutagenized Dhh1 at residues that were previously shown to be required for these activities (Cheng et al., 2005; Dutta et al., 2011). These include residues in the conserved Q-motif (F66R, Q73A - which we termed Dhh1$^{Q\text{-}motif}$; Dutta et al., 2011), which are needed for Dhh1 ATP binding, as well as residues shown to crosslink to RNA (S322A, S340A, R370A) **(Table 2.1)**.

Table 2.1

Dhh1 mutants generated in this study

Name	Mutation(s)	Biochemical Activity Affected
Q-motif	F66R,Q73A	ATP-binding
DQAD	E195Q	ATP-hydrolysis
1X-RNA	S322A	RNA-binding
2X-RNA	S322A,S340A	RNA-binding
3X-RNA	S322A,S340A, R370A	RNA-binding
INT	K91A,T344A	Enhanced ATP-hydrolysis

Table 2.1: Dhh1 mutants generated in this study

We first expressed Dhh1$^{Q\text{-}motif}$ and a triple RNA binding point mutant, Dhh1$^{3X\text{-}RNA}$, as GFP fusion proteins in *dhh1Δ* cells to ask whether these activities were important for Dhh1 localization. Upon glucose starvation, Dhh1$^{Q\text{-}motif}$-GFP and Dhh1$^{3X\text{-}RNA}$-GFP were unable to efficiently localize to PB foci compared to *dhh1Δ* cells expressing wild-type Dhh1-GFP **(Fig 2.1 A-D)**. This demonstrates that both RNA binding and ATP binding are required for Dhh1 localization to PBs. Dhh1$^{Q\text{-}motif}$-GFP cells also had a severe defect in overall PB formation, as seen by a loss in Dcp2-mCherry foci, a marker for PBs **(Fig 2.1 A-B)**. However, while loss of RNA binding dramatically affected the localization of Dhh1 to PBs, cells expressing Dhh1$^{3X\text{-}RNA}$-GFP showed

only a small defect in PB formation **(Fig 2.1 C-D)**. This suggests that Dhh1 RNA binding does not affect PB formation *per se*, and either that PBs can form in the absence of RNA or that RNAs can also be trafficked into PBs by an additional factor. If Dhh1 RNA binding is important for delivering RNA to PBs, one prediction would be that RNA binding mutations could prevent the constitutive PB localization of the ATPase-deficient allele, $Dhh1^{DQAD}$ in glucose replete conditions. Indeed, *dhh1Δ* cells expressing a combined ATPase deficient-RNA-binding mutant, $Dhh1^{DQAD\ +3X\text{-}RNA}$-GFP, no longer formed constitutive PBs **(Fig 2.1 E-F)**. These results demonstrate that RNA binding is necessary for localization of Dhh1 to PBs, and suggest that RNA binding facilitates Dhh1 PB entry, while ATP hydrolysis is required for PB exit.

Fig 2.1

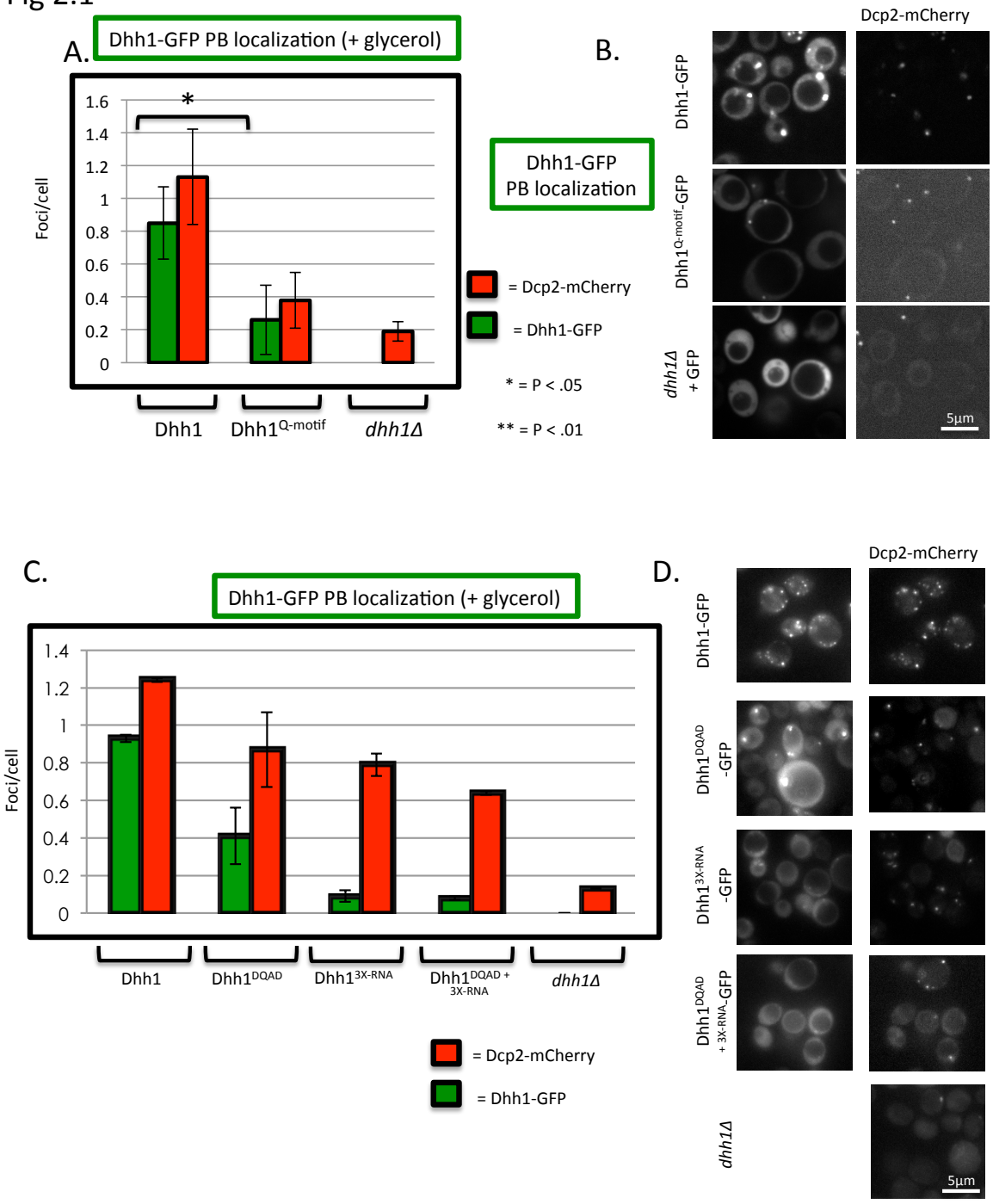
A.
Dhh1-GFP PB localization (+ glycerol)
Foci/cell
1.6
1.4
1.2
1
0.8
0.6
0.4
0.2
0
*
Dhh1
Dhh1Q-motif
dhh1Δ
Dhh1-GFP PB localization
= Dcp2-mCherry
= Dhh1-GFP
* = P < .05
** = P < .01
B.
Dcp2-mCherry
Dhh1-GFP
Dhh1Q-motif-GFP
dhh1Δ + GFP
5µm
C.
Dhh1-GFP PB localization (+ glycerol)
Foci/cell
1.4
1.2
1
0.8
0.6
0.4
0.2
0
Dhh1
Dhh1DQAD
Dhh13X-RNA
Dhh1DQAD + 3X-RNA
dhh1Δ
= Dcp2-mCherry
= Dhh1-GFP
D.
Dcp2-mCherry
Dhh1-GFP
Dhh1DQAD -GFP
Dhh13X-RNA -GFP
Dhh1DQAD + 3X-RNA-GFP
dhh1Δ
5µm

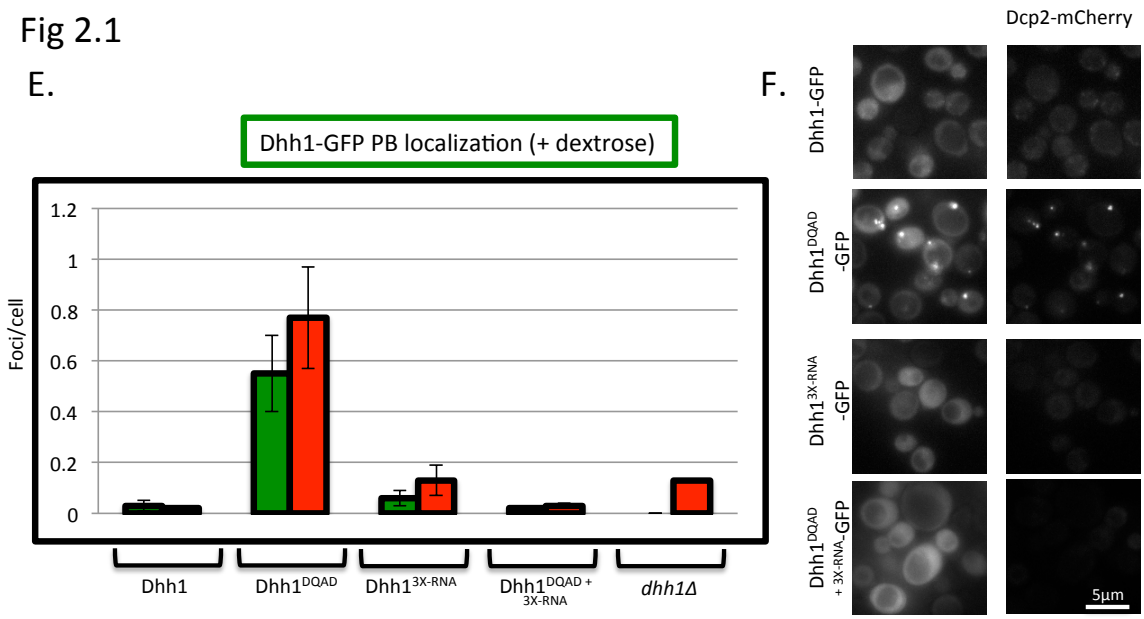

Figure 2.1: Loss of ATP binding and RNA binding disrupt Dhh1 localization to PBs

(A) Dhh1-GFP, Dhh1^{Qmotif}-GFP, or GFP were coexpressed with Dcp2-mCherry in *dhh1Δ* cells. After growth to mid-log phase, cells were shifted from glucose to glycerol as described previously (Passos and Parker 2008). Dhh1 localization and PB formation were quantified, using Dcp2-mCherry as a PB marker. (B) Dhh1-GFP, Dhh1$^{Q\text{-}motif}$-GFP, and GFP localization following a shift from glucose to glycerol. (C) Dhh1 PB localization and formation were quantified as in (A) in *dhh1Δ* cells expressing Dhh1-GFP, Dhh1^{DQAD}-GFP, Dhh1$^{3X\text{-}RNA}$-GFP, or Dhh1$^{DQAD + 3X\text{-}RNA}$-GFP. (D) Dhh1-GFP, Dhh1^{DQAD}-GFP, Dhh1$^{3X\text{-}RNA}$-GFP, or Dhh1$^{DQAD + 3X\text{-}RNA}$-GFP localization following a shift from glucose to glycerol. (E) Quantification of Dhh1-GFP, Dhh1^{DQAD}-GFP, Dhh1$^{3X\text{-}RNA}$-GFP, Dhh1$^{DQAD + 3X\text{-}RNA}$-GFP or *dhh1Δ* localization grown continuously in glucose. (F) Dhh1-GFP, Dhh1^{DQAD}-GFP, Dhh1$^{3X\text{-}RNA}$-GFP, or Dhh1$^{DQAD + 3X\text{-}RNA}$-GFP localization in cells continuously grown in glucose.

Loss of Dhh1 ATP binding and RNA binding has differential affects on mRNA decay and translation repression

In addition to examining effects of ATP and RNA binding on Dhh1 localization, we also sought to characterize whether these activities were required for Dhh1 functions in mRNA decay and translation repression. Previously, our lab engineered a stem loop aptamer (PP7L) into the 3'UTR of the *FBA1* gene that is recognized with high affinity by the bacteriophage PP7 coat protein (PP7-CP) (Hogg and Collins, 2007; Lim and Peabody, 2002). In addition, our previous study showed that recruitment of Dhh1 to the mRNA using this PP7 system is sufficient to stimulate mRNA decay and translation repression of a tethered mRNA reporter,

FBA1-PP7L (Carroll et al., 2011). In this study, we expressed a Dhh1$^{Q\text{-motif}}$-PP7CP fusion protein in *DHH1*, *dhh1Δ*, and *dcp1Δdhh1Δ* yeast and examined *FBA1* mRNA and protein levels compared with wild-type Dhh1-PP7CP or a GFP-PP7CP tether, which does not affect *FBA1* mRNA or protein levels when tethered (Carroll et al., 2011). As expected, tethering wild-type Dhh1 to *FBA1* in the presence or absence of endogenous Dhh1 caused a decrease in steady state *FBA1* mRNA and protein levels compared with a GFP tether **(Fig 2.2A-F)**. Tethering Dhh1$^{Q\text{-motif}}$-PP7CP led to a similar decrease in *FBA1* mRNA and protein levels, demonstrating the Dhh1$^{Q\text{-motif}}$ can stimulate decay of a tethered mRNA **(Fig 2.2 A-F)**. Yeast strains deficient in decapping provide a unique tool for uncoupling Dhh1 function in decay and translation repression. In *dcp1Δ* cells, Dhh1 is unable to lower *FBA1-PP7L* mRNA levels (Carroll et al., 2011), but is still able to lower Fba1 protein levels. We expressed Dhh1$^{Q\text{-motif}}$ –PP7CP in *dcp1Δdhh1Δ* yeast and saw that tethering of the Dhh$^{Q\text{-motif}}$-PP7CP to *FBA1*, like wild-type Dhh1-PP7CP, still lowered Fba1 protein levels under conditions where *FBA1* mRNA levels were stabilized due to loss of decapping activity **(Fig 2.2 G-I)**. This suggests robust ATP binding is not required for Dhh1 to stimulate mRNA decay and translation repression after association with the RNA.

To assess the role of Dhh1 RNA binding on mRNA decay and translation repression, we expressed single, double, and triple point mutants of RNA binding, Dhh1$^{1X\text{-}RNA}$, Dhh1$^{2X\text{-}RNA}$, and Dhh1$^{3X\text{-}RNA}$ as PP7CP fusion proteins in *dhh1Δ* cells, and observed their effect on *FBA1* mRNA and proteins levels compared with a GFP-PP7CP tether or in the absence of tether **(Fig 2.2 J-L)**. While tethering Dhh1$^{1X\text{-}RNA}$-PP7CP lowered *FBA1-PP7L* mRNA and Fba1 protein levels similar to wild-type Dhh1-PP7CP, Dhh1$^{2X\text{-}RNA}$-PP7CP, and Dhh1$^{3X\text{-}RNA}$-PP7CP showed increasingly higher *FBA1* mRNA and protein levels. These results suggest that tethering Dhh1 to mRNA is not sufficient to stimulate mRNA decay and translation repression, and that robust RNA binding is required to inactivate the mRNA. This is especially surprising given the expectation that mutations that affect RNA binding may be overcome by the increase in local concentration of Dhh1 at the RNA through tethering. One possible explanation for the loss of function by Dhh1$^{3X\text{-}RNA}$-PP7CP is that these mutations cause a severe misfolding of Dhh1, leading to the expression of a nonfunctional protein. However, cells expressing Dhh1$^{3X\text{-}RNA}$-GFP show only a partial defect in PB formation **(Fig 2.1 C-D)**. In addition, Western blot of Dhh1$^{3X\text{-}RNA}$ compared with wild-type Dhh1 showed that the two proteins are expressed to similar levels (data not shown). Moreover, affinity purification of Dhh1$^{3X\text{-}RNA}$-GFP followed by multidimensional protein identification technology mass spectrometry (MudPIT) revealed that it still interacts with all the major mRNA decay machinery, including Dcp1, Dcp2, Edc3, Lsm1-7, Pat1, Xrn1, Ccr4 and Not1 **(Appendix I, Fig. 4.3 A)**, suggesting Dhh1$^{3X\text{-}RNA}$ is still properly folded.

DDX6, the mammalian ortholog of Dhh1 can multimerize on RNA *in vitro* and is present in roughly 10-fold molecular excess over mRNA (Ernoult-Lange et al., 2012). Moreover, Dhh1 is also in large excess over mRNA in yeast (Gygi et al., 1999). Therefore, one possibility is that multiple copies of Dhh1 need to bind the mRNA in order to stimulate decay or translation repression. To test if wild-type Dhh1 could rescue Dhh1$^{3X\text{-}RNA}$-PP7CP functions in mRNA decay and translation repression, we

expressed Dhh1$^{1X\text{-}RNA}$-PP7CP, Dhh1$^{2X\text{-}RNA}$-PP7CP, and Dhh1$^{3X\text{-}RNA}$-PP7CP in *DHH1* cells and observed their effect on *FBA1* mRNA and proteins levels compared with a GFP-PP7CP tether or in the absence of tether. The presence of wild-type Dhh1 was unable to lower mRNA and protein levels of Dhh1$^{3X\text{-}RNA}$-PP7CP-tethered *FBA1* **(Fig 2.2 M-O)**. Thus, while loss of ATP binding did not strongly affect mRNA decay and translation repression of Dhh1-associated mRNA, RNA binding by Dhh1 is a critical event to initiate repression and decay of an mRNA.

Fig 2.2

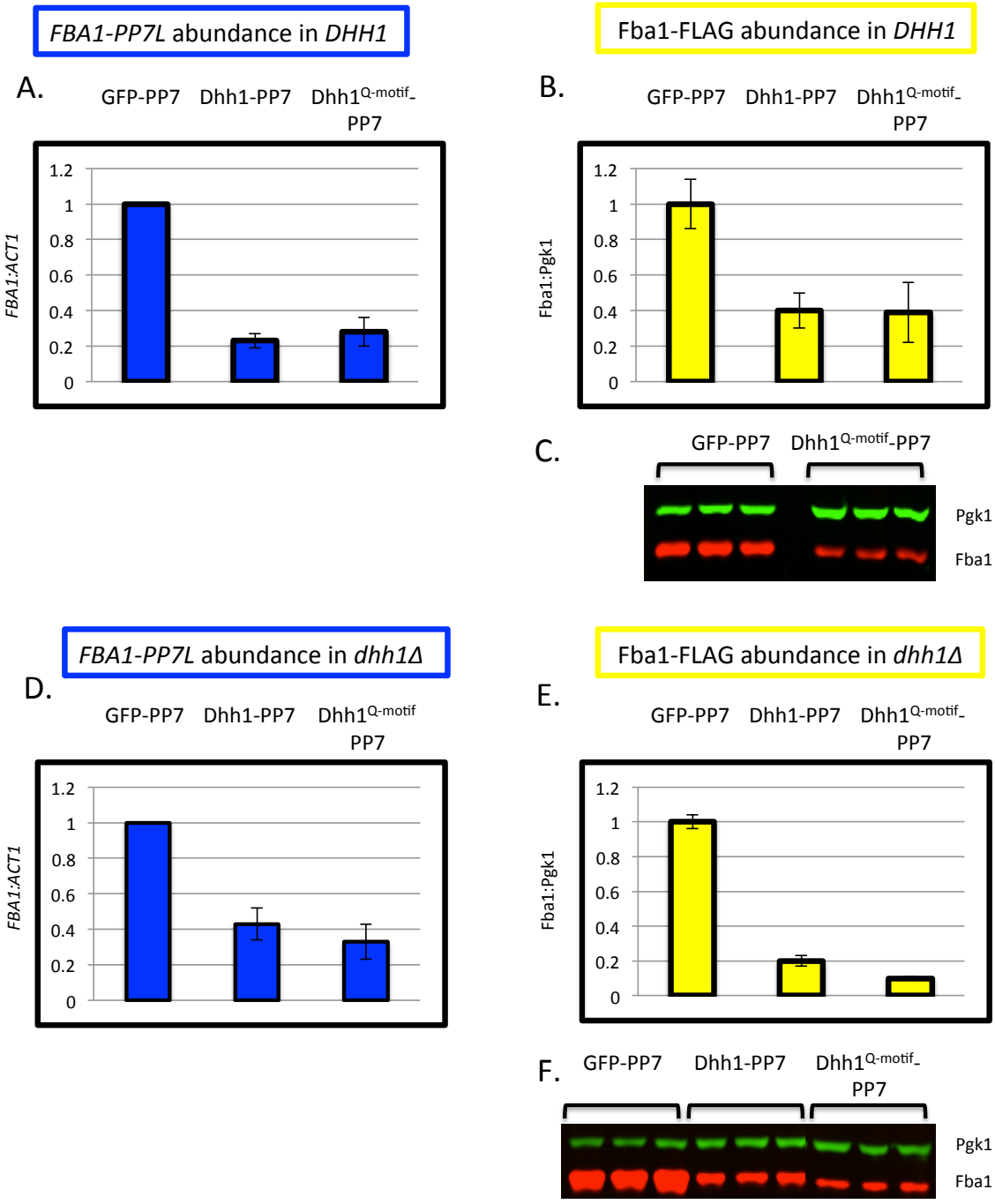
FBA1-PP7L abundance in *DHH1*
A.
GFP-PP7
Dhh1-PP7
Dhh1Q-motif-PP7
FBA1:ACT1
1.2
1
0.8
0.6
0.4
0.2
0
Fba1-FLAG abundance in *DHH1*
B.
GFP-PP7
Dhh1-PP7
Dhh1Q-motif-PP7
Fba1:Pgk1
1.2
1
0.8
0.6
0.4
0.2
0
C.
GFP-PP7
Dhh1Q-motif-PP7
Pgk1
Fba1
FBA1-PP7L abundance in *dhh1Δ*
D.
GFP-PP7
Dhh1-PP7
Dhh1Q-motif PP7
FBA1:ACT1
1.2
1
0.8
0.6
0.4
0.2
0
Fba1-FLAG abundance in *dhh1Δ*
E.
GFP-PP7
Dhh1-PP7
Dhh1Q-motif-PP7
Fba1:Pgk1
1.2
1
0.8
0.6
0.4
0.2
0
F.
GFP-PP7
Dhh1-PP7
Dhh1Q-motif-PP7
Pgk1
Fba1

Fig 2.2

FBA1-PP7L abundance in *dcp1Δdhh1Δ*

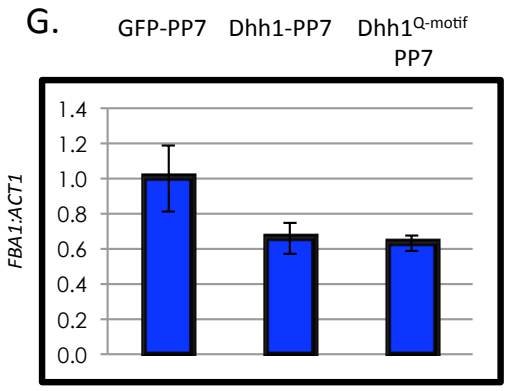

Fba1-FLAG abundance in *dcp1Δdhh1Δ*

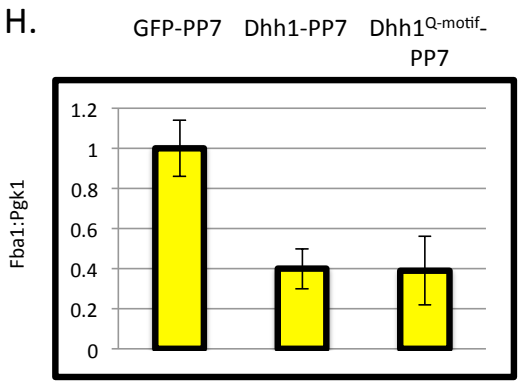

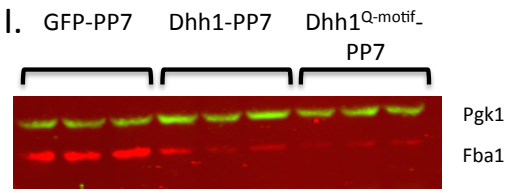

Fig 2.2

J.

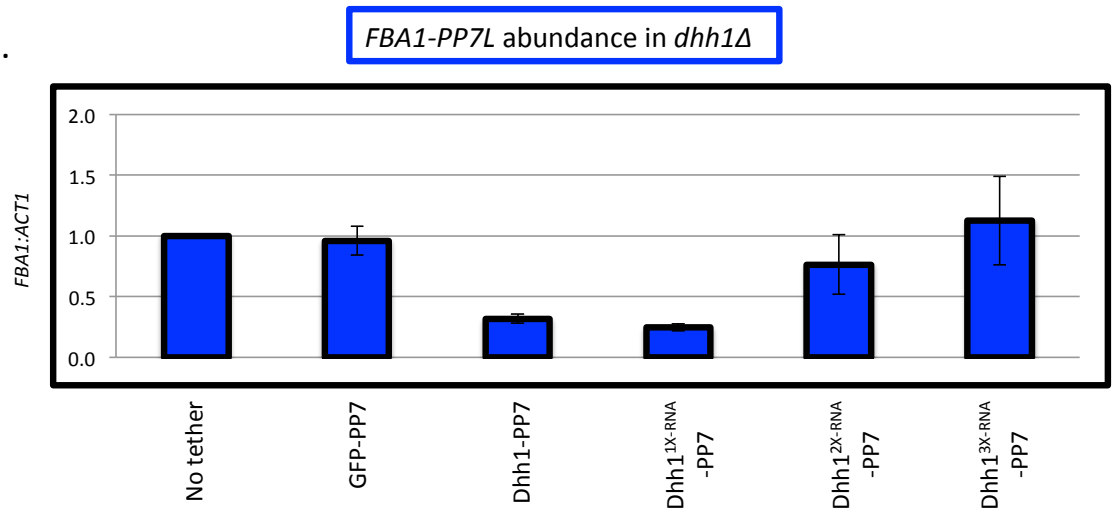
FBA1-PP7L abundance in dhh1Δ
FBA1:ACT1
2.0
1.5
1.0
0.5
0.0
No tether
GFP-PP7
Dhh1-PP7
Dhh1 1X-RNA -PP7
Dhh1 2X-RNA -PP7
Dhh1 3X-RNA -PP7

K.

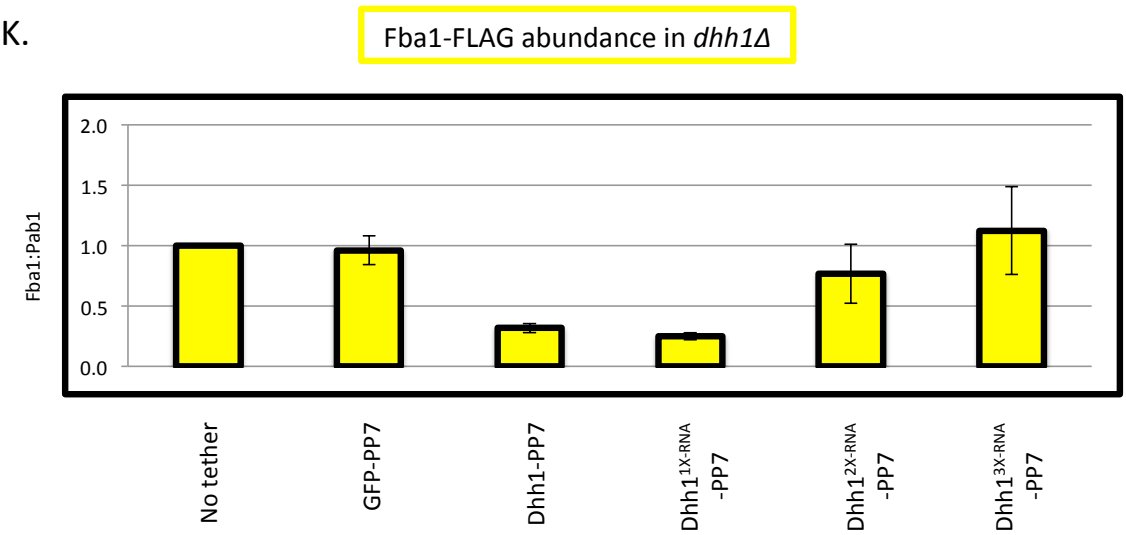
Fba1-FLAG abundance in dhh1Δ
Fba1:Pab1
2.0
1.5
1.0
0.5
0.0
No tether
GFP-PP7
Dhh1-PP7
Dhh1 1X-RNA -PP7
Dhh1 2X-RNA -PP7
Dhh1 3X-RNA -PP7

L.

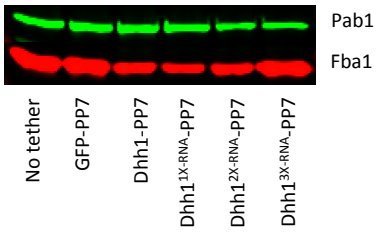
Pab1
Fba1
No tether
GFP-PP7
Dhh1-PP7
Dhh1 1X-RNA -PP7
Dhh1 2X-RNA -PP7
Dhh1 3X-RNA -PP7

Fig 2.2

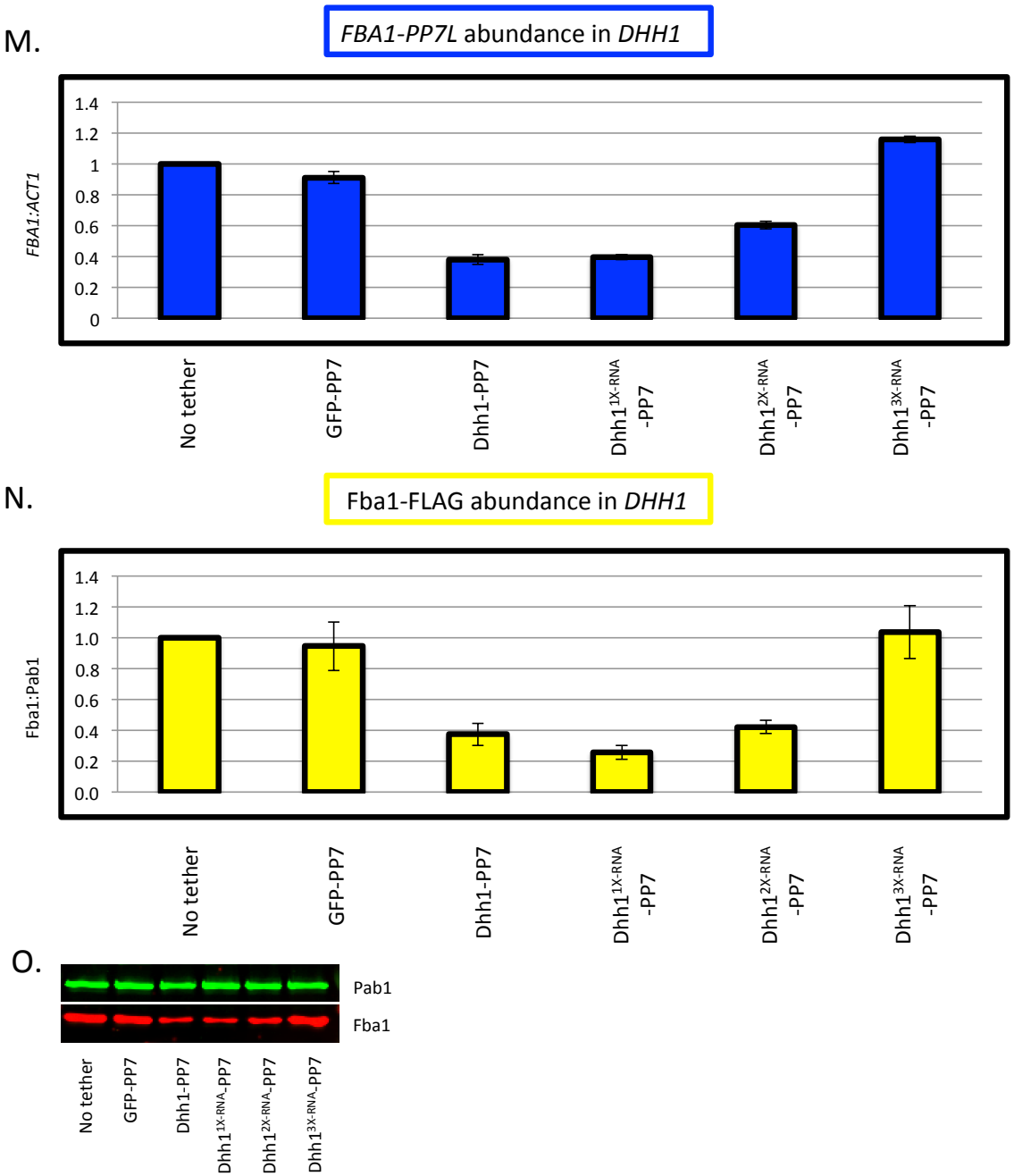

Figure 2.2: RNA binding activity, but not ATP binding activity, is required for decay translation repression of Dhh1-bound mRNA
(A,D,G,J,M) *FBA1-PP7L* abundance was measured by RT-qPCR in DHH1, *dhh1Δ*, or *dcp1Δdhh1Δ* cells expressing GFP-PP7CP, Dhh1-PP7CP, or Dhh1$^{Q\text{-motif}}$-PP7CP fusion proteins (A,D,G – for ATP binding effects) or GFP-PP7CP, Dhh1-PP7CP, Dhh1$^{1X\text{-RNA}}$-PP7CP, Dhh1$^{2X\text{-RNA}}$-PP7, or Dhh1$^{3X\text{-RNA}}$-PP7 (J,M – for RNA binding effects). *FBA1-PP7L* levels were normalized to the *ACT1* gene. (B,E,H,K,N) Western blot

quantification of Fba1-FLAG abundance. Relative Fba1 amounts were normalized to a loading control, either Pgk1 or Pab1. (C,F,I,L,O) Western blot image of biological triplicate samples of Fba1 protein and Pgk1 or Pab1 protein. Mean values ± standard deviation were determined from at least three independent experiments.

Dhh1$^{Q\text{-}motif}$ is unable to robustly bind to proteins in the Ccr4-NOT complex:

Dhh1 ATP binding and RNA binding mutants show differential effects on Dhh1 localization and function in mRNA decay and translation repression. One possible explanation for differences in function between these mutants could be that they are unable to associate with proteins that are required for normal Dhh1 function. To investigate this, we expressed C-terminal Tandem Affinity Purification (TAP)-tagged Dhh1, Dhh1$^{Q\text{-}motif}$, and Dhh1$^{3X\text{-}RNA}$ in *dhh1Δ* cells and isolated wild-type and mutant Dhh1 complexes by affinity purification (Oeffinger et al., 2007). Interestingly, Dhh1$^{3X\text{-}RNA}$-TAP did not show appreciable changes in complex composition compared to Dhh1-TAP, as assessed by multidimensional protein identification technology (MudPIT) mass spectrometry (data not shown). However, Dhh1$^{Q\text{-}motif}$-TAP revealed a dramatic loss of interaction with proteins that are members of the Ccr4-NOT complex **(Table 2.2 A-B)**. In particular, Not1, the central scaffold of the Ccr4-NOT complex, and Ccr4, the catalytic deadenylase subunit, which showed higher sequence coverage and a greater number of peptide spectra than other Ccr4-NOT members in wild-type purifications **(Table 2.2 C)**, were dramatically decreased in Dhh1$^{Q\text{-}motif}$-TAP samples.

In order to validate our large-scale mass spectrometry data, we C-terminally tagged Not1 and Ccr4 with 3HA and GFP respectively, and assessed interaction with Dhh1-TAP and Dhh1$^{Q\text{-}motif}$-TAP by co-immunoprecipitation (Co-IP). Indeed, Not1-3HA showed a roughly 75% reduction in binding to Dhh1$^{Q\text{-}motif}$-TAP compared with Dhh1-TAP **(Fig 2.3 A-B)**. Ccr4-GFP showed a similar decrease in interaction **(Fig 2.3 C-D)**. Thus, Dhh1 ATP binding is required for robust interaction with the Ccr4-NOT complex.

Table 2.2

A. Dhh1-TAP

CCR4-NOT subunits	Unique Peptides	Identical Peptides
DHH1	57	439
CCR4	27	86
POP2	3	4
NOT1	62	176
CDC36	7	19
MOT2	15	25
CAF130	5	11
NOT3	19	51
CAF40	11	26
NOT5	22	51

B. Dhh1$^{Q\text{-}motif}$-TAP

CCR4-NOT subunits	Unique Peptides	Identical Peptides
DHH1$^{Q\text{-}motif}$	39	456
CCR4	4	7
POP2	-	-
NOT1	18	34
CDC36	-	-
MOT2	6	10
CAF130	2	3
NOT3	4	8
CAF40	-	-
NOT5	4	12

C.

Protein	Dhh1-TAP	Dhh1$^{Q\text{-}motif}$-TAP
Ccr4	38.7%	5.5%
Not1	28.1%	11.9%

Table 2.2: Mass spectrometry of affinity purified Dhh1-TAP and Dhh1$^{Q\text{-}motif}$-TAP mRNP complexes

(A-B) Dhh1-TAP and Dhh1$^{Q\text{-}motif}$-TAP mRNPs were purified from *dhh1Δ* yeast and interacting proteins were identified by multidimensional protein identification technology MudPIT mass spectrometry. Bait protein is highlighted in blue, with resulting Ccr4-NOT associated proteins listed below. Unique peptide fragments as well as total number of peptides are reported. (C) Total sequence coverage of Ccr4 and Not1 peptides in Dhh1-TAP and Dhh1$^{Q\text{-}motif}$-TAP pulldowns. MS data is presented from 1 of 3 biological replicates.

Fig 2.3

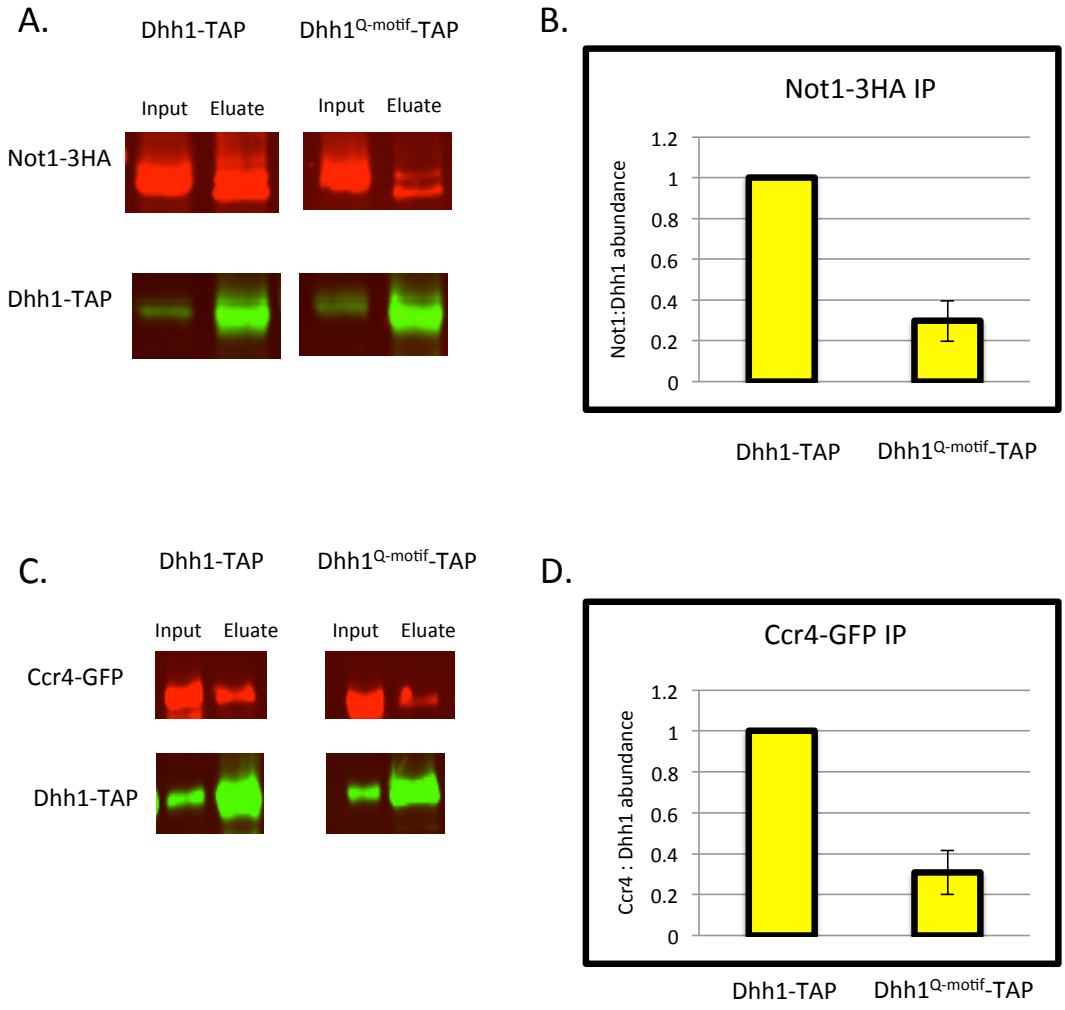

Figure 2.3: An ATP-binding mutant of Dhh1 shows defects in Ccr4-NOT complex interaction *in vivo*
Dhh1-TAP and Dhh1$^{Q\text{-motif}}$-TAP were expressed in *dhh1Δ* yeast and affinity purified by IgG-coupled magnetic beads and co-precipitating proteins were assessed by Western blot. (A, C) Western Blot of Not1-3HA and Ccr4-GFP proteins co-precipitating with Dhh1-TAP or Dhh1$^{Q\text{-motif}}$-TAP. (B, D) Western blot quantification of Not1-3HA or Ccr4-GFP abundance. Not1 and Ccr4 signals were normalized to Dhh1 signal. Bar graphs represent averages with standard error of the mean from three independent experiments.

Ccr4-NOT complex recruitment to PBs relies on an ATP-bound conformation of Dhh1

Next, we wanted to test whether the cellular localization of the Ccr4-NOT complex was disrupted in Dhh1$^{Q\text{-motif}}$ expressing cells. Ccr4 and Not1 have

previously been shown to localize to PBs, which form upon glucose removal in *S. cerevisiae* (Cougot et al., 2004; Sheth and Parker, 2003). We monitored the localization of Ccr4-GFP and Not1-GFP in *dhh1Δ* cells expressing either Dhh1 or Dhh1$^{Q\text{-}motif}$. Following glucose starvation, Not1-GFP and Ccr4-GFP localized to PBs **(Fig 2.4 B, D)**. However, PB localization of Not1-GFP and Ccr4-GFP was not as robust as Dhh1-GFP, with 1 in every 3 cells containing a Not1-GFP or Ccr4-GFP focus, compared to 1 Dhh1-GFP focus in every cell **(**compare **Fig 2.4 A, C** and **Fig 2.1 A, C)**. This is consistent with previous reports that Ccr4-NOT proteins localize to PB less efficiently than other mRNA decay factors (Teixeira and Parker, 2007). Not1-GFP and Ccr4-GFP PB localization were further reduced in cells expressing Dhh1$^{Q\text{-}motif}$ compared with wild-type Dhh1 **(Fig 2.4 B, D)**. However, although the total number of PBs was lower in Dhh1$^{Q\text{-}motif}$-expressing cells, the overall ratios of Not1 and Ccr4 in PBs appeared to be similar to wild-type. Thus, while a functional Dhh1 Q-motif is required for efficient PB localization of Not1 and Ccr4, we cannot exclude that Dhh1 ATP binding may indirectly affect Ccr4-NOT localization by disrupting general PB formation.

Fig 2.4

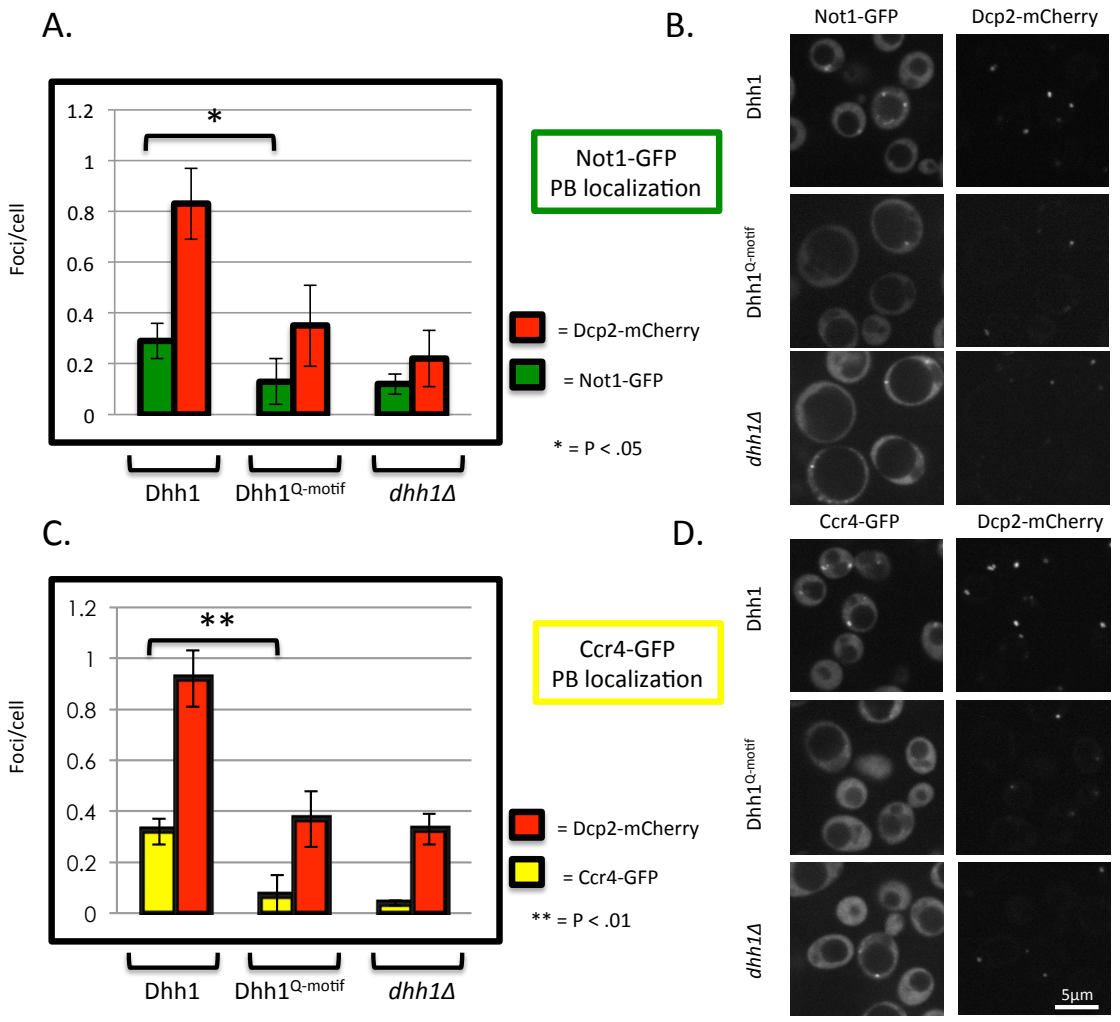

Figure 2.4: Ccr4-NOT recruitment to PBs relies on an ATP-bound conformation of Dhh1

(A) Not1-GFP was coexpressed with Dcp2-mCherry in Dhh1, Dhh1$^{Q\text{-motif}}$, or *dhh1Δ* cells. After growth to mid-log, cells were shifted from glucose to glycerol as described previously (Passos and Parker 2008). Dhh1 PB localization and formation were quantified, using Dcp2-mCherry as a PB marker. (B) Not1-GFP and Dcp2-mCherry localization following shift from glucose to glycerol. (C) Ccr4-GFP PB localization and formation were quantified as in (A) in yeast expressing Dhh1, Dhh1$^{Q\text{-motif}}$, or *dhh1Δ*. (D) Ccr4-GFP and Dcp2-mCherry localization following shift from glucose to glycerol.

Mutants in Dhh1 that disrupt binding to Not1 form constitutive PBs, similar to an ATPase-deficient Dhh1 mutant.

Recently, the mammalian orthologs of Dhh1 and Not1, DDX6 and CNOT1, were shown to directly bind one another *in vitro* (Chen et al., 2014; Mathys et al., 2014; Rouya et al., 2014). In addition, the crystal structures of CNOT1 and Not1 contain an alpha helical middle domain of initiation factor 4G (MIF4G)-like motif, similar to eIF4G and Gle1, two known activators of the DEAD box proteins eIF4A and Dbp5 respectively (Basquin et al., 2012; Montpetit et al., 2011; Schütz et al., 2008). Primary sequence alignments of Dhh1 and Not1 orthologs showed that the residues predicted to mediate binding of these two factors are highly conserved (Rouya et al., 2014; data not shown). Furthermore, CNOT1 was able to stimulate ATP hydrolysis of DDX6 *in vitro* (Mathys et al., 2014).

Given that Dhh1 ATPase activity appears to be critical for proper Dhh1 localization to, and recycling from PBs, we generated a panel of mutants predicted to disrupt Dhh1 interaction with Not1 at one of three conserved surfaces (referred to as Patch 1, 2, and 3, see **Fig 1.9** and Mathys et al. 2014) **(Table 2.3)**. Patch1 mutants were generated by mutating arginine (R) and phenylalanine (F) residues in the N-terminal RecA surface of Dhh1 to glutamic acid (R55E and/or F62E). Similarly, glutamic acid substitutions were also made at C-terminal RecA residues at the Patch 2 surface (Q282E and N284E) and Patch 3 surface (R335E). Localization of GFP fusions of these Dhh1 mutant proteins was monitored in vegetatively growing *dhh1Δ* cells, and compared to previously characterized Dhh1 mutants, Dhh1$^{Q\text{-}motif}$, Dhh1^{DQAD}, and Dhh1^{INT} – a mutant of Dhh1 shown to have enhanced ATPase activity *in vitro* (Dutta et al., 2011). As expected, Dhh1-GFP, Dhh1$^{Q\text{-}motif}$-GFP, and Dhh1^{INT}-GFP showed a diffuse cytoplasmic localization in glucose replete conditions, while ATPase deficient Dhh1^{DQAD}-GFP robustly localized to PBs (**Fig 2.5 A**, data not shown). Individually, point mutations in Patch 1 and Patch 2 did not alter Dhh1 localization compared with wild-type protein **(Fig 2.5 B, F)**. However, a mutation in the Dhh1 C-terminus, R335E, on Patch 3, led to a significant increase in Dhh1 foci **(Fig 2.5 B, F)**. Furthermore, combining mutations from all three patches caused a dramatic increase in Dhh1 foci per cell, similar to the ATPase-deficient allele, Dhh1^{DQAD}-GFP **(Fig 2.5 C, D, F)**. These foci colocalize with Dcp2-mCherry **(Fig 2.5 E)**, demonstrating that these foci are *bona fide* PBs.

In order to determine if Dhh1-Not1 binding mutants could stimulate mRNA decay, we expressed a PP7CP fusion protein of the most severe mutant, Dhh1$^{5X\text{-}Not1}$ **(Table 2.3)** - a Dhh1 mutant that possesses five amino acid substitutions across all three conserved patches that disrupt Not1 binding - in *dhh1Δ* cells with the *FBA1-PP7L*. Indeed, Dhh1$^{5X\text{-}Not1}$-PP7CP lowered *FBA1-PP7L* mRNA and protein levels to a similar degree as Dhh1-PP7CP, when compared to GFP-PP7CP, suggesting that interaction between Dhh1 and Not1 is dispensable for mRNA decay **(Fig 2.6 A-B)**. Furthermore, mutations in the three patches did not dramatically alter Dhh1 expression levels **(Fig 2.7)**. Thus, loss of interaction with Not1 causes mislocalization of Dhh1 and a constitutive formation of PBs in the absence of stress, phenocopying the ATPase deficient Dhh1^{DQAD} mutant, which also forms constitutive

PBs and cannot actively shuttle in and out of PBs (Carroll et al., 2011). These observations strongly suggest that Not1 plays a key role in stimulating Dhh1's ATPase cycle *in vivo*, and that proper binding to Not1 is critical for Dhh1 recycling from PB foci.

Table 2.3

Dhh1 mutations in Not1 binding surface

Patch	Mutation(s)	Name
Patch 1	R55E	
	F62E	
	R55E, F62E	
Patch 2	Q282E, N284E	
Patch 3	R335E	
Patch 1 + 2	R55E, Q282E, N284E	
	F62E, Q282E, N284E	
Patch 1 + 3	R55E, R335E	
	F62E, R335E	
	R55E, F62E, R335 E	
Patch 2 + 3	Q282E, N284E, R335E	$Dhh1^{3X\text{-}Not1}$
Patch 1 + 2 + 3	R55E, Q282E, N284E, R335E	
	F62E, Q282E, N284E, R335E	
	R55E, F62E, Q282E, N284E, R335E	$Dhh1^{5X\text{-}Not1}$

Table 2.3: Dhh1 mutants in Not1 binding surface generated in this study.
A panel of Dhh1-GFP point mutants were generated by site directed mutagenesis and expressed in *dhh1Δ* yeast to identify defects in Dhh1 localization. The residues that bridge the interaction between Dhh1 and Not1 are highly conserved across evolution, and are identical in DDX6, the mammalian ortholog of Dhh1 (data not shown, Mathys et al., 2014).

Fig 2.5

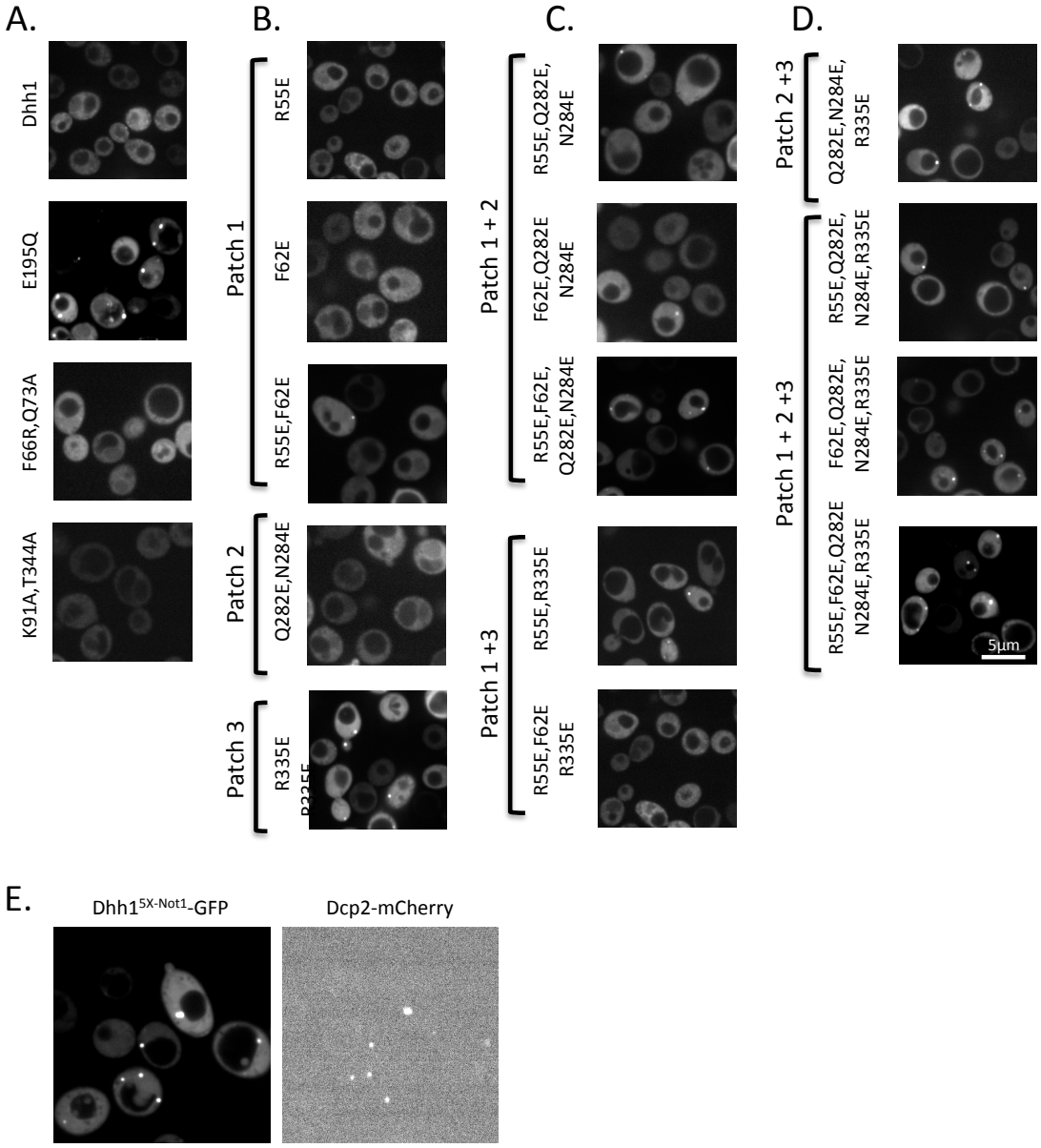
A.
Dhh1
E195Q
F66R,Q73A
K91A,T344A
B.
Patch 1
R55E
F62E
R55E,F62E
Patch 2
Q282E,N284E
Patch 3
R335E
C.
Patch 1 + 2
R55E,Q282E, N284E
F62E,Q282E N284E
R55E,F62E, Q282E,N284E
Patch 1 +3
R55E,R335E
R55E,F62E R335E
D.
Patch 2 +3
Q282E,N284E, R335E
Patch 1 + 2 +3
R55E,Q282E, N284E,R335E
F62E,Q282E, N284E,R335E
R55E,F62E,Q282E N284E,R335E
5µm
E.
Dhh1^5X-Not1-GFP
Dcp2-mCherry

Fig 2.5

F.

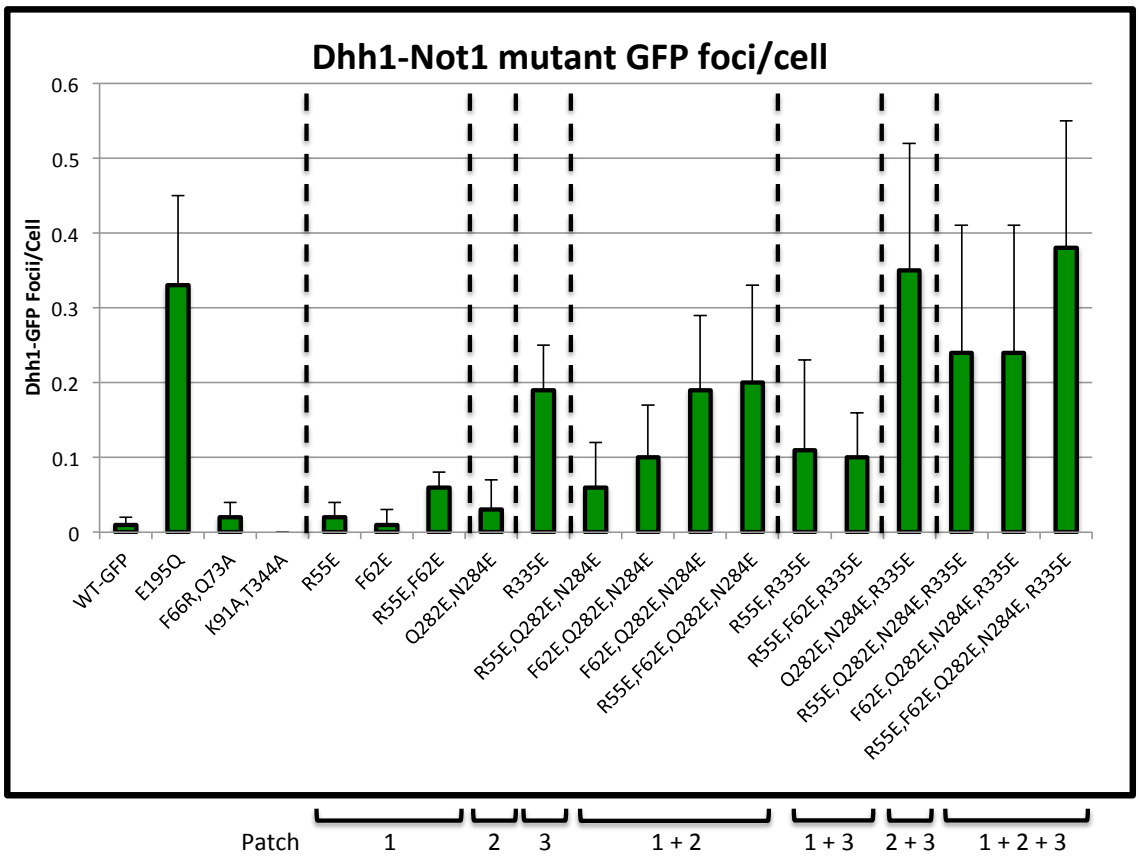

Figure 2.5: Mutants in Dhh1 predicted to affect binding to Not1 form constitutive PBs, similar to an ATPase-dead Dhh1 mutant.

Dhh1 mutants predicted to be deficient in Not1 binding were generated by site directed mutagenesis and expressed as GFP fusion proteins in *dhh1Δ* cells grown continuously in glucose. Dhh1-GFP foci were quantified as in Fig 2.1. (A) Dhh1-GFP, Dhh1^{DQAD}-GFP, Dhh1$^{Q\text{-}motif}$-GFP, and Dhh1^{INT}-GFP localization. (B) Localization of Dhh1-Not1 mutants in the N-terminal RecA Patch 1 surface, or the C-terminal RecA Patch 2 or Patch 3 surfaces. (C) Localization of Dhh1-Not1 mutants in Dhh1 Patch (1 + 2) or Patch (1 + 3). (D) Localization of Dhh1-Not1 mutants in Dhh1 Patch (2 + 3) or Patch (1 + 2 + 3). (E) Co-localization of Dhh1$^{5X\text{-}Not1}$-GFP and Dcp2-mCherry in cells grown in dextrose to mid-log phase. (F) Quantitation of wild-type and mutant Dhh1-GFP foci. The Dhh1-Not1 surface patches that were mutagenized are indicated below the graph.

Fig 2.6

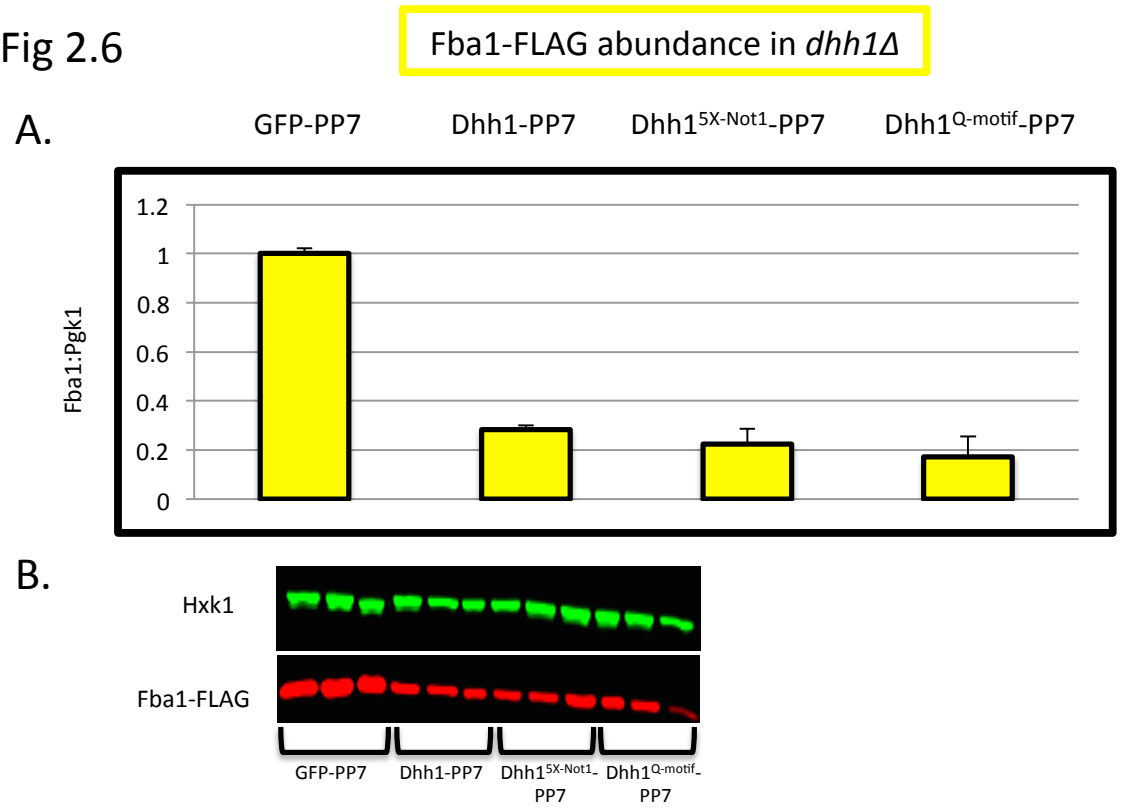

Fig 2.6: Dhh1$^{5X\text{-}Not1}$-PP7CP stimulates decay of tethered *FBA1-PP7L* mRNA
(A) Western blot quantification of Fba1-FLAG abundance in *dhh1Δ* cells expressing GFP-PP7CP, Dhh1-PP7CP, Dhh1$^{5X\text{-}Not1}$-PP7CP or Dhh1$^{Q\text{-}motif}$-PP7CP fusion proteins. Relative Fba1 amounts were normalized to Hxk1 as a loading control. (B) Western blot image of biological triplicate samples of Fba1 protein and Hxk1. Lanes were cropped in order to place the three replicates side-by-side. Mean values ± standard deviation were determined from at least three independent experiments.

Fig 2.7

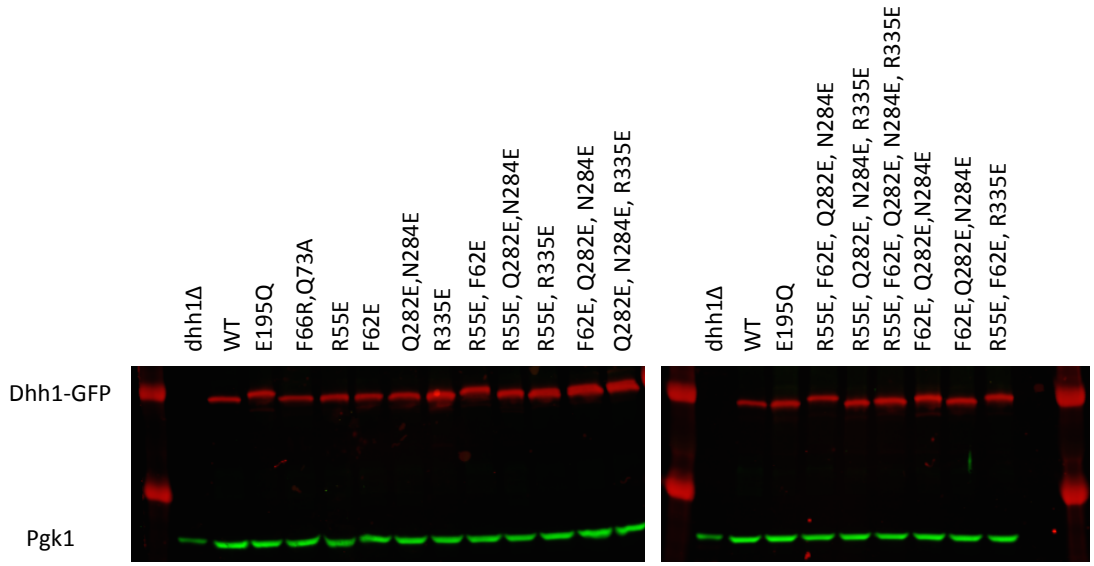

Fig 2.7: Mutations in Dhh1-Not1 binding surface do not affect expression of Dhh1
Dhh1 mutants predicted to be deficient in Not1 binding were generated by site directed mutagenesis and expressed as GFP fusion proteins in *dhh1Δ* cells grown to mid-log phase in glucose. Western blot of wild-type and mutant Dhh1-GFP proteins. Pgk1 was used as a loading control.

Dhh1$^{5X\text{-}Not1}$ displays altered PB dynamics

Previous work has shown that Dhh1 ATP hydrolysis is required for its dynamic localization to PBs (Carroll et al., 2011). To assess whether Not1 interaction was required for proper Dhh1 recycling from PBs, we expressed Dhh1, Dhh1^{DQAD}, and Dhh1$^{5X\text{-}Not1}$-GFP in *dhh1Δ* cells and measured their dynamics by fluorescence recovery after photobleaching (FRAP). As shown previously, Dhh1-GFP shuttles rapidly in and out of PBs, while ATPase-deficient Dhh1^{DQAD}-GFP recovery was severely diminished (**Fig 2.8 A, B**; Carroll et al. 2011). In cells expressing *DHH1*$^{5X\text{-}Not1}$-GFP, a majority of PBs (9 out of 12 traces) showed a significantly diminished recovery, similar to Dhh1^{DQAD}-GFP **(Fig 2.8 B vs. D)**. The median percent fluorescent recovery of Dhh1$^{5X\text{-}Not1}$-GFP was 0.39 ± 0.08, similar to Dhh1^{DQAD}-GFP (0.35 ± 0.09), while Dhh1-GFP recovery was measured at 0.71 ± 0.11 **(Fig 2.8 E)**. Interestingly, a small number of Dhh1$^{5X\text{-}Not1}$-GFP PBs (3 out of 12 traces) showed complete fluorescent recovery **(Fig 2.8 C)**. At present, the significance of this result remains unclear, however, the presence of some dynamic foci could be consistent with Dhh1$^{5X\text{-}Not1}$-GFP having only a partial loss in Not1 binding and/or residual ATPase activity. Taken together, these data suggest that Not1-stimualted ATP hydrolysis by Dhh1 regulates the dynamics of PB foci, and support a mechanism

where Not1 activates Dhh1 ATPase activity *in vivo* to facilitate recycling and release of Dhh1 out of PBs.

Fig 2.8

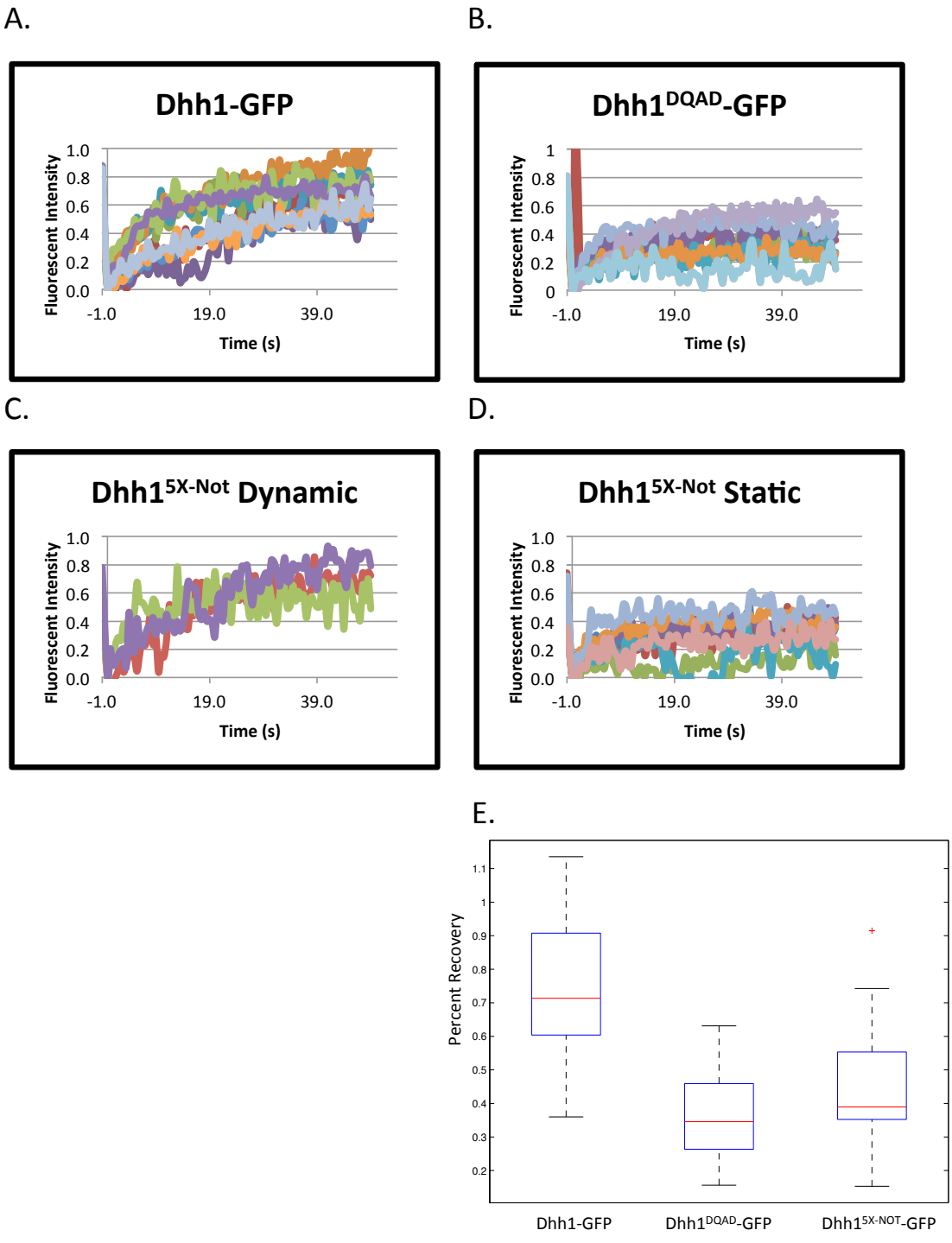

Figure 2.8: Mutants in Dhh1 predicted to affect binding to Not1 show a loss of dynamic PB localization
Dhh1-GFP, Dhh1^{DQAD}-GFP, and Dhh1$^{5X\text{-}Not1}$-GFP were expressed in *dhh1Δ* cells and grown to mid-log phase and shifted from glucose to glycerol as described in Fig 2.1. PBs were bleached with a 488nm laser and fluorescence intensity was measured for 50s. (A) Fluorescent recovery of Dhh1-GFP, (B) Dhh1^{DQAD}-GFP, and (C and D) Dhh1$^{5X\text{-}Not1}$-GFP. (C) Dynamic Dhh1$^{5X\text{-}Not1}$-GFP PB traces with recovery curves similar to Dhh1-GFP, and (D) static Dhh1$^{5X\text{-}Not1}$-GFP PB traces with recovery curves similar to Dhh1^{DQAD}-GFP. Graphs show recovery curves of at least 10 PBs from one representative experiment. Three independent experiments were performed with 10 or more PBs bleached per experiment (Dhh1$^{5X\text{-}Not1}$-GFP "dynamic" shows only 3 traces, Dhh1$^{5X\text{-}Not1}$-GFP "static" shows 9 traces). (E) PB traces were curve fitted using a MatLab program described in the methods, and percentage of fluorescent recovery for strains expressing Dhh1-GFP, Dhh1^{DQAD}-GFP, or Dhh1$^{5X\text{-}Not1}$-GFP is shown. Static and dynamic traces in the Dhh1$^{5X\text{-}Not1}$-GFP conditions are plotted in the same box plot. Boxes correspond to upper and lower quartiles, and whiskers correspond to maximum and minimum values, with outliers indicated as a (+).

Loss of Dhh1 ATP hydrolysis does not affect localization of other PB components

While Dhh1 dynamically localizes to PBs, the dynamics of other PB factors in yeast have not been reported. Moreover, it is unclear how Dhh1's ATPase cycle affects the recycling of other PB components in and out of PBs. For example, loss of Dhh1 ATP hydrolysis may lead to a loss in dynamic localization of other PB components. In order to test if Dhh1 ATPase activity affects recycling of known PB proteins, we expressed wild-type Dhh1 or Dhh1^{DQAD} in *dhh1Δ* cells, along with GFP fusion proteins of several mRNA decay factors, such as Pat1, Xrn1, Dcp1, Dcp2, and Edc3.

Surprisingly, loss of Dhh1 ATP hydrolysis did not appear to significantly alter the recycling of any PB protein measured **(Fig 2.9)**. Furthermore, the localization patterns of the factors measured were separated into two distinct classes: dynamic PB factors, like Xrn1 and Pat1 **(Fig 2.9 A-B)**, and resident PB factors, like Dcp1, Dcp2, and Edc3 **(Fig 2.9 C-D)**. For example, the dynamic PB factors, Xrn1-GFP and Pat1-GFP, both showed dynamic localization to PBs irrespective of Dhh1 ATPase activity **(Fig 2.9 A-B)**. While these proteins appeared to recover over longer time scales than did Dhh1, the patterns were unaltered by expression of Dhh1^{DQAD}. In contrast, Dcp1, Dcp2, and Edc3 did not dynamically localize to PB in the presence of Dhh1 or Dhh1^{DQAD} **(Fig 2.9 C-D)**, suggesting these factors are resident PB proteins that are needed for proper PB assembly. Consistent with this observation, Dcp2 and Edc3 are critical scaffolding proteins that are required for robust PB formation (Decker et al., 2007; Fromm et al., 2012; Teixeira and Parker, 2007). Similarly, Dcp1, Dcp2, and Edc3 from *Schizosaccharomyces pombe* were also recently shown to be sufficient to spontaneously self assemble PB-like structures *in vitro* (Fromm et al.,

2014). Overall, the dynamics of PB components are not significantly affected by loss of Dhh1 ATPase activity.

Fig 2.9

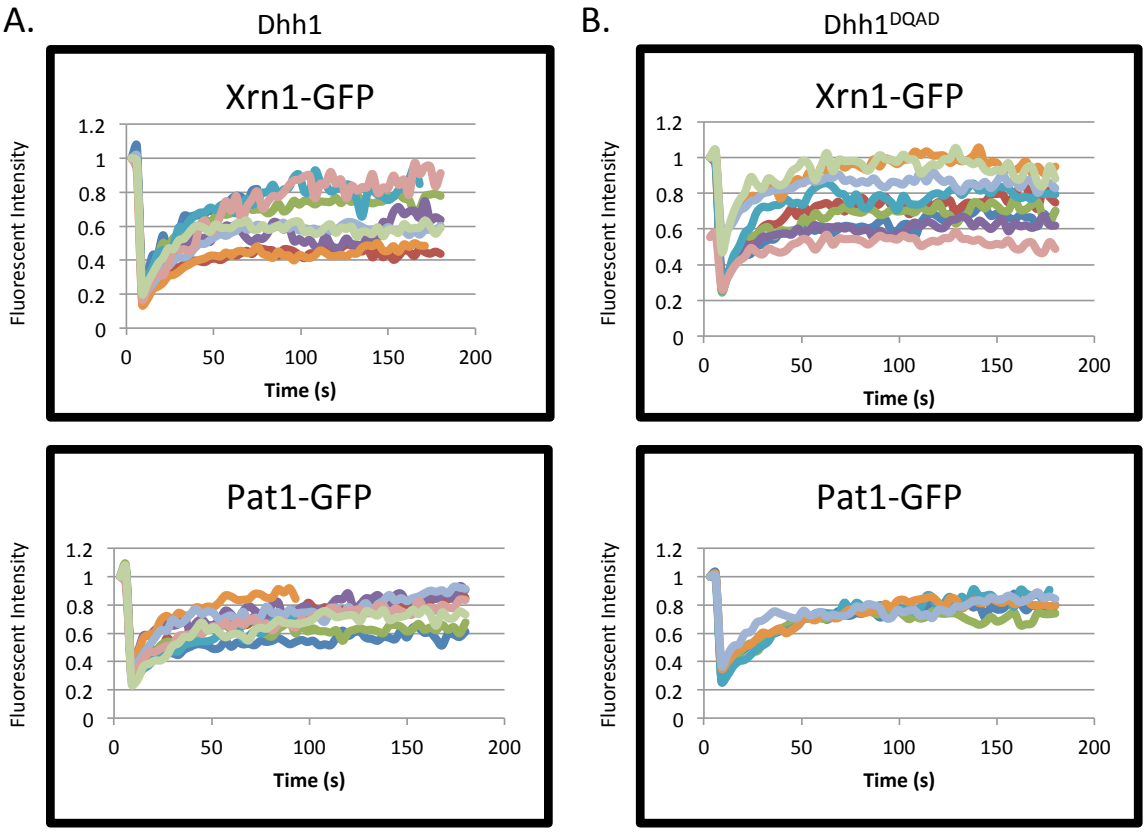

Fig 2.9

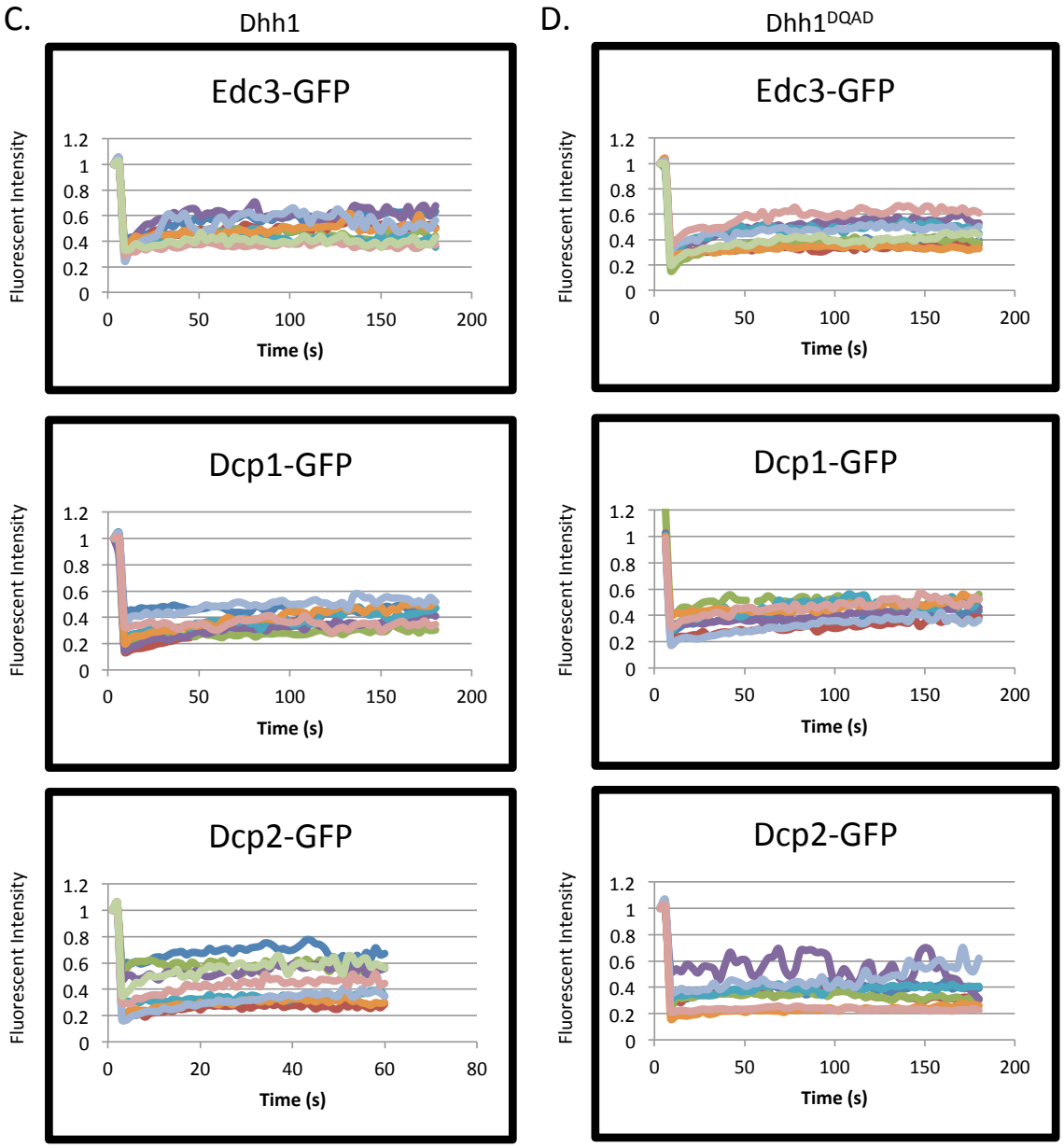

Figure 2.9: Loss of Dhh1 ATP hydrolysis does not affect localization of other PB components

Dhh1 or Dhh1^{DQAD} were expressed in *dhh1Δ* cells along with GFP-fusion proteins of known mRNA decay factors. Cells were grown to mid-log phase and shifted from glucose to glycerol as described in Fig 2.1. PBs were bleached with a 405nm laser and fluorescence intensity was measured for up to 3 min. (A-B) Fluorescent recovery of "dynamic" PB proteins in cells expressing (A) Dhh1 or (B) Dhh1^{DQAD}. (C-D) Fluorescent recovery of "resident" PB proteins in cells expressing (C) Dhh1 or (D) Dhh1^{DQAD}. Graphs show recovery curves of at least 8 PBs from one

representative experiment. Three independent experiments were performed with 8 or more PBs bleached per experiment.

Discussion

In this study, we show that Dhh1 ATP and RNA binding mutants have differential effects on Dhh1 localization, PB formation, mRNA decay, and translation repression **(Figs 2.1 and 2.2)**. Because we were unable to purify full-length Dhh1 in bacterial expression systems, however, we could not directly validate loss of RNA and ATP binding of Dhh1 mutants *in vitro*. Still, the Dhh1 mutants used in this study show localization defects similar to those seen for Dhh1 ATP and RNA binding mutants from previous studies (Dutta et al., 2011). ATP binding, as assessed with the Dhh1$^{Q\text{-motif}}$ mutant, is not required to stimulate mRNA decay or to repress translation of a bound mRNA. In contrast, RNA-binding is critical for mRNA decay and translation repression by Dhh1. In addition, while Dhh1 ATP and RNA binding activities are important for Dhh1 localization to PBs, expression of a Dhh1 RNA binding mutant has only a modest defect in PB formation. One possible explanation for this observation may be that the primary function of Dhh1 may not be to seed PB complex formation directly, but rather to transport mRNA to PBs. Consistent with this hypothesis, defects in Dhh1 ATP hydrolysis do not affect the PB dynamics of several mRNA decay factors **(Fig 2.9)**, suggesting that Dhh1 may primarily function by delivering RNA substrates to seed decay mRNP oligomerization, rather than scaffolding decay and translation repression factors directly. Interestingly, Dcp1, Dcp2, and Edc3 do not dynamically localize to PBs in all conditions tested. Thus, these factors are termed resident PB proteins that likely are required for higher order PB assembly.

Surprisingly, while Dhh1 RNA binding mutants still interact with the normal complement of mRNA decay factors, the ATP binding mutant Dhh1$^{Q\text{-motif}}$ no longer robustly binds to proteins of the Ccr4-NOT complex, in particular Not1 and Ccr4. Furthermore, we demonstrate that Dhh1 interaction with Not1 is crucial for dynamic localization of Dhh1 to PBs **(Fig 2.5, 2.8)**. Disruption of the interaction between the C-terminal RecA domain of Dhh1 and the Not1 MIF4G domain causes Dhh1 to localize to PBs in the absence of stress, similar to the ATPase-deficient allele, Dhh1^{DQAD}. Furthermore, a Dhh1 mutant protein that is unable to bind robustly to Not1 no longer dynamically shuttles in and out of PBs. Taken together, these observations suggest that Not1, through the concave surface of its MIF4G domain, is an activator of Dhh1 ATP hydrolysis *in vivo*, and regulates the residence of Dhh1 in PB foci. The notion of Not1 as an activator of Dhh1 ATP hydrolysis is consistent with the other DEAD-box-activator pairs that have been recently identified. For example, Gle1, a cytoplasmic nuclear pore complex protein, facilitates mRNA export by binding to the DEAD-box protein Dbp5 and stimulating it to release RNA (Montpetit et al., 2011). Similarly, eIF4G also stimulates ATP hydrolysis of eIF4A, docking with the N and C-terminal RecA domains in a similar manner to both Dbp5-Gle1 and Dhh1-Not1 (Chen et al., 2014; Mathys et al., 2014; Montpetit et al., 2011; Özeş et al., 2011; Rouya et al., 2014). Further examples of this type of regulation have yet to be

identified, largely because MIF4G-containing proteins do not possess a high primary sequence similarity. However, it is becoming apparent that the MIF4G domain is a common motif among proteins that regulate DEAD-box function.

There are two possible models to explain the relationship between Dhh1 and Not1 **(Fig 2.10)**. First, Not1 could activate an RNPase-like function of Dhh1. Following recruitment of Dhh1 to the mRNA, Not1 would activate the Dhh1 ATPase to remodel the mRNP so that other decay factors may be recruited to the mRNA. This model predicts that mutations affecting Dhh1-Not1 interaction would display slower decay kinetics of the transcriptome. Alternatively, Not1 could function as a negative regulator of Dhh1, stimulating its ATPase activity to prevent the formation of a "degradation complex" on an mRNA. In this model, mutants that affect Dhh1-Not1 interaction would be expected to show an enhanced rate of mRNA turnover. To differentiate between these models, it would be of great interest to measure the stability of individual tethered mRNAs or the transcriptome in cells expressing wild-type Dhh1 and Dhh1$^{5X\text{-}Not1}$ to determine whether mRNAs become more or less stable following a disruption of the Dhh1-Not1 interaction.

Furthermore, there is evidence that the Ccr4-NOT complex can also promote transcriptional elongation (Kruk et al., 2011), and thus may already be recruited to the mRNA during transcription. Therefore, one interesting possibility is that the Ccr4-NOT complex may function as a timer of mRNA half-life, marking an mRNA throughout its lifetime. Once deadenylation is complete, Dhh1 is no longer removed from the mRNA by Not1, which allows the formation of a mature decapping complex and either repression or degradation of the mRNA. Trapping intermediates in this mRNP maturation pathway and examining their composition will be critical to evaluating the validity of this model. Future work should also identify the precise step of the Dhh1 ATPase cycle that is controlled by Not1, as well as whether or not Not1 regulates Dhh1 function outside of PB foci.

Fig 2.10

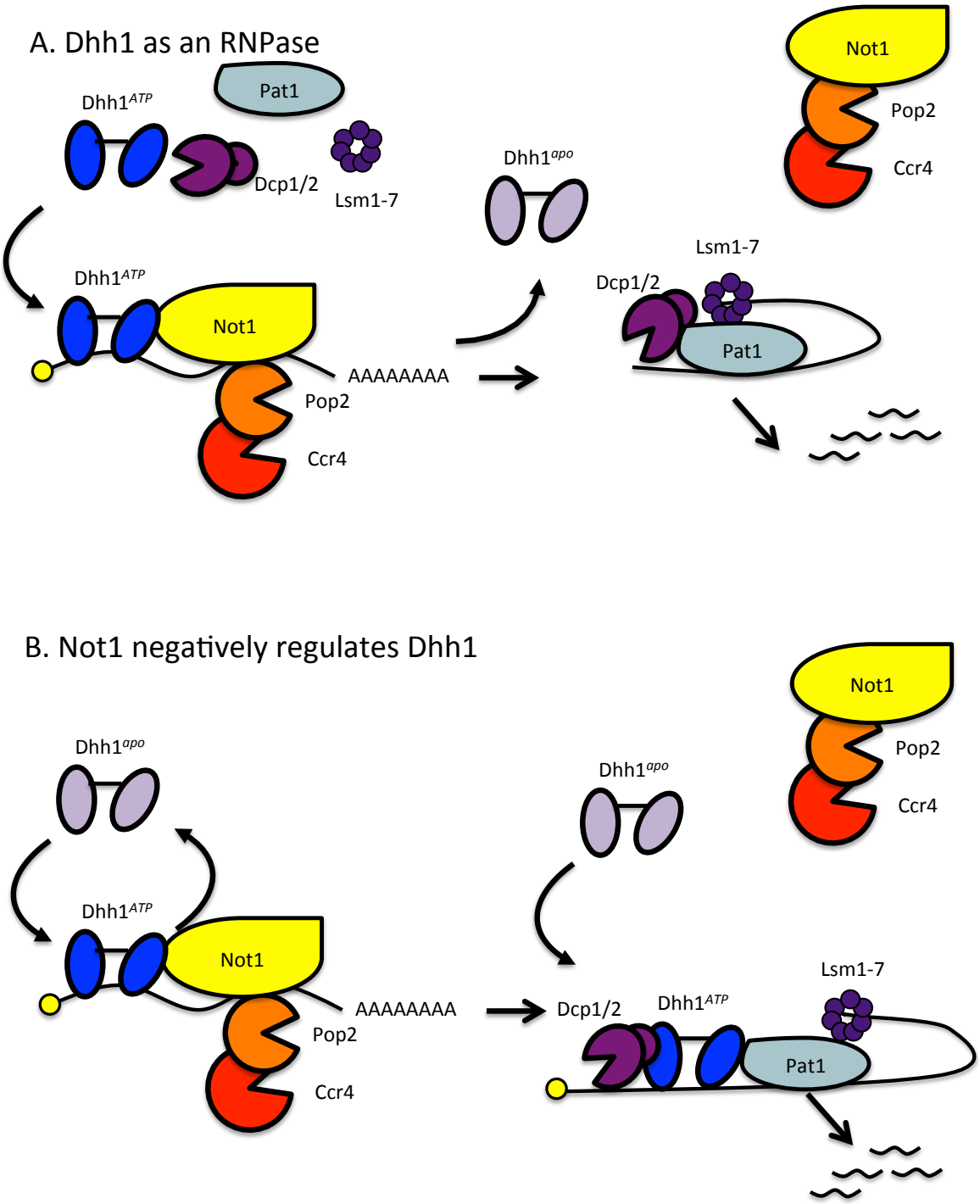

Fig 2.10: Models of Dhh1 interaction with Not1
Two hypothetical models of the interaction between Dhh1 and Not1: (A) Not1 activates Dhh1 ATPase activity, allowing Dhh1 to remodel the mRNP either by displacing translation factors or by stimulating the binding of decay factors to the mRNA. (B) Not1 negatively regulates Dhh1 ATPase activity to prevent Dhh1 from scaffolding mRNA decay factors on the mRNA. After deadenylation, the Ccr4-NOT

complex no longer remains bound to the mRNA, allowing Dhh1 to assemble a decapping complex on the mRNA to initiate decapping and decay or PB assembly.

Experimental Procedures

Construction of yeast strains and plasmids:

Construction of plasmids for this study (Table S1) was performed using standard molecular cloning techniques. Yeast deletion strains were made by PCR-based homologous recombination transformations, using integration and tagging vectors as previously described (Longtine et al. 1998, Carroll et al 2011). Double knockout strains were made either using the PCR-based transformation method described above, or by mating and dissection of sporulated yeast.

The generation of bacteriophage PP7-CP and PP7-loop tagging plasmids was described previously (Carroll et al. 2011), and were gifts from B. Hogg and K. Collins (University of California, Berkeley, Berkeley, CA; Hogg and Collins 2007).

Dhh1 mutagenesis:

Mutations in Dhh1 were generated using a QuikChange II site-directed mutagenesis kit (Agilent Technologies) using PFu Ultra or PFu Turbo. Mutagenic oligonucleotides were designed using the Agilent Technologies primer design platform. Plasmids generated are listed below in **Table 2.5**.

Tethering assay:

Sample preparation was performed as previously described (Carroll et al 2011). Briefly, yeast cells were grown to mid-log phase (OD_{600} = 0.4-0.8) in synthetic media containing 2% dextrose. Cells were collected by centrifugation and lysed in 1X Phospho-buffered saline (PBS) with 0.1% Tween-20 and protease inhibitors. Lysis was performed using three 1-min pulses using a multi-bead beater (company). Extract was clarified by centrifugation, and extract was split for protein and RNA measurements. Protein samples were normalized by total protein content by Bradford Assay (Bio-Rad Laboratories). RNA was isolated using the RNeasy RNA isolation kit (Qiagen).

For hot acid phenol extraction, frozen cell pellets were resuspended in 600uL TES buffer (10mM Tris-HCl pH=7.5, 10mM EDTA, 0.5% SDS). Acid saturated phenol was added and cells were incubated at 65° C for 1 hour with occasional vortexing. Samples were transferred to ice for 5 minutes and spun at 4° C at max speed. The aqueous phase was extracted and a second phenol extraction was done, followed by a chloroform extraction and ethanol precipitation. RNA was stored at -80° C.

Immunoprecipitation:

Yeast were inoculated in synthetic media containing 2% dextrose and grown overnight to saturation, then backdiluted the following day in 1L synthetic media

and grown to OD_{600} = 0.4-1.0. Cells were harvested by centrifugation at 3800 rpm for 10 minutes, resuspended briefly in resuspension buffer (20mM HEPES, 1.2% polyvinylpyrrolidone, 1mM DTT, 1:100 Solution P, 1:1000 Pepstatin A), and spun at 3100 rpm for 15 minutes, then frozen in liquid nitrogen and stored at -80° C. Yeast extracts were lysed with a Retsch planetary ball mill for six cycles of 30 Hz for 3 min with cooling in liquid nitrogen between cycles. 0.25g of lysate was then resuspended in 9mL TBT buffer (20mM HEPES, pH7.4, 110mM KOAc, 2mM MgCl2, 0.5% Triton, 0.1% Tween 20, 1:100 Solution P, 1:1000 DTT, 1:5000 SuperRNasin (Ambion), 1:5000 Antifoam B (Sigma)). The lysate was homogenized and spun briefly for 1 min at 1500 x *g*, followed by clarification of lysate through 2.7µm and 1.6µm GD/X Glass Microfiber syringe filters (25mm, Whatman). The lysates were then incubated with 5mg rabbit IgG (Sigma)-coupled magnetic beads (DynaI) – corresponding to 400ul bead slurry at 20mg/uL slurry) – and were rotated at 4°C for 30 min. The beads were washed three times with 1mL TBT buffer, and a final wash in 1 ml of 100 mM ammonium acetate, pH = 7.4, 0.1 mM MgCl2, 0.2% Tween-20 for 5 min while rotating. Protein complexes were eluted from the beads directly in SDS-PAGE sample buffer (for Western blot) or twice with 500µl of fresh aqueous 500mM NH_4OH, 0.5mM EDTA solution for 20 minutes with rotation (for mass spectrometry). The eluates were then pooled and lyophilized overnight in a SpeedVac (ThermoSavant) and prepared for mass spectrometry.

RT-qPCR:

RNA was isolated as described above and quantified using a NanoDrop spectrophotometer (Fischer Scientific). cDNA was generated by reverse transcription of 1µg of RNA using a random hexamer oligonucleotides (Invitrogen) and Superscript II (Invitrogen). Quantitative PCR was performed in real time using the StepOnePlus (Applied Biosystems) with gene specific primers and a SYBR-Green ROX mix (Thermo Scientific) supplemented with gene specific primers.

Western Blot:

Proteins from yeast lysates were separated by SDS-PAGE and transferred to nitrocellulose membrane (GE Health Sciences). Membranes were blocked in phosphor-buffered saline (PBS) with 4% non-fat milk, followed by incubation with primary antibody over night and secondary antibody for 45 minutes. Membranes were analyzed and quantified using an infrared imaging system (Odyssey; LI-COR Biosciences). The following primary antibodies were used for detection of tagged proteins: anti-FLAG, , anti-HA, anti-GFP, anti-Pgk1, anti-Pab1, anti-Xpo1, and anti-Hxk1. Fluorophore-coupled goat anti-mouse AlexaFluor 680 (Invitrogen) and goat anti-rabbit IRdye800 (Rockland Immunochemicals) were used as secondary antibodies.

Microscopy:

Samples were grown overnight in in synthetic media containing 2% dextrose,

backdiluted to OD_{600} = 0.05 or 0.1 the following day, and grown to mid-log phase (OD_{600}= 0.3-0.8). Cells were harvested by centrifugation and washed in ¼ volumes of fresh synthetic media +/- 2% dextrose, then harvested again and resuspended in 1 volume of fresh synthetic media +/- 2% dextrose and grown 15 minutes at 30° C. Cells were harvested once more and washed as described above, then plated onto Concavalin A-treated MatTek dishes (MatTek) in induction media and visualized at room temperature by epifluorescent microscopy or by confocal microscopy using an Andor/Nikon Spinning Disk Confocal Microscope. All cells were observed using a 100X-oil immersion objective (NA = 1.49) and images were captured using an iXon Ultra 897 EMCCD camera (Andor) using Metamorph Microscopy Automation & Image Analysis software (Metamorph). All images unless otherwise indicated are collapsed Z-stacks. Unless otherwise indicated, three independent experiments were performed and foci/cell values in the bar graphs representing the mean with standard deviation of the mean (SDM). Quantitation is described below.

Fluorescence Recovery After Photobleaching (FRAP):

Samples were grown overnight in synthetic media at 30° C, backdiluted to OD_{600} = 0.05 or 0.1 the following day, and grown to mid-log phase (OD_{600}= 0.3-0.8). Cells were shifted into SC media containing 3% glycerol or no sugar as described above, and mounted on Concavalin A-treated MatTek dishes (MatTek) in induction media and visualized under the microscope at room temperature. Dhh1-GFP, $Dhh1^{DQAD}$-GFP, and $Dhh1^{5X\text{-}Not1}$-GFP photobleaching experiments were performed on the Leica SP8 Laser Scanning Confocal Microscope or the Andor/Nikon Spinning Disk Confocal Microscope. Images were acquired from a single plane with a 2.92nm pinhole.

Using the Leica SP8 Laser Scanning Confocal Microscope, photobleached PBs were subjected to 5-10 pulses with an argon laser at 488nm. Images were collected at 500ms intervals for approximately 40 seconds after bleach. Using the Andor/Nikon Spinning Disk Confocal Microscope, photobleached PBs were pulsed once for 500ms using a 405nm laser and images were collected at 500ms or 3s intervals for 60 seconds or 3 minutes. Recovery curves were generated by normalization to the bleach point and quantified in ImageJ/FIJI. Percent of fluorescent recovery values were determined by curve fitting using the equation: $f(t) = A(1-e^{-rt})$. Fluorescent plateau values were determined from individual PB traces and represented in the boxplot in Fig 2.7 E .

Image Quantitation:

An ImageJ/FIJI script was used to quantify PB foci number and size as described previously (Passos and Parker, 2008). Briefly, z-stacks were collapsed by max intensity and cell images were sharpened, background-subtracted, and thresholded using the Otsu Thresholding plugin. Thresholded image LUTs were inverted and measured, with size cut offs of less than 7 pixel and greater than 500 pixels to produce foci number and size. Cell number was quantified using the Cell Counter

plugin to generate foci per cell averages. Greater than 100 cells were counted for three independent experiments and reported as mean averages of foci per cell ± standard deviation.

Table 2.4: Yeast strains used in this study

Yeast Strains	Genotype	Source
W303	MATa/a ade2-1 ura3-1 his3-11,15 trp1-1 leu203, 112 can1-100	This study
KWY2532	W303a *dhh1Δ*::NatMX *FBA1-FLAG-PP7L*::KanMX	Carroll et al. (2011)
KWY4448	W303a *dhh1Δ*::KanMX *P(DHH1)-DHH1-CBP-TEV-ZZ*::*URA3*	This study
KWY4449	W303a *dhh1Δ*::KanMX *P(DHH1)-DHH1^{DQAD}-CBP-TEV-ZZ*::*URA3*	This study
KWY4450	W303a *dhh1Δ*::KanMX *P(DHH1)-DHH1$^{Q\text{-}motif}$-CBP-TEV-ZZ*::*URA3*	This study
KWY4451	W303a *dhh1Δ*::KanMX *P(DHH1)-DHH1$^{3X\text{-}RNA}$-CBP-TEV-ZZ*::*URA3*	This study
KWY4452	W303a *dhh1Δ*::KanMX *P(DHH1)-DHH1^{INT}-CBP-TEV-ZZ*::*URA3*	This study
KWY4466	W303a *dhh1Δ*::KanMX	This study
KWY4574	W303a *dhh1Δ*::KanMX *NOT1-3HA*::HisMX	This study
KWY2193	W303α *dhh1Δ*::KanMX *DCP2-mCHERRY*::NatMX	Carroll et al. (2011)
KWY3266	W303α *dhh1Δ*::KanMX *CCR4-GFP*::HisMX *DCP2-mCHERRY*::NatMX	Carroll et al. (2011)
KWY4597	W303α *dhh1Δ*::KanMX *NOT1-GFP*::HisMX *DCP2-mCHERRY*::NatMX	Carroll et al. (2011)

Table 2.5: Plasmids used in this study

Plasmid	Description	Source
pKW2304	pRS316 PDhh1-GFP; *URA3* marker	Carroll et al (2011)
pKW2312	pRS316 PDhh1-Dhh1-GFP; *URA3* marker	Carroll et al (2011)
pKW2313	pRS316 PDhh1-Dhh1^{DQAD}-GFP; *URA3* marker	Carroll et al (2011)
pKW2420	pRS316 PDhh1-GFP-PP7CP; *URA3* marker	Carroll et al (2011)
pKW2321	pRS316 PDhh1-Dhh1-PP7CP; *URA3* marker	Carroll et al (2011)
pKW2322	pRS316 PDhh1-Dhh1^{DQAD}-PP7CP; *URA3* marker	Carroll et al (2011)
pKW2421	pRS316 PDhh1-Dhh1-CBP-TEV-ZZ; *URA3* marker	Carroll et al (2011)
pKW2422	pRS316 PDhh1-Dhh1^{DQAD}-CBP-TEV-ZZ; *URA3* marker	Carroll et al (2011)
pKW2800	pRS316 PDhh1-Dhh1 ^{INT}-GFP; *URA3* marker	This study
pKW2864	pRS316 PDhh1-Dhh1$^{1X\text{-}RNA}$-PP7CP; *URA3* marker	This study
pKW2865	pRS316 PDhh1-Dhh1$^{2X\text{-}RNA}$-PP7CP; *URA3* marker	This study
pKW2866	pRS316 PDhh1-Dhh1$^{3X\text{-}RNA}$-PP7CP; *URA3* marker	This study
pKW2867	pRS316 PDhh1-Dhh1$^{3X\text{-}RNA}$-GFP; *URA3* marker	This study
pKW3040	pRS316 PDhh1-Dhh1$^{3X\text{-}RNA/DQAD}$-GFP; *URA3* marker	This study
pKW3072	pRS316 PDhh1-Dhh1$^{Q\text{-}motif}$-GFP; *URA3* marker	This study
pKW3073	pRS316 PDhh1-Dhh1$^{Q\text{-}motif}$-PP7CP; *URA3* marker	This study
pKW3074	pRS316 PDhh1-Dhh1$^{Q\text{-}motif}$-CBP-TEV-ZZ; *URA3* marker	This study
pKW3126	pRS316 PDhh1-Dhh1$^{3X\text{-}RNA}$-CBP-TEV-ZZ; *URA3* marker	This study
pKW3127	pRS316 PDhh1-Dhh1^{INT}-CBP-TEV-ZZ; *URA3* marker	This study
pKW3321	pRS316 PDhh1-Dhh1$^{(R55E)}$-GFP; *URA3* marker	This study
pKW3322	pRS316 PDhh1-Dhh1$^{(F62E)}$-GFP; *URA3* marker	This study
pKW3323	pRS316 PDhh1-Dhh1$^{(Q282E,N284E)}$-GFP; *URA3* marker	This study
pKW3324	pRS316 PDhh1-Dhh1$^{(R335E)}$-GFP; *URA3* marker	This study
pKW3325	pRS316 PDhh1-Dhh1$^{(R55E,F62E)}$-GFP; *URA3* marker	This study
pKW3326	pRS316 PDhh1-Dhh1$^{(R55E,Q282E,N284E)}$-GFP; *URA3* marker	This study
pKW3327	pRS316 PDhh1-Dhh1$^{(R55E,R335E)}$-GFP; *URA3* marker	This study
pKW3328	pRS316 PDhh1-Dhh1$^{(F62E,Q282E,N284E)}$-GFP; *URA3* marker	This study
pKW3329	pRS316 PDhh1-Dhh1$^{(Q282E,N284E,R335E)}$-GFP; *URA3* marker	This study
pKW3330	pRS316 PDhh1-Dhh1$^{(R55E,F62E,Q282E,N284E)}$-GFP; *URA3* marker	This study
pKW3331	pRS316 PDhh1-Dhh1$^{(R55E,Q282E,N284E,R335E)}$-GFP; *URA3* marker	This study
pKW3332	pRS316 PDhh1-Dhh1$^{(F62E,Q282E,N284E,R335E)}$-GFP; *URA3* marker	This study
pKW3333	pRS316 PDhh1-Dhh1$^{(R55E,F62E,Q282E,N284E,R335E)}$-GFP; *URA3* marker	This study
pKW3335	pRS316 PDhh1-Dhh1$^{(R55E,R335E)}$-GFP; *URA3* marker	This study
pKW3349	pRS316 PDhh1-Dhh1$^{(R55E,F62E,Q282E,N284E,R335E)}$-CBP-TEV-ZZ; *URA3* marker	This study
pKW3352	pRS316 PDhh1-Dhh1$^{(R55E,F62E,Q282E,N284E,R335E)}$-PP7CP; *URA3* marker	This study

References:

Aizer, A., Kalo, A., Kafri, P., Shraga, A., Ben-Yishay, R., Jacob, A., Kinor, N., and Shav-Tal, Y. (2014). Quantifying mRNA targeting to P-bodies in living human cells reveals their dual role in mRNA decay and storage. J. Cell Sci. *127*, 4443–4456.

Anderson, P., and Kedersha, N. (2009). Stress granules. Curr. Biol. CB *19*, R397–R398.

Basquin, J., Roudko, V.V., Rode, M., Basquin, C., Séraphin, B., and Conti, E. (2012). Architecture of the nuclease module of the yeast Ccr4-not complex: the Not1-Caf1-Ccr4 interaction. Mol. Cell *48*, 207–218.

Brown, C.E., and Sachs, A.B. (1998). Poly(A) tail length control in Saccharomyces cerevisiae occurs by message-specific deadenylation. Mol. Cell. Biol. *18*, 6548–6559.

Buchan, J.R., Muhlrad, D., and Parker, R. (2008). P bodies promote stress granule assembly in Saccharomyces cerevisiae. J. Cell Biol. *183*, 441–455.

Carroll, J.S., Munchel, S.E., and Weis, K. (2011). The DExD/H box ATPase Dhh1 functions in translational repression, mRNA decay, and processing body dynamics. J. Cell Biol. *194*, 527–537.

Chen, Y., Boland, A., Kuzuoğlu-Öztürk, D., Bawankar, P., Loh, B., Chang, C.-T., Weichenrieder, O., and Izaurralde, E. (2014). A DDX6-CNOT1 complex and W-binding pockets in CNOT9 reveal direct links between miRNA target recognition and silencing. Mol. Cell *54*, 737–750.

Cheng, Z., Coller, J., Parker, R., and Song, H. (2005). Crystal structure and functional analysis of DEAD-box protein Dhh1p. RNA N. Y. N *11*, 1258–1270.

Chlebowski, A., Lubas, M., Jensen, T.H., and Dziembowski, A. (2013). RNA decay machines: the exosome. Biochim. Biophys. Acta *1829*, 552–560.

Coller, J., and Parker, R. (2004). Eukaryotic mRNA decapping. Annu. Rev. Biochem. *73*, 861–890.

Coller, J., and Parker, R. (2005). General translational repression by activators of mRNA decapping. Cell *122*, 875–886.

Cordin, O., Banroques, J., Tanner, N.K., and Linder, P. (2006). The DEAD-box protein family of RNA helicases. Gene *367*, 17–37.

Cougot, N., Babajko, S., and Séraphin, B. (2004). Cytoplasmic foci are sites of mRNA decay in human cells. J. Cell Biol. *165*, 31–40.

Decker, C.J., and Parker, R. (2012). P-bodies and stress granules: possible roles in the control of translation and mRNA degradation. Cold Spring Harb. Perspect. Biol. *4*, a012286.

Decker, C.J., Teixeira, D., and Parker, R. (2007). Edc3p and a glutamine/asparagine-rich domain of Lsm4p function in processing body assembly in Saccharomyces cerevisiae. J. Cell Biol. *179*, 437–449.

Dutta, A., Zheng, S., Jain, D., Cameron, C.E., and Reese, J.C. (2011). Intermolecular interactions within the abundant DEAD-box protein Dhh1 regulate its activity in vivo. J. Biol. Chem. *286*, 27454–27470.

Erickson, S.L., and Lykke-Andersen, J. (2011). Cytoplasmic mRNP granules at a glance. J. Cell Sci. *124*, 293–297.

Ernoult-Lange, M., Baconnais, S., Harper, M., Minshall, N., Souquere, S., Boudier, T., Bénard, M., Andrey, P., Pierron, G., Kress, M., et al. (2012). Multiple binding of repressed mRNAs by the P-body protein Rck/p54. RNA N. Y. N *18*, 1702–1715.

Eulalio, A., Behm-Ansmant, I., Schweizer, D., and Izaurralde, E. (2007). P-body formation is a consequence, not the cause, of RNA-mediated gene silencing. Mol. Cell. Biol. *27*, 3970–3981.

Fischer, N., and Weis, K. (2002). The DEAD box protein Dhh1 stimulates the decapping enzyme Dcp1. EMBO J. *21*, 2788–2797.

Franks, T.M., and Lykke-Andersen, J. (2008). The control of mRNA decapping and P-body formation. Mol. Cell *32*, 605–615.

Fromm, S.A., Truffault, V., Kamenz, J., Braun, J.E., Hoffmann, N.A., Izaurralde, E., and Sprangers, R. (2012). The structural basis of Edc3- and Scd6-mediated activation of the Dcp1:Dcp2 mRNA decapping complex. EMBO J. *31*, 279–290.

Fromm, S.A., Kamenz, J., Nöldeke, E.R., Neu, A., Zocher, G., and Sprangers, R. (2014). In vitro reconstitution of a cellular phase-transition process that involves the mRNA decapping machinery. Angew. Chem. Int. Ed Engl. *53*, 7354–7359.

Garneau, N.L., Wilusz, J., and Wilusz, C.J. (2007). The highways and byways of mRNA decay. Nat. Rev. Mol. Cell Biol. *8*, 113–126.

Gygi, S.P., Rochon, Y., Franza, B.R., and Aebersold, R. (1999). Correlation between protein and mRNA abundance in yeast. Mol. Cell. Biol. *19*, 1720–1730.

Hogg, J.R., and Collins, K. (2007). RNA-based affinity purification reveals 7SK RNPs with distinct composition and regulation. RNA N. Y. N *13*, 868–880.

Kiebler, M.A., and Bassell, G.J. (2006). Neuronal RNA granules: movers and makers. Neuron *51*, 685–690.

Kruk, J.A., Dutta, A., Fu, J., Gilmour, D.S., and Reese, J.C. (2011). The multifunctional Ccr4-Not complex directly promotes transcription elongation. Genes Dev. *25*, 581–593.

Lavut, A., and Raveh, D. (2012). Sequestration of highly expressed mRNAs in cytoplasmic granules, P-bodies, and stress granules enhances cell viability. PLoS Genet. *8*, e1002527.

Lim, F., and Peabody, D.S. (2002). RNA recognition site of PP7 coat protein. Nucleic Acids Res. *30*, 4138–4144.

Linder, P., and Jankowsky, E. (2011). From unwinding to clamping - the DEAD box RNA helicase family. Nat. Rev. Mol. Cell Biol. *12*, 505–516.

Maillet, L., and Collart, M.A. (2002). Interaction between Not1p, a component of the Ccr4-not complex, a global regulator of transcription, and Dhh1p, a putative RNA helicase. J. Biol. Chem. *277*, 2835–2842.

Mathys, H., Basquin, J., Ozgur, S., Czarnocki-Cieciura, M., Bonneau, F., Aartse, A., Dziembowski, A., Nowotny, M., Conti, E., and Filipowicz, W. (2014). Structural and biochemical insights to the role of the CCR4-NOT complex and DDX6 ATPase in microRNA repression. Mol. Cell *54*, 751–765.

Montpetit, B., Thomsen, N.D., Helmke, K.J., Seeliger, M.A., Berger, J.M., and Weis, K. (2011). A conserved mechanism of DEAD-box ATPase activation by nucleoporins and InsP6 in mRNA export. Nature *472*, 238–242.

Muhlrad, D., and Parker, R. (1992). Mutations affecting stability and deadenylation of the yeast MFA2 transcript. Genes Dev. *6*, 2100–2111.

Oeffinger, M., Wei, K.E., Rogers, R., DeGrasse, J.A., Chait, B.T., Aitchison, J.D., and Rout, M.P. (2007). Comprehensive analysis of diverse ribonucleoprotein complexes. Nat. Methods *4*, 951–956.

Özeş, A.R., Feoktistova, K., Avanzino, B.C., and Fraser, C.S. (2011). Duplex unwinding and ATPase activities of the DEAD-box helicase eIF4A are coupled by eIF4G and eIF4B. J. Mol. Biol. *412*, 674–687.

Parker, R. (2012). RNA degradation in Saccharomyces cerevisae. Genetics *191*, 671–702.

Pause, A., and Sonenberg, N. (1992). Mutational analysis of a DEAD box RNA helicase: the mammalian translation initiation factor eIF-4A. EMBO J. *11*, 2643–2654.

Petit, A.-P., Wohlbold, L., Bawankar, P., Huntzinger, E., Schmidt, S., Izaurralde, E., and Weichenrieder, O. (2012). The structural basis for the interaction between the CAF1 nuclease and the NOT1 scaffold of the human CCR4-NOT deadenylase complex. Nucleic Acids Res. *40*, 11058–11072.

Ramachandran, V., Shah, K.H., and Herman, P.K. (2011). The cAMP-dependent protein kinase signaling pathway is a key regulator of P body foci formation. Mol. Cell *43*, 973–981.

Rouya, C., Siddiqui, N., Morita, M., Duchaine, T.F., Fabian, M.R., and Sonenberg, N. (2014). Human DDX6 effects miRNA-mediated gene silencing via direct binding to CNOT1. RNA N. Y. N *20*, 1398–1409.

Russell, R., Jarmoskaite, I., and Lambowitz, A.M. (2013). Toward a molecular understanding of RNA remodeling by DEAD-box proteins. RNA Biol. *10*, 44–55.

Schütz, P., Bumann, M., Oberholzer, A.E., Bieniossek, C., Trachsel, H., Altmann, M., and Baumann, U. (2008). Crystal structure of the yeast eIF4A-eIF4G complex: an RNA-helicase controlled by protein-protein interactions. Proc. Natl. Acad. Sci. U. S. A. *105*, 9564–9569.

Shah, K.H., Zhang, B., Ramachandran, V., and Herman, P.K. (2013). Processing body and stress granule assembly occur by independent and differentially regulated pathways in Saccharomyces cerevisiae. Genetics *193*, 109–123.

Sharif, H., Ozgur, S., Sharma, K., Basquin, C., Urlaub, H., and Conti, E. (2013). Structural analysis of the yeast Dhh1-Pat1 complex reveals how Dhh1 engages Pat1, Edc3 and RNA in mutually exclusive interactions. Nucleic Acids Res. *41*, 8377–8390.

Sheth, U., and Parker, R. (2003). Decapping and decay of messenger RNA occur in cytoplasmic processing bodies. Science *300*, 805–808.

Sweet, T., Kovalak, C., and Coller, J. (2012). The DEAD-box protein Dhh1 promotes decapping by slowing ribosome movement. PLoS Biol. *10*, e1001342.

Teixeira, D., and Parker, R. (2007). Analysis of P-body assembly in Saccharomyces cerevisiae. Mol. Biol. Cell *18*, 2274–2287.

Tritschler, F., Braun, J.E., Eulalio, A., Truffault, V., Izaurralde, E., and Weichenrieder, O. (2009). Structural basis for the mutually exclusive anchoring of P body components EDC3 and Tral to the DEAD box protein DDX6/Me31B. Mol. Cell *33*, 661–668.

Voronina, E. (2013). The diverse functions of germline P-granules in Caenorhabditis elegans. Mol. Reprod. Dev. *80*, 624–631.

Chapter III: Dhh1 requires distinct factors to stimulate mRNA decay and repress translation

Introduction

How messenger ribonucleic acids (mRNAs) transit between a translationally active state and an inactive state is an important, yet poorly understood aspect of post-transcriptional gene expression. Moreover, improper regulation and/or kinetics of mRNA inactivation can dramatically affect growth and development, and can lead to disease. mRNAs that are not actively translated can be targeted for mRNA decay or storage. In logarithmically growing *S. cerevisiae*, the default mRNA inactivation pathway is thought to be degradation in a deadenylation-dependent manner, initiated by removal of the poly(A) tail by the Pan2-3 heterodimer and/or the Pop2 and Ccr4 deadenylases of the Ccr4-NOT complex (Garneau et al., 2007; Wolf and Passmore, 2014). Following deadenylation, an mRNA can undergo degradation through one of two conserved mechanisms. The ten-subunit exosome complex can degrade the mRNA from the 3' end, with the 5' cap removed by DcpS – the scavenger decapping enzyme (Makino et al., 2013; Milac et al., 2014). However, current evidence in yeast suggests that the predominant mechanism of bulk mRNA decay occurs in a 5'-3' direction, with the Dcp1-Dcp2 decapping complex removing the 5' cap, followed by exonucleolytic degradation by the 5'-3' exonuclease Xrn1 (Parker, 2012). While removal of the 5' cap is thought to mark an irreversible step in mRNA decay, deadenylated mRNAs can exist in complex with other protein factors in a nontranslating messenger ribonucleoprotein complex (mRNP) (Franks and Lykke-Andersen, 2008). However, the signals that partition mRNAs for either storage or degradation are poorly understood.

Several additional protein factors outside of the canonical mRNA decay machinery have been implicated in mRNA turnover, yet the functions of these proteins remain poorly understood. This includes the DEAD-box ATPase Dhh1, which is postulated to regulate mRNA inactivation. It is unclear however, how Dhh1 employs its ATPase activity to regulate mRNP activity or composition. Initially, Dhh1 was identified as a multicopy suppressor of Pop2, and was shown to stimulate mRNA decapping activity *in vitro* (Fischer and Weis, 2002; Hata et al., 1998). However, recent evidence has shown that Dhh1 has additional functional roles in both 5'-3' mRNA turnover and translation repression of bulk cytoplasmic mRNA in *Saccharomyces cerevisiae* (Carroll et al., 2011; Coller and Parker, 2005; Sweet et al., 2012). Dhh1 can inhibit translation initiation by blocking assembly of the 48S preinitiation complex *in vitro* (Coller and Parker, 2005). Additionally, Dhh1 association on the mRNA leads to an accumulation of ribosomes on the mRNA, and can stimulate decay of an mRNA blocked during translation elongation (Sweet et al., 2012). However, the signals that stimulate Dhh1 to bind mRNA and initiate these processes have not yet been identified. Moreover, not only are important steps of Dhh1 recruitment to an mRNA poorly understood, the function of Dhh1 while bound to the message is also unclear.

To further characterize the functional role of Dhh1, our lab used a PP7-based tethering system to bypass unknown signaling events that are needed to recruit Dhh1 to an mRNA (Carroll et al., 2011; Hogg and Collins, 2007; Lim and Peabody, 2002). I used this tool to investigate whether Dhh1 requires distinct factors to stimulate mRNA turnover and repress translation after mRNA binding. We tethered

Dhh1 to a reporter mRNA in yeast lacking *EDC3*, *SCD6*, *PAT1*, or *LSM1* – genes implicated in mRNA turnover whose precise functions are unknown (Kshirsagar and Parker, 2004; Marnef and Standart, 2010; Tanaka et al., 2006) and assessed the role of Dhh1 function in mRNA decay and translation repression.

These experiments reveal that Dhh1 requires *LSM1* to stimulate mRNA turnover, suggesting that the Lsm1-7 ring complex functions after Dhh1-mRNA binding at a late stage in decapping. Interestingly, while *PAT1* is expendable for Dhh1-mediated mRNA decay, it is required for translation repression by Dhh1. This effect is specific to Pat1, as loss of Scd6 and Edc3, two other proteins known to bind to Dhh1 at the same surface as Pat1 do not cause defects in translation repression of a Dhh1-bound mRNA. These findings show that Dhh1 requires distinct protein factors to trigger both translation repression and mRNA decay, and suggest that translational repression is a separable path from mRNA decay.

Results

In order to assess requirements of Dhh1 function after binding to an mRNA, I utilized a reporter mRNA engineered by our lab. A stem loop aptamer that is recognized with high affinity by the bacteriophage PP7 coat protein (PP7-CP) was inserted into the 3'UTR of the *FBA1* gene (*FBA1-PP7L*) (Carroll et al., 2011). *FBA1,* the gene encoding the fructose 1,6-bisphosphate aldolase enzyme is among the most abundant mRNAs in yeast, and is essential for vegetative growth (Holstege et al., 1998). When the *FBA1-PP7L* reporter is co-expressed with either *DHH1-PP7CP* or *GFP-PP7CP*, Dhh1 tethering is sufficient to stimulate mRNA decay compared to the GFP tether or in the absence of tether (Carroll et al., 2011, **Fig 3.1, Fig 3.2 A**). In an effort to further characterize the role of Dhh1 in mRNA decay and translation repression, we utilized the Dhh1-PP7CP-based tethering assay in cells lacking genes that are implicated in translation repression or mRNA turnover to ask if these factors were necessary for either function of Dhh1.

Fig 3.1

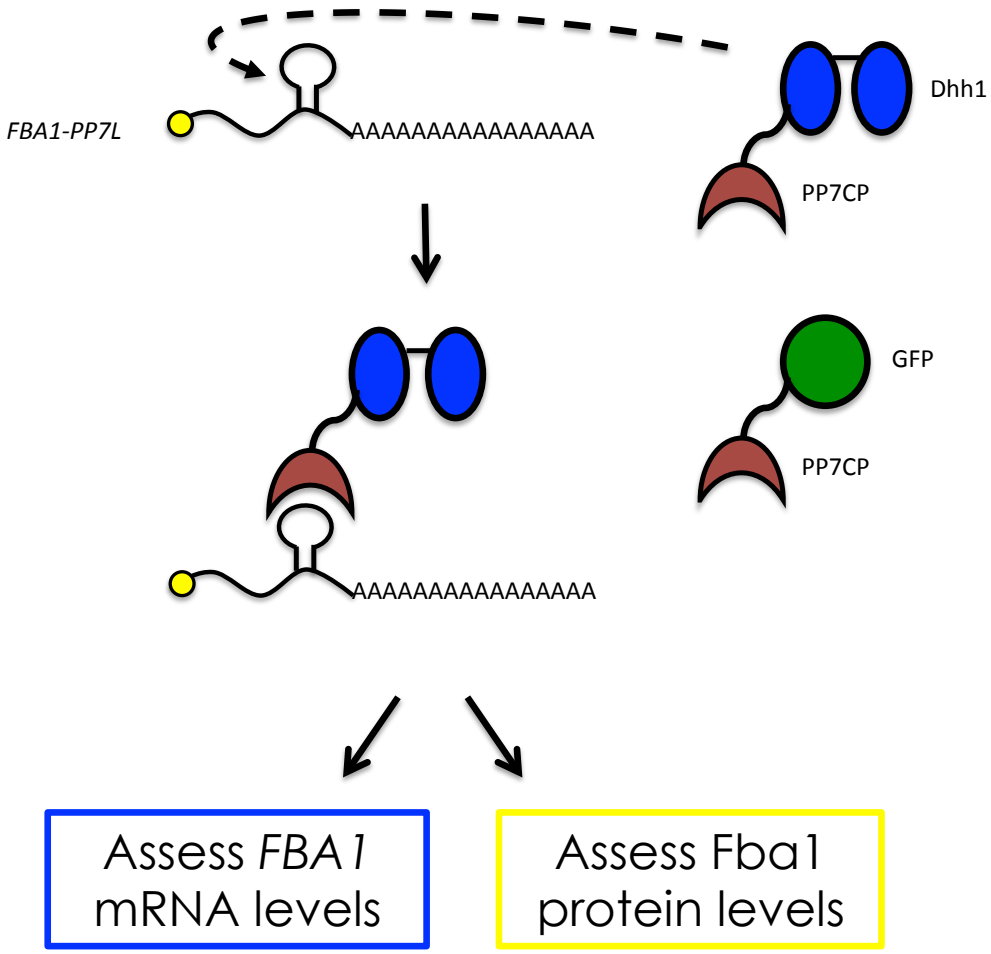

Fig 3.1: Schematic depicting Dhh1 tethered-function assay
GFP and Dhh1 were fused to the bacteriophage PP7 coat protein (PP7CP), which binds with high affinity to a stem loop structure inserted into the 3'UTR of *FBA1* (*FBA1-PP7L*). *GFP-PP7CP* or *DHH1-PP7CP* fusion proteins were expressed in several yeast strains lacking genes involved in mRNA turnover. Both steady state *FBA1* mRNA (blue bar graphs) and Fba1 protein levels (yellow bar graphs) were determined by RT-qPCR and Western Blot respectively.

Dhh1 can stimulate decay of a bound mRNA in the absence of *EDC3*, *SCD6*, and *PAT1*

Edc3, Scd6, and Pat1, are factors known to participate in mRNA decay and translation repression. They each bind directly to Dhh1 at overlapping surfaces (Sharif et al., 2013; Tritschler et al., 2008, 2009). Edc3 and Pat1 also interact with

several other components involved in mRNA turnover, and are critical for the formation of large mRNA-protein granules called Processing Bodies (PBs), which are postulated sites of mRNA decay and storage. While Scd6 was shown to bind to Dcp1 and to stimulate decapping *in vitro* (Fromm et al., 2012; Tritschler et al., 2008), it is primarily thought to function as a translational repressor in yeast and other organisms (Krüger et al., 2013; Rajyaguru et al., 2012). We therefore wanted to examine whether Dhh1 requires these factors to translationally repress and/or decay a transcript. We first expressed *DHH1-PP7CP* or *GFP-PP7CP* in strains containing *FBA1-PP7L* in wild-type cells, or in cells lacking *EDC3*, *SCD6*, or *PAT1* and assessed *FBA1* mRNA levels to determine whether the activities of these genes were required for Dhh1's function in mRNA decay.

Tethering Dhh1 to *FBA1* in wild-type yeast caused a reduction of *FBA1* mRNA levels, in agreement with previously published data (**Fig 3.2 A**; Carroll et al., 2011). Similarly, tethering Dhh1 to *FBA1* also caused a decrease in *FBA1* mRNA levels in *edc3Δ*, *scd6Δ*, and *pat1Δ* cells, demonstrating that these factors are not individually needed to stimulate mRNA turnover by Dhh1 **(Fig 3.2 A-D)**. As expected, this drop in *FBA1* mRNA levels lead to a similar decrease in Fba1 protein levels **(Fig 3.3 A-D)**. Edc3, Scd6, and Pat1 all have been shown to interact with Dhh1 using a phenylalanine-glycine-phenylalanine (FDF)-motif that docks with an FDF binding pocket in the C-terminal RecA domain of Dhh1 (Sharif et al., 2013; Tritschler et al., 2009). It is therefore possible that loss of *EDC3*, *SCD6*, or *PAT1* individually may be compensated by increased occupancy of Dhh1 by other factors, which would mask any effects due to loss of a single protein. To rule out redundancy of these factors in decay, *edc3Δ scd6Δ* and *edc3Δ pat1Δ* yeast were generated and *FBA1* mRNA and protein levels were assessed. In both pairwise deletions, Dhh1 tethering nonetheless stimulated decay of *FBA1* **(Fig 3.2 E-F)**. As in *edc3Δ*, *scd6Δ*, and *pat1Δ* single mutants, Fba1 protein levels and mRNA levels were also correlated in the double mutants **(Fig 3.3 E-F)**. Dhh1 can therefore stimulate decay of a tethered mRNA in strains lacking multiple FDF-motif proteins. However, to determine whether Edc3, Scd6, and Pat1 are truly dispensable for decay by Dhh1, *pat1Δ scd6Δ* and *edc3Δ pat1Δ scd6Δ* mutants would have to be assessed.

Fig 3.2

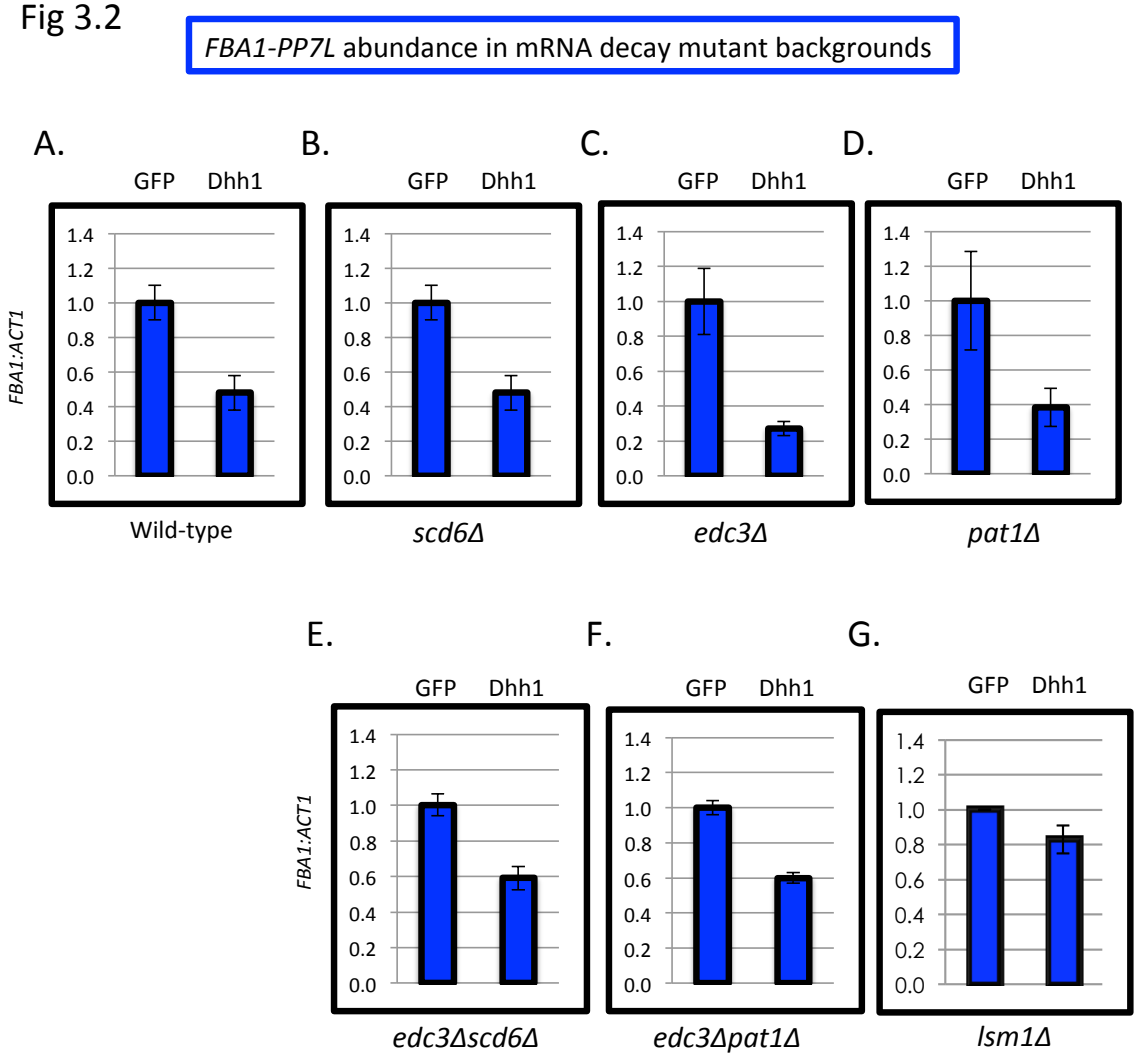

Figure 3.2: Dhh1 stimulates decay of bound mRNA without *EDC3*, *SCD6*, and *PAT1*

(A) *FBA1-PP7L* was coexpressed with *GFP-PP7CP* or *DHH1-PP7CP* in wild-type or (B) *scd6Δ*, (C) *edc3Δ*, (D) *pat1Δ*, (E) *edc3Δ scd6Δ*, (F) *edcΔ pat1Δ*, (G) and *lsm1Δ* cells. *FBA1-PP7L* mRNA levels were determined by RT-qPCR, and were normalized to the *ACT1* gene. Mean values ± standard deviation were determined from at least three independent experiments.

Fig 3.3

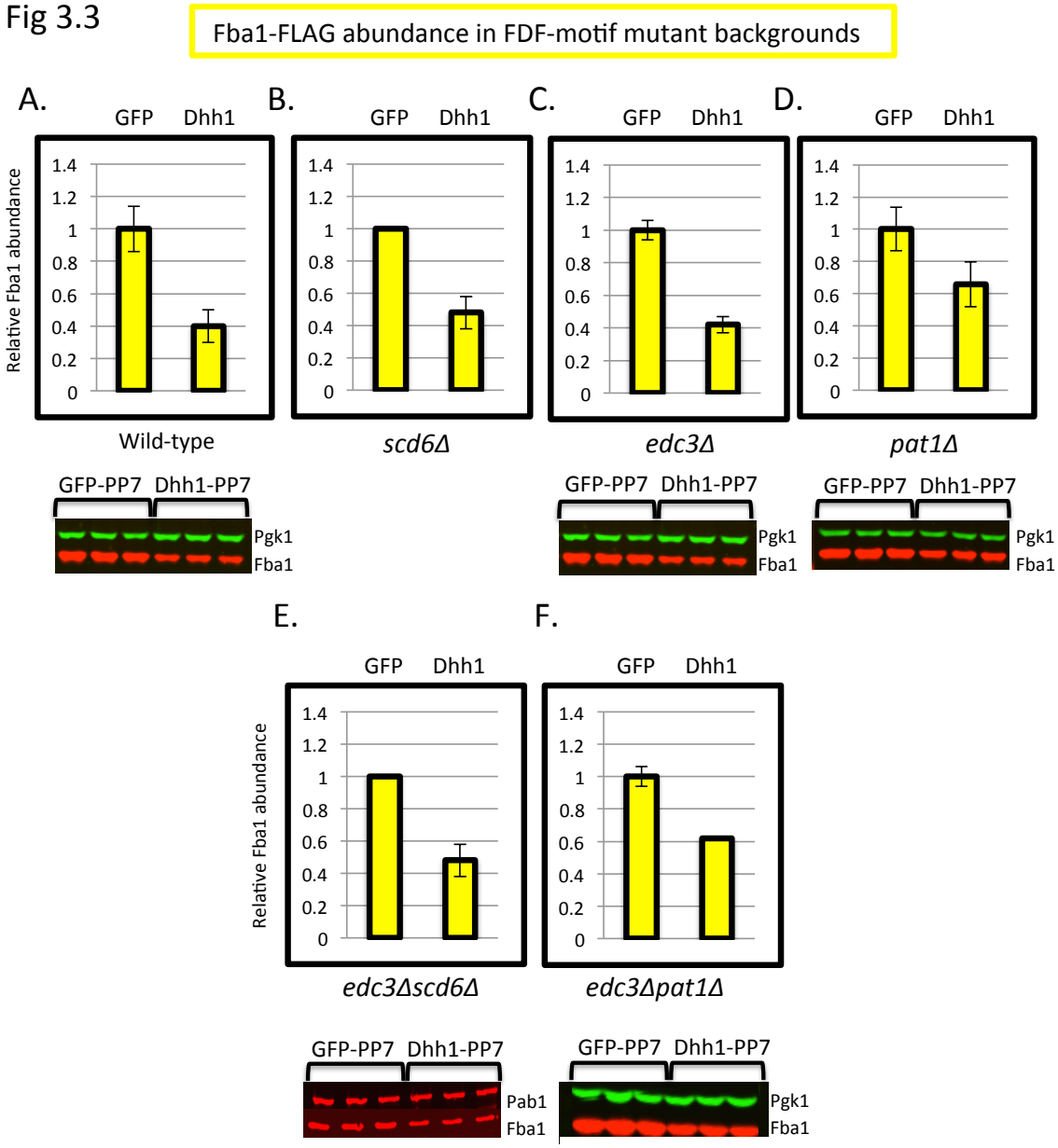

Fig 3.3 Tethering Dhh1 to *FBA1* mRNA lowers Fba1 protein levels in wild-type, *edc3Δ*, *scd6Δ*, *pat1Δ*, *edc3Δ scd6Δ*, and *edc3Δ pat1Δ* cells

(A) *FBA1-PP7L* was coexpressed with *GFP-PP7CP* or *DHH1-PP7CP* in wild-type and (B) *scd6Δ*, (C) *edc3Δ* , (D) *pat1Δ*, (E) *edc3Δ scd6Δ*, (F) *edcΔ pat1Δ*, (G) and *lsm1Δ* cells and Fba1 protein levels were determined by Western blot. Fba1 protein was normalized to Pab1 or Pgk1 levels as a loading control. Biological triplicate samples of Fba1 protein in *GFP-PP7CP* or *DHH1-PP7CP* conditions are shown below the bar graphs for each condition. Mean protein values ± standard deviation were determined from at least three independent experiments

Lsm1 is required for the decay of a Dhh1-bound mRNA, but not to repress translation

Next, we wanted to assess the role of the Lsm1-7 complex in Dhh1-tethered mRNA decay. The Lsm1-7 complex forms a heptameric ring that is thought to be recruited to an mRNA following deadenylation (Garneau et al., 2007). Moreover, the Lsm1-7 complex can specifically bind to oligoadenylated mRNAs *in vitro* and *in vivo* (Chowdhury and Tharun, 2008; Chowdhury et al., 2007), and was therefore suggested that it functions at – or immediately following – the deadenylation step. To test if Dhh1 requires the Lsm1-7 complex to stimulate decay of a tethered mRNA, we expressed *GFP-PP7CP* or *DHH1-PP7CP* in *lsm1Δ* cells, which fail to form a heptameric ring complex (Tharun et al., 2000). Interestingly, tethering Dhh1 to *FBA1* mRNA in an *lsm1Δ* mutant prevented Dhh1-mediated decay, with mRNA levels stabilized to a similar level as observed in *xrn1Δ* and *dcp1Δ* mutant cells **(Fig 3.2 G)** (Carroll et al., 2011). Dhh1 therefore requires *LSM1* in order to stimulate mRNA decay. Although this result does not rule out that the Lsm1-7 complex may also function at an earlier step in mRNA decay, it suggests that Lsm1-7 plays an important role at a step downstream of Dhh1-mRNA binding.

If the Lsm1-7 complex functions after Dhh1-mRNA binding, it may no longer require Dhh1 once recruited to the mRNA. To test this, we built an *LSM1-PP7CP* fusion protein and expressed it in wild-type and *dhh1Δ* yeast along with *FBA1-PP7L.* Much like tethering Dhh1, tethering Lsm1 to *FBA1* in wild-type cells led to a decrease in *FBA1* mRNA levels compared to a non-tethered control, demonstrating that Lsm1 is sufficient to stimulate decay of a bound mRNA **(Fig 3.4 A).** Fba1 protein levels were also decreased in cells where Lsm1 was tethered to *FBA1* mRNA **(Fig 3.5)**. Importantly, in *dhh1Δ* yeast, Lsm1-PP7CP can still stimulate *FBA1* mRNA decay **(Fig 3.4 B)**. Of note, *FBA1* mRNA levels of Lsm1-tethered mRNA were reduced to a significantly lower level in *dhh1Δ* cells, which may indicate that degradation may be enhanced by loss of Dhh1. However, more experiments will be needed to confirm that the increase in *FBA1* turnover is specifically due to the loss of *DHH1*, rather than differences between the two strain backgrounds. Regardless, these results show that Lsm1 functions at a step in mRNA decay after Dhh1-mRNA binding.

Fig 3.4

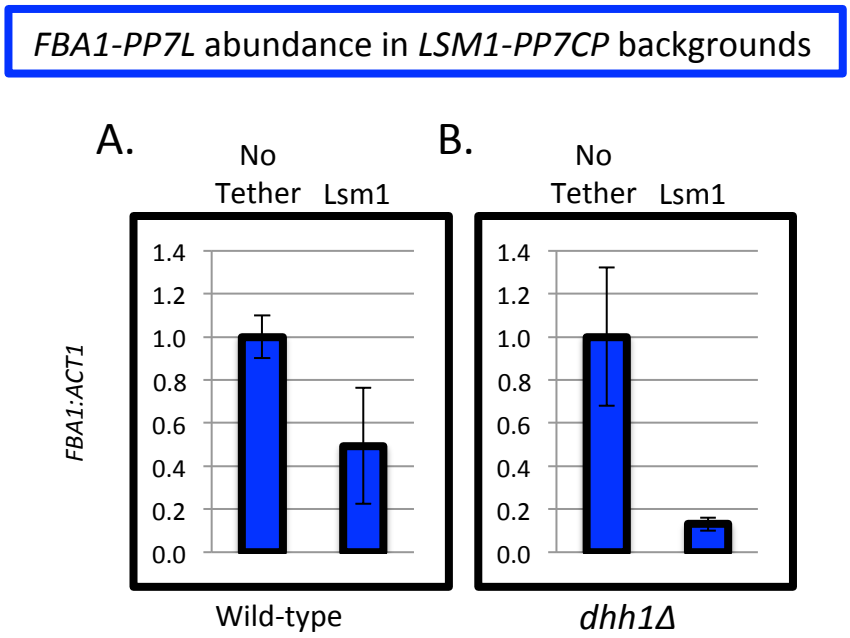

Figure 3.4: Lsm1 stimulates decay of a tethered mRNA independent of Dhh1
(A) *FBA1-PP7L* was coexpressed with *LSM1-PP7CP* or in the absence of tether in wild-type cells or (B) *dhh1Δ* cells. mRNA levels were determined by RT-qPCR. *FBA1* levels were normalized to the *ACT1* gene. Mean values ± standard deviation were determined from at least three independent experiments.

Fig 3.5

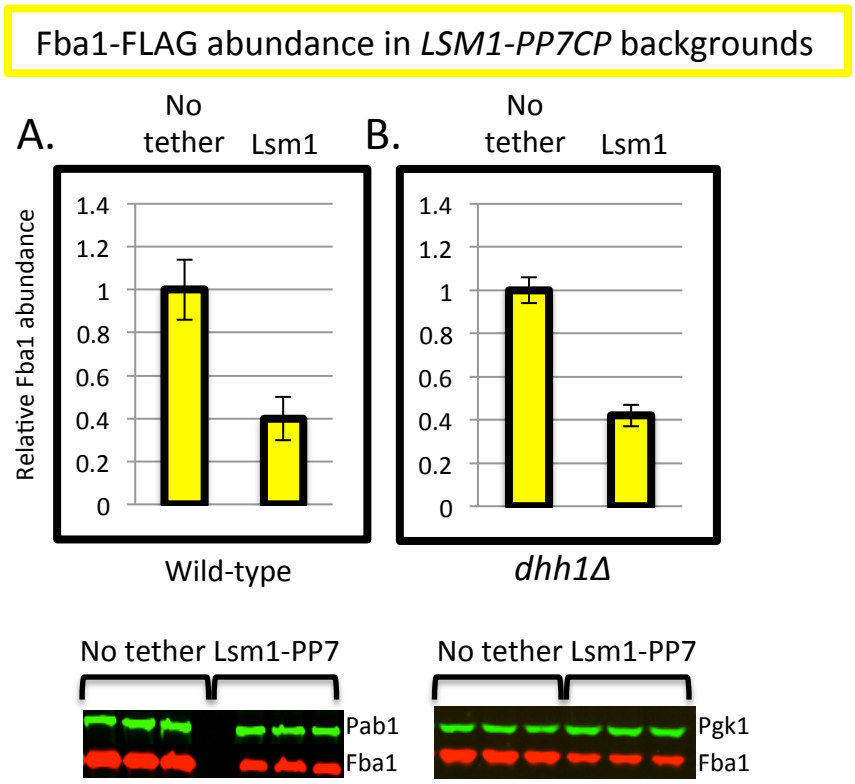

Fig 3.5 Tethering Lsm1 to *FBA1* mRNA lowers Fba1 protein levels in wild-type and *dhh1Δ* cells:
(A) *FBA1-PP7L* was coexpressed with *GFP-PP7CP* or *DHH1-PP7CP* in wild-type and (B) *dhh1Δ* cells and Fba1 protein levels were determined by Western blot. Fba1 protein was normalized to Pab1 or Pgk1 levels as a loading control. Biological triplicate samples of Fba1 protein in *LSM1*-PP7CP or no tether conditions are shown below the bar graphs for each condition. Mean protein values ± standard deviation were determined from at least three independent experiments.

Interestingly, although recruitment of Dhh1 to *FBA1* mRNA via tethering could not lower mRNA levels in the absence of *LSM1*, Fba1 protein levels nonetheless decreased **(Fig 3.6 A-B)**. This suggests that in the absence of *LSM1,* Dhh1 can still repress mRNA translation. Thus, the *lsm1Δ* strain phenocopies the Dhh1-*FBA1* tethering results observed in *dcp1Δ* cells **(Fig 3.6 A-B**; Carroll et al., 2011). One possible explanation for a decrease in Fba1 protein levels under these conditions is that the *FBA1* mRNA accumulates in a deadenylated state that is refractory for translation. To test whether or not deadenylation contributed to the reduction of Fba1 protein levels, we performed an RNase H cleavage assay to determine the poly(A) status of GFP and Dhh1-tethered *FBA1* mRNA in *lsm1Δdhh1Δ* cells. *FBA1* mRNA showed a large mobility range in both GFP and Dhh1 tethering samples that

was lost upon treatment of the RNA with oligo(dT) and RNase H, consistent with the presence of a poly(A) tail **(Fig 3.6 C)**. Poly(A)-analysis of both GFP and Dhh1-tethered *FBA1* in *dcp1Δ dhh1Δ* yeast also showed a similar trend **(Fig 3.6 D)**. These results show that translational repression of a Dhh1-tethered mRNA is not due to loss of the poly(A) tail, and that Dhh1 represses translation independent of deadenylation.

Fig 3.6

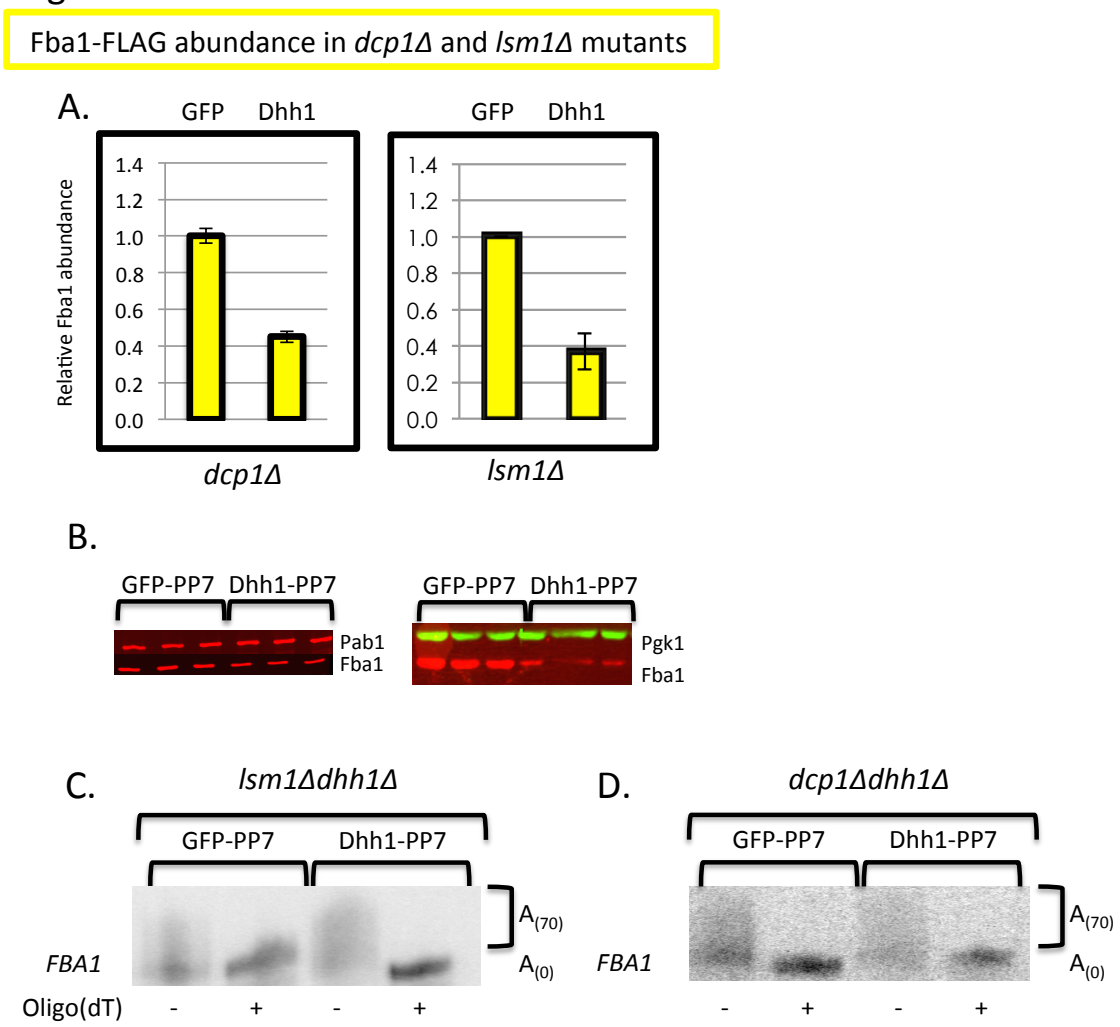

Figure 3.6: Lsm1 can stimulate mRNA decay of a bound mRNA when tethered independent of *DHH1*

(A-B) *FBA1-PP7L* was coexpressed with *GFP-PP7CP* or *DHH1-PP7CP* in *dcp1Δ* and *lsm1Δ* cells and Fba1 protein levels were determined by Western blot. Fba1 protein was normalized to Pab1 or Pgk1 levels as a loading control. Biological triplicate samples of Fba1 protein in GFP-PP7CP or Dhh1-PP7CP conditions are shown below the bar graphs for each condition. Mean protein values ± standard deviation were determined from at least three independent experiments. (C) RNase H assay to determine *FBA1* poly(A) status. Dhh-PP7CP or GFP-PP7CP were expressed in *lsm1Δ*

dhh1Δ cells or (D) in *dcp1Δ dhh1Δ* cells. RNA was extracted and resolved on a Urea-PAGE gel followed by Northern blot. Poly(A) status was determined by incubating RNA samples with an internal antisense *FBA1* probe to cleave *FBA1* (about 1.1 kb) to a shorter form (0.28 kb), and treated with (+) or without (-) an oligo(dT) probe to cleave poly(A) tails. $A_{(70)}$ indicates poly(A) mRNA, and $A_{(0)}$ indicates deadenylated mRNA.

Dhh1 requires Pat1 to repress translation of a bound mRNA

The analysis of *FBA1* poly(A) status suggests that Dhh1 represses translation of a bound mRNA in a deadenylation-independent manner. However, the factors needed for Dhh1-mediated translation repression are still unknown. The fact that Dhh1 can repress translation in *dcp1Δ* and *lsm1Δ* cells allows us to uncouple changes in Fba1 protein levels due to translational repression and *FBA1* mRNA decay and to further investigate the mechanism of Dhh1 in translation repression. We therfore performed a similar analysis as in Figure 1, by expressing *DHH1-PP7CP* or *GFP-PP7CP* in *dcp1Δ* cells, or *dcp1Δ scd6Δ*, *dcp1Δ edc3Δ*, and *dcp1Δ pat1Δ* double mutant cells and analyzed Fba1 protein levels. As expected, loss of *DCP1* prevented degradation of Dhh1-tethered *FBA1*, leading to a stabilization of *FBA1* mRNA but a decrease in Fba1 protein **(Fig 3.7 A, E)**. *FBA1* mRNA levels were also stabilized in *dcp1Δ scd6Δ*, *dcp1Δ edc3Δ*, and *dcp1Δ pat1Δ* cells, consistent with a block in mRNA decay **(Fig 3.7 B-D).** Similarly to *dcp1Δ* cells, tethering Dhh1 to *FBA1* mRNA in *dcp1Δ edc3Δ* cells still caused a decrease in Fba1 protein levels **(Fig 3.7 G)**, suggesting that Edc3 is dispensable for translation repression of a Dhh1-bound mRNA. In *dcp1Δ scd6Δ* mutant cells, there was a small – but significant – increase in Fba1 protein levels **(Fig 3.7 F)**, which may indicate that a pool of Fba1 protein is repressed by Dhh1 in an Scd6-dependent manner. Most strikingly, however, tethering Dhh1 to *FBA1* mRNA in *dcp1Δ pat1Δ* mutants showed a complete loss of Fba1 translational repression **(Fig 3.7 H)**. Still, Dhh1 is able to stimulate mRNA decay of a bound reporter in the absence of Pat1 **(Fig 3.2 D)**, suggesting there are different requirements for Pat1 in Dhh1-mediated translation repression and mRNA decay, and that these pathways are functionally separable from one another.

Fig 3.7

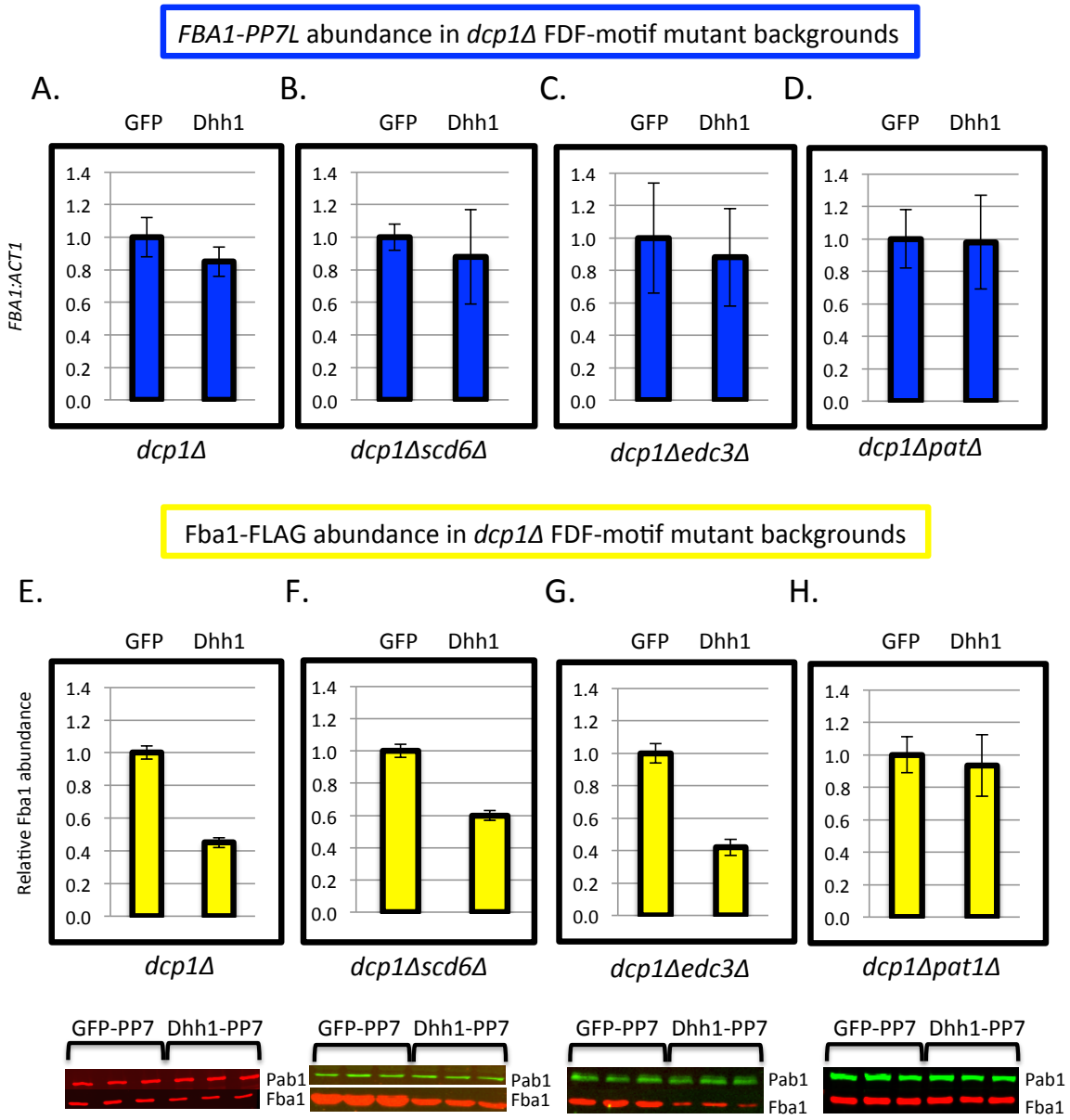

Fig 3.7: Dhh1 requires Pat1 to repress translation of a target mRNA:
(A, E) *FBA1-PP7L* was coexpressed with *GFP-PP7CP* or *DHH1-PP7CP* in *dcp1Δ* cells and (B, F) *dcp1Δ scd6Δ*, (C, G) *dcp1Δ edc3Δ*, and (D, H) *dcp1Δ pat1Δ*, cells. *FBA1-PP7L* mRNA levels were determined by RT-qPCR, and were normalized to the *ACT1* gene in (A-D). Fba1 protein levels were determined by Western blot in (E-H). Fba1 protein was normalized to Pab1 or Pgk1 levels as a loading control. Biological triplicate samples of Fba1 protein in GFP-PP7CP or Dhh1-PP7CP conditions are shown below the bar graphs for each condition. Mean protein values ± standard deviation were determined from at least three independent experiments

Pat1 is unable to repress translation of a bound mRNA

As Dhh1 is unable to repress translation in the absence of *PAT1*, we wanted to assess whether Pat1 functions in translation repression at a step after Dhh1-mRNA binding, similar to how Lsm1 is required for mRNA decay after Dhh1 binds to the message. Like Dhh1, Pat1 was also previously shown to repress translation *in vitro* and *in vivo*, and yeast lacking *PAT1* show an increase in S^{35}-methionine incorporation *in vivo* compared to wild-type yeast (Coller and Parker, 2005). Furthermore, Pat1 has also been shown to repress translation at, or prior to, the initiation step *in vitro* by blocking the formation of the 48S-preinitation complex (Nissan et al., 2010). Much like Dhh1 and Lsm1, tethering of Pat1 to *FBA1* mRNA caused a dramatic decrease in mRNA and protein levels in wild-type cells **(Fig 3.8 A, D)**, which demonstrates that Pat1 can stimulate degradation of a bound mRNA. Moreover, Dhh1 and Edc3 were not required for decay of Pat1-tethered *FBA1* mRNA **(Fig 3.9 B-C)**. To interrogate whether Pat1 can also repress translation when bound to an mRNA, we tethered Pat1-PP7CP to *FBA1-PP7L* in wild-type, *dcp1Δ,* and *lsm1Δ* cells. As expected, loss of *DCP1* or *LSM1* significantly stabilized Pat1-tethered *FBA1* mRNA levels **(Fig 3.8 B-C)**. However, when tethered to the *FBA1-PP7L* reporter in *dcp1Δ* or *lsm1Δ* cells, Pat1-PP7CP was unable to lower Fba1 protein levels, unlike Dhh1 **(Fig 3.8 E-F)**. This result is surprising, given Pat1's previously described role in translation repression (Coller and Parker, 2005; Nissan et al. 2010). While the lack of Pat1 activity in translation repression could be an artifact of tethering, it can still stimulate mRNA decay **(Fig 3.8 A)**, which suggests that tethering Pat1 does not abrogate its function. Nonetheless, Pat1 and Dhh1 appear to have distinct functions in mRNA decay and translation repression while at the mRNA, and Pat1 recruitment to an mRNA alone is not sufficient for translational repression.

Fig 3.8

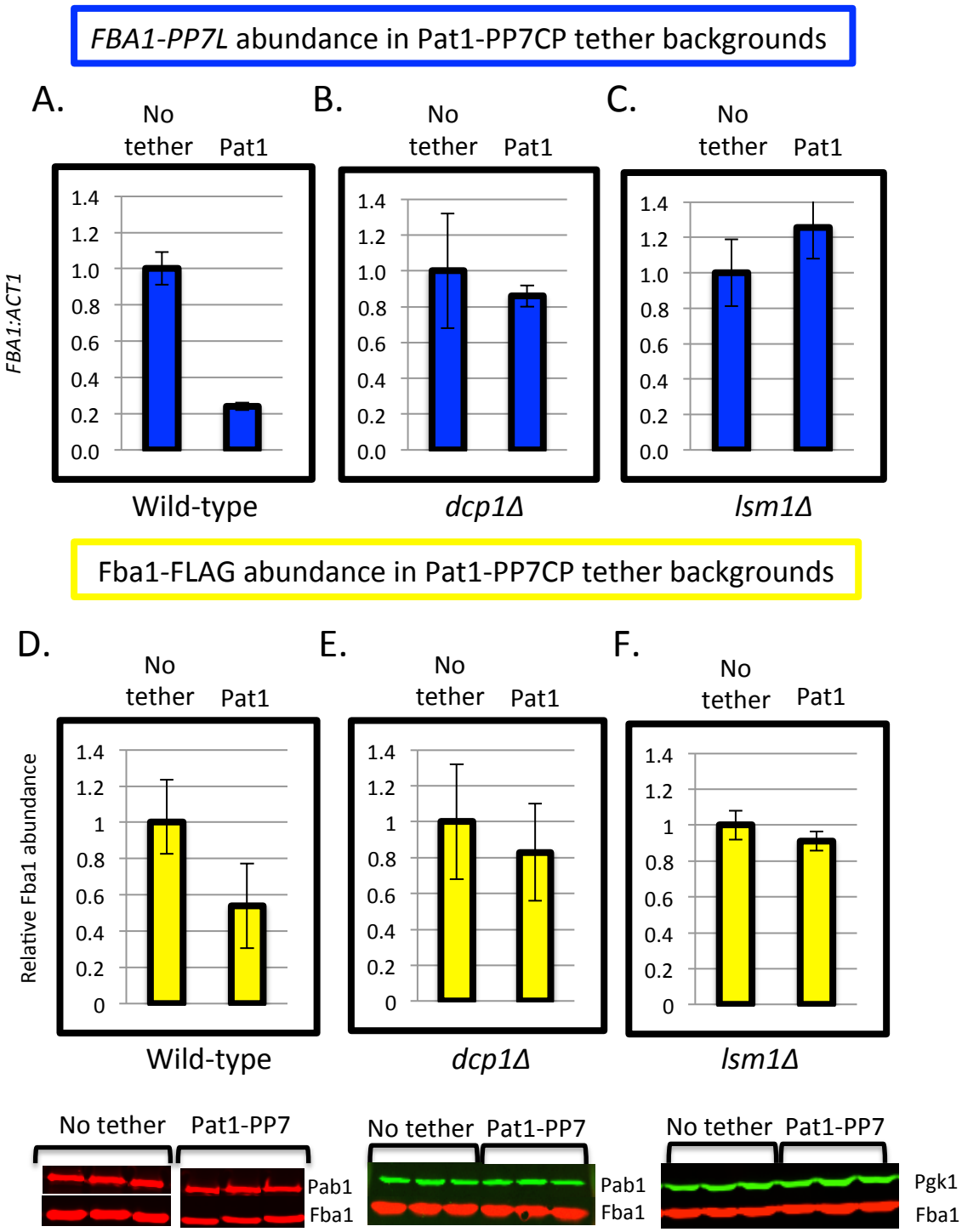

Fig 3.8: Pat1 can stimulate decay of a bound mRNA, but cannot repress translation

(A, D) *FBA1-PP7L* was coexpressed with *PAT1-PP7CP* or in the absence of tether in wild-type (B, E) *dcp1Δ*, (C, F) or *lsm1Δ* cells. *FBA1-PP7L* mRNA levels were determined by RT-qPCR, and were normalized to the *ACT1* gene in (A-D). Fba1

protein levels were determined by Western blot in (D-F). Fba1 protein was normalized to Pab1 or Pgk1 levels as a loading control. Biological triplicate samples of Fba1 protein in *PAT1-PP7CP* or no tether conditions are shown below the bar graphs for each condition. Mean protein values ± standard deviation were determined from at least three independent experiments

Fig 3.9

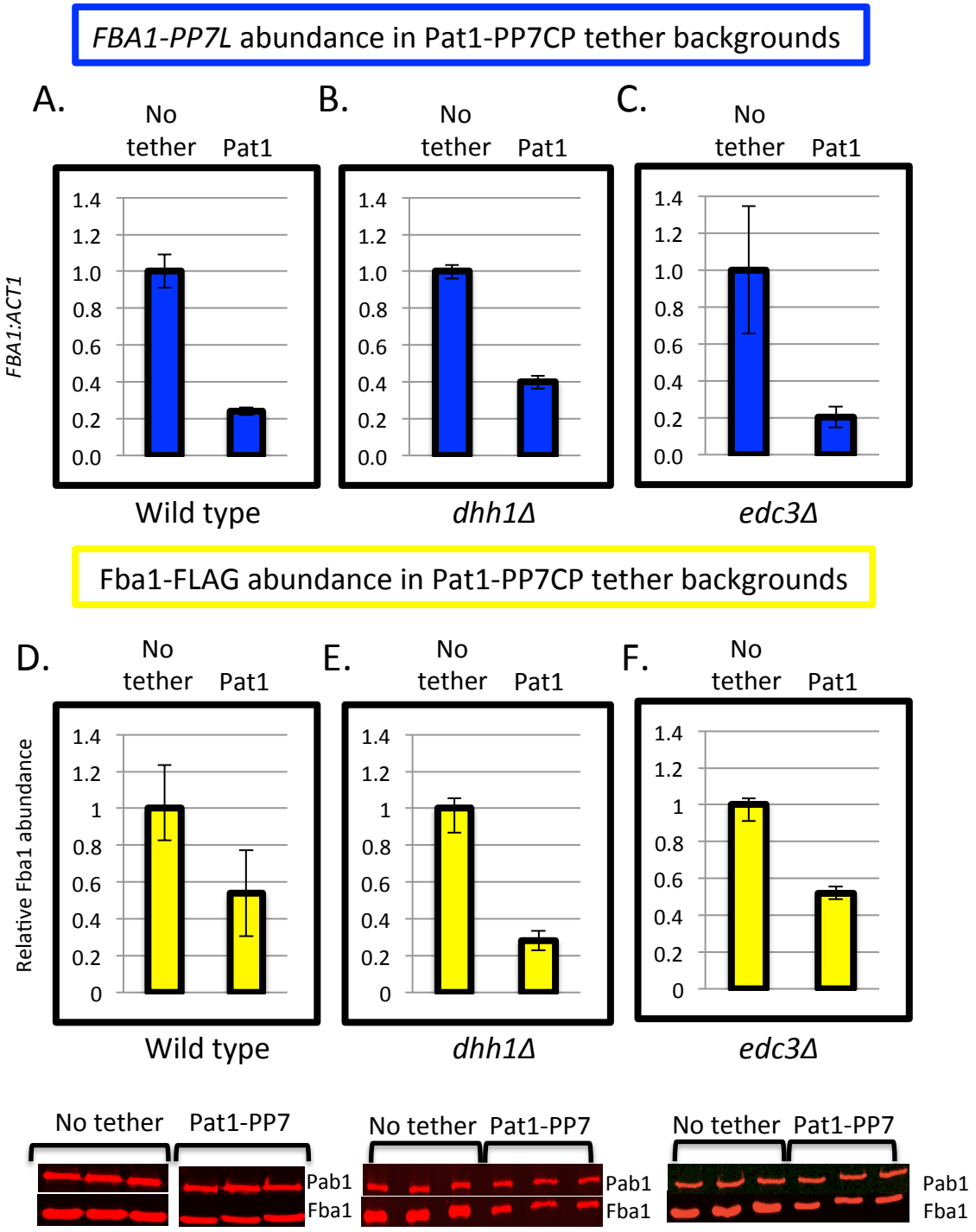

Fig 3.9: Pat1 can stimulate mRNA decay independent of Dhh1 and (A, D) *FBA1-PP7L* was coexpressed with *PAT1-PP7CP* or in the absence of tether in wild-type cells or in (B, E) *dhh1Δ*, or (C, F) *edc3Δ* cells. *FBA1-PP7L* mRNA levels were determined by RT-qPCR in (A-C) Fba1 protein levels were determined by Western blot in (D-F). Fba1 protein was normalized to Pab1 or Pgk1 levels as a loading

control. Biological triplicate samples of Fba1 protein in *PAT1*-PP7CP or no tether conditions are shown below the bar graphs for each condition. Mean protein values ± standard deviation were determined from at least three independent experiments. Wild-type *FBA1* mRNA and protein graphs (A and D) are the same as shown in Fig 3.8 and are used as references for comparison.

Discussion

In this study we utilized a PP7-based tethering assay in an effort to interrogate the mechanistic requirements of mRNA turnover and translation repression in *S. cerevisiae*. In summary, we show using this approach that Dhh1 differentially utilizes mRNA decay factors for distinct functions in translation repression and mRNA turnover, and provide some mechanistic understanding of the essential requirements for these activities **(Fig 3.10)**. One caveat of this approach is that it may not recapitulate the means by which mRNA decay factors are normally recruited to the mRNA, and that tethered protein factors may not be fully functional. However, because we have not yet identified how decay factors are normally recruited to the mRNA, the PP7 tethering system is a powerful tool for assessing requirements of mRNA turnover and translation repression following Dhh1-mRNA binding *in vivo*.

We took advantage of the Dhh1-PP7CP-based tethering assay to assess the function of several factors that have been recently described to associate with decay-competent and translationally repressed mRNPs but whose mechanistic role in mRNA decay is unknown. This includes the FDF-motif containing proteins Scd6, Edc3, and Pat1 (Decker et al., 2007; Kshirsagar and Parker, 2004; Tanaka et al., 2006). We demonstrate that mRNA decay of a Dhh1-bound mRNA is not affected in *scd6Δ*, *edc3Δ*, and *pat1Δ* mutant cells, suggesting these factors are not required for degradation. One explanation for this observation is that Dhh1 is able to efficiently bind Dcp1 and Dcp2 in the absence of these factors once it is recruited to the mRNA, which is consistent with previous observations that Dhh1 can bind to Dcp2 directly (Decker et al., 2007). An alternative explanation is that Edc3, Scd6, and Pat1 only participate in the degradation of specific mRNAs.

Interestingly, *LSM1* was required for degradation of a Dhh1-bound mRNA. The Lsm1-7 complex binds preferentially to oligoadenylated mRNAs *in vitro* and *in vivo* (Chowdhury and Tharun, 2008; Chowdhury et al., 2007), which could explain how deadenylated mRNAs are first targeted for mRNA decay. However, more recent work also suggests that the Lsm1-7 complex may activate decapping following RNA binding (Chowdhury and Tharun, 2009). Furthermore, *lsm1Δ* mutants form constitutive PBs, similar to *dcp1Δ* and *xrn1Δ* cells (Teixeira et al.,2007). Together, these data suggest that in addition to recognition of oligoadenylated mRNAs, Lsm1 also functions at late step in decapping or decay.

Our lab previously showed that Dhh1 can repress translation of a bound mRNA in the absence of decapping or exonuclease activity (Carroll et al., 2011). In this study, we demonstrate that translational repression is not due to loss of the poly(A) tail, which could indirectly decrease the translational competency of the

mRNA. Furthermore, we show that Dhh1 requires Pat1 for translational repression, based on the observation that Dhh1 cannot lower Fba1 protein levels in the absence of *PAT1* in *dcp1Δ* cells, where mRNA decay and translation repression are uncoupled. In contrast, Edc3 and Scd6, which bind to the C-terminal RecA domain of Dhh1 through an FDF-motif peptide in a similar manner as Pat1 (Sharif et al., 2013; Tritschler et al., 2009), do not disrupt translation repression of a Dhh1-tethered mRNA. This indicates that Pat1 is specifically required for Dhh1 function as a translational repressor. Surprisingly, despite evidence that Pat1 can repress translation at the initiation step (Coller and Parker, 2005; Nissan et al., 2010), Pat1 does not repress translation when tethered to *FBA1*. It is conceivable that the inability of Pat1 to repress translation is an artifact of tethering. For instance, Pat1 may be too confined by tethering to function properly, or may be ineffective when targeted specifically to the 3'UTR. However, Pat1 is thought to strongly bind to proteins of the Lsm1-7 complex, and contributes to its RNA binding activity, making it likely to associate with the 3' end of messages (Chowdhury et al., 2007, 2012, 2014). Moreover, crosslinking and immunoprecipitation (CLIP) experiments show that Pat1 preferentially binds to the 3' end of the mRNA (Mitchell et al., 2013). One alternative explanation is that Pat1 must interact with Dhh1 to repress translation of a bound mRNA, or that Pat1 inhibits translation by a mechanism that does not involve direct RNA binding. Although, Pat1 cannot repress translation of a bound mRNA, it can nonetheless stimulate its degradation, which suggests translation repression and mRNA decay may be independent pathways with unique requirements.

In mammalian cells, multiple copies of Rck/p54 – the mammalian ortholog of Dhh1 – can bind to mRNA *in vivo* (Ernoult-Lange et al., 2012). Furthermore, Dhh1 is also present in considerable excess over mRNA in both mammalian cells and yeast (Ernoult-Lange et al., 2012; Gygi et al., 1999). Together, this may suggest that multiple Dhh1 proteins bind to an mRNA in order to repress its translation or stimulate its degradation. Consistent with this hypothesis, CLIP studies have shown that Dhh1 can bind many targets with more than one copy (Mitchell et al., 2013).

One possible mechanism for Dhh1 function in translation repression is that Pat1 binding to Dhh1 is required for Dhh1 multimerization on the RNA. Multimerization by Dhh1 could disrupt mRNA circularization and therefore the interaction between Pab1 and eIF4G that is needed for efficient translation. As a result, the mRNA would no longer be translationally competent, and instead would be targeted for either storage and/or degradation. This hypothesis implies that Dhh1 would not repress translation at a specific step *per se*, and is consistent with observations that Dhh1 represses translation at the level of both elongation and initiation (Coller and Parker, 2005; Sweet et al., 2012).

An unresolved question in mRNA turnover is whether or not mRNA decay and translation repression occur at distinct cellular locations. Given that mRNA decay factors localize in cytoplasmic processing bodies (PBs) during stress, one hypothesis is that mRNAs destined for decay are targeted to PB foci. However, while PBs were initially identified as sites of mRNA decay (Sheth and Parker, 2003), increasing evidence suggests that these granules are primarily sites of translation repression and mRNA storage (Aizer et al., 2014; Buchan, 2014; Lavut and Raveh,

2012; Zid and O'Shea, 2014). Thus, following stress, Dhh1 may trigger translational repression by shuttling mRNAs into PBs in a Pat1-dependent manner, while mRNAs destined for decay are degraded in the cytoplasm. Future work is needed to determine if translation repression and mRNA decay happen in specific locations within the cell, and if these two functions of Dhh1 are independent of one another or are part of the same path.

Fig 3.10

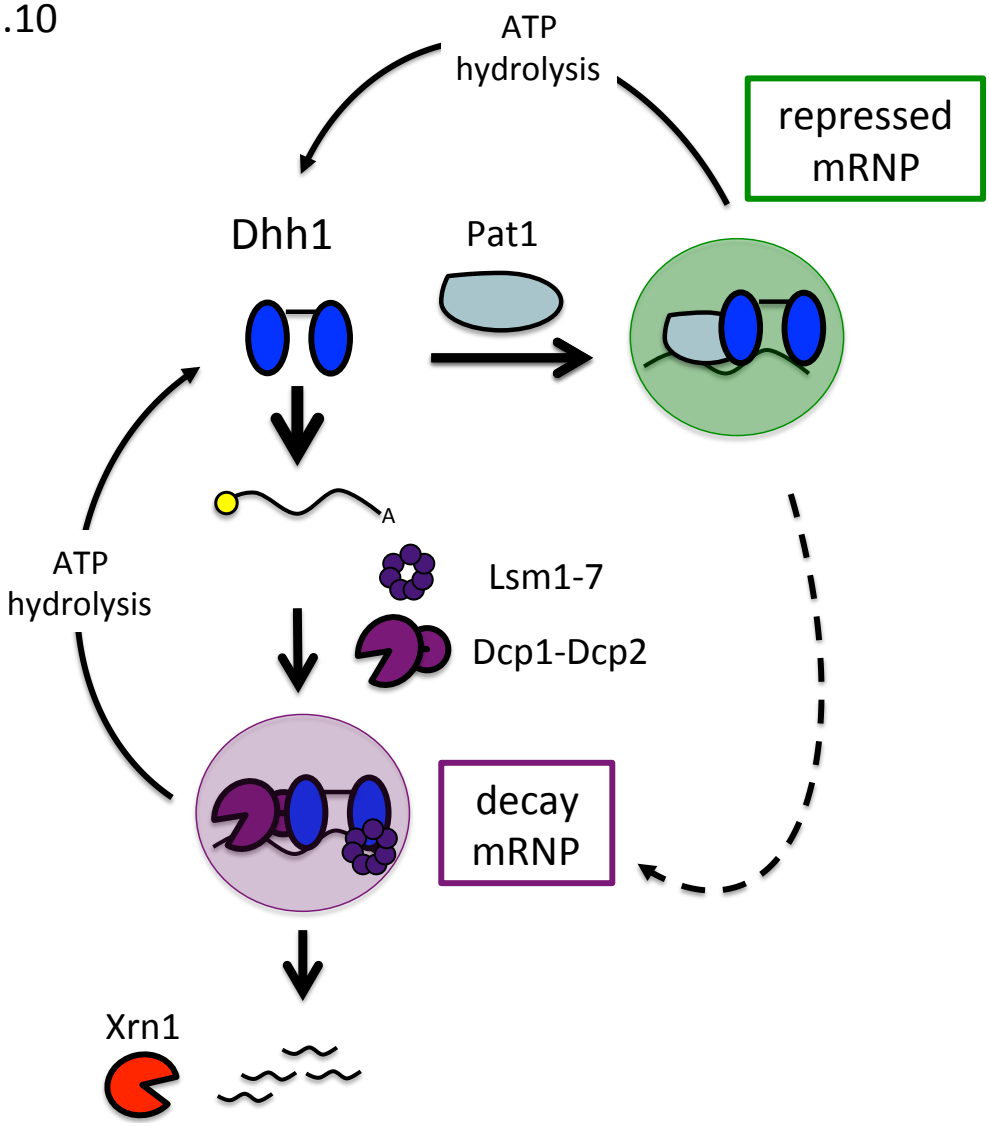

Figure 3.10: Model of Dhh1 functions in translation repression and mRNA decay

Dhh1 has distinct requirements to repress translation and stimulate decay of a bound mRNA. Following Dhh1 binding, the Lsm1-7 complex, the Dcp1-Dcp2 decapping coenzyme, and Xrn1 are required to degrade mRNA. In contrast, Pat1 is not needed for mRNA degradation, but is required for Dhh1 to repress translation of a bound mRNA.

Experimental Procedures

Construction of yeast strains and plasmids:

Construction of plasmids for this study (Table S1) was performed using standard molecular cloning techniques. Yeast deletion strains were made by PCR-based homologous recombination transformations, using integration and tagging vectors as previously described (Longtine et al. 1998, Carroll et al 2011). Double knockout strains were made either using the PCR-based transformation method described above, or by mating and dissection of sporulated yeast.

The generation of bacteriophage PP7-CP and PP7-loop tagging plasmids was described previously (Carroll et al. 2011), and were gifts from B. Hogg and K. Collins (University of California, Berkeley, Berkeley, CA; Hogg and Collins 2007).

Tethering assay:

Sample preparation was performed as previously described (Carroll et al 2011). Briefly, yeast cells were grown to mid-log phase (OD_{600} = 0.4-0.8) in synthetic media containing 2% dextrose. Cells were collected by centrifugation and lysed in 1X Phospho-buffered saline (PBS) with 0.1% Tween-20 and protease inhibitors. Lysis was performed using three 1-min pulses using a multi-bead beater (Biospec Products). Extract was clarified by centrifugation, and extract was split for protein and RNA measurements. Protein samples were normalized by total protein content by Bradford Assay (Bio-Rad Laboratories). RNA was isolated using the RNeasy RNA isolation kit (Qiagen) or by hot acid phenol extraction. RNA samples were treated with DNase I (Ambion) to remove contaminating genomic DNA.

For hot acid phenol extraction, frozen cell pellets were resuspended in 600uL TES buffer (10mM Tris-HCl pH=7.5, 10mM EDTA, 0.5% SDS). Acid saturated phenol was added and cells were incubated at 65° C for 1 hour with occasional vortexing. Samples were transferred to ice for 5 minutes and spun at 4° C at max speed. The aqueous phase was extracted and a second phenol extraction was done, followed by a chloroform extraction and ethanol precipitation. RNA was stored at -80° C.

RT-qPCR:

RNA was isolated as described above and quantified using a NanoDrop spectrophotometer (Fischer Scientific). cDNA was generated by reverse transcription of 1μg of RNA using a random hexamer oligonucleotides (Invitrogen) and Superscript II (Invitrogen). Quantitative PCR was performed in real time using the StepOnePlus (Applied Biosystems) with gene specific primers and a SYBR-Green ROX mix (Thermo Scientific) supplemented with gene specific primers.

Poly(A) assay:

RNA was isolated as described above and quantified using a NanoDrop spectrophotometer (Fischer Scientific). 15ug RNA was combined with a probe

antisense to the 3' end of *FBA1* mRNA and with or without an oligo(dT) probe and heated for 5 minutes at 85°C, followed by slow cooling to 37° C. RNA samples were incubated with RNaseOUT (Invitrogen) and RNase H (Invitrogen) for 1 hour at 37° C, followed by phenol:chloroform:isoamyl alcohol extraction of RNA and ethanol precipitation. RNA was resuspended in loading buffer and resolved by urea-PAGE northern blot.

Northern Blot:
RNA was isolated as described above and quantified using a NanoDrop spectrophotometer (Fischer Scientific) and separated on a 6% Urea-PAGE gel. RNA was transferred to a nitrocellulose membrane (GE Healthcare Life Sciences) and treated with antisense oligonucleotide specific to the gene of interest, end labeled with ATP-γ-^{32}P with T4 polynucleotide kinase (New England Biolabs, Inc.). Probes were hybridized overnight at 42°C in Church buffer. Membranes were washed at 42°C once with 5X saline-sodium citrate (SSC) buffer with 0.1% SDS for 30 minutes and once with 1X SSC with 0.1% SDS. RNA was visualized with a Typhoon Trio Imager (GE Healthcare).

Western Blot:

Proteins from yeast lysates were separated by SDS-PAGE and transferred to nitrocellulose membrane (GE Health Sciences). Membranes were blocked in phosphor-buffered saline (PBS) with 4% non-fat milk, followed by incubation with primary antibody over night and secondary antibody for 45 minutes. Membranes were analyzed and quantified using an infrared imaging system (Odyssey; LI-COR Biosciences). The following primary antibodies were used for detection of tagged proteins: anti-FLAG, anti-Pgk1, anti-Pab1, and anti-Xpo1. Fluorophore-coupled goat anti-mouse AlexaFlour 680 (Invitrogen) and goat anti-rabit IRdye800 (Rockland Immunochemicals) were used as secondary antibodies.

Table 3.1: Yeast Strains used in this study

Yeast Strains	Genotype	Source
KWY2180	W303α *PAT1-PP7CP*::HisMX *FBA1-FLAG-PP7L*::KanMX	This study
KWY2209	W303α *FBA1-FLAG-PP7L*::NatMX	Carroll et al. (2011)
KWY2532	W303a *dhh1Δ*::NatMX *FBA1-FLAG-PP7L*::KanMX	Carroll et al. (2011)
KWY2546	W303a *edc3Δ*::LEU2 *FBA1-FLAG-PP7L*::KanMX	This study
KWY2790	W303α stm1Δ::KanMX *FBA1-FLAG-PP7L*::NatMX	This study
KWY2791	W303α *scd6Δ*::KanMX *FBA1-FLAG-PP7L*::NatMX	This study
KWY2958	W303α *edc3Δ*::LEU2 *scd6Δ*::KanMX *FBA1-FLAG-PP7L*::NatMX	This study
KWY3023	W303α *dcp1Δ*::KanMX *pat1Δ*::HisMX *FBA1-FLAG-PP7L*::NatMX	This study
KWY3089	W303a *dhh1Δ*::NatMX *PAT1-PP7CP*::HisMX *FBA1-FLAG-PP7L*::KanMX	This study
KWY3091	W303a *edc3Δ*::*LEU2 PAT1-PP7CP*::HisMX *FBA1-FLAG-PP7L*::KanMX	This study
KWY3093	W303a *dhh1Δ*::NatMX *FBA1-FLAG-PP7L*::KanMX	This study
KWY3776	W303a *dcp1Δ*::HisMX *scd6Δ*::KanMX *FBA1-FLAG-PP7L*::NatMX	This study
KWY3778	W303a *dcp1Δ*::HisMX *edc3Δ*::*LEU2* *FBA1-FLAG-PP7L*::NatMX	This study
KWY3787	W303α *lsm1Δ*::*TRP1 FBA1-FLAG-PP7L*::NatMX	This study
KWY3903	W303α *dhh1Δ*::KanMX *FBA1-FLAG-PP7L*::NatMX	This study
KWY3905	W303α *dhh1Δ*::KanMX *FBA1-FLAG-PP7L*::NatMX *LSM1-PP7CP*::HisMx	This study
KWY3906	W303α *pat1Δ*::KanMX *FBA1-FLAG-PP7L*::NatMX	This study
KWY3908	W303α *pat1Δ*::KanMX *LSM1-PP7CP*::HisMX *FBA1-FLAG-PP7L*::NatMX	This study
KWY4578	W303α *edc3Δ*::*LEU2 pat1Δ*::KanMX *FBA1-FLAG-PP7L*::NatMX	This study

Table 3.2: Plasmids used in this study

Plasmid	Description	Source
pKW2420	pRS316 PDhh1-GFP-PP7CP; *URA3* marker	Carroll et al (2011)
pKW2321	pRS316 PDhh1-Dhh1-PP7CP; *URA3* marker	Carroll et al (2011)

References

Aizer, A., Kalo, A., Kafri, P., Shraga, A., Ben-Yishay, R., Jacob, A., Kinor, N., and Shav-Tal, Y. (2014). Quantifying mRNA targeting to P-bodies in living human cells reveals their dual role in mRNA decay and storage. J. Cell Sci. *127*, 4443–4456.

Brangwynne, C.P., Eckmann, C.R., Courson, D.S., Rybarska, A., Hoege, C., Gharakhani, J., Jülicher, F., and Hyman, A.A. (2009). Germline P granules are liquid droplets that localize by controlled dissolution/condensation. Science *324*, 1729–1732.

Buchan, J.R. (2014). mRNP granules: Assembly, function, and connections with disease. RNA Biol. *11*.

Carroll, J.S., Munchel, S.E., and Weis, K. (2011). The DExD/H box ATPase Dhh1 functions in translational repression, mRNA decay, and processing body dynamics. J. Cell Biol. *194*, 527–537.

Chowdhury, A., and Tharun, S. (2008). lsm1 mutations impairing the ability of the Lsm1p-7p-Pat1p complex to preferentially bind to oligoadenylated RNA affect mRNA decay in vivo. RNA N. Y. N *14*, 2149–2158.

Chowdhury, A., and Tharun, S. (2009). Activation of decapping involves binding of the mRNA and facilitation of the post-binding steps by the Lsm1-7-Pat1 complex. RNA N. Y. N *15*, 1837–1848.

Chowdhury, A., Mukhopadhyay, J., and Tharun, S. (2007). The decapping activator Lsm1p-7p-Pat1p complex has the intrinsic ability to distinguish between oligoadenylated and polyadenylated RNAs. RNA N. Y. N *13*, 998–1016.

Chowdhury, A., Raju, K.K., Kalurupalle, S., and Tharun, S. (2012). Both Sm-domain and C-terminal extension of Lsm1 are important for the RNA-binding activity of the Lsm1-7-Pat1 complex. RNA N. Y. N *18*, 936–944.

Chowdhury, A., Kalurupalle, S., and Tharun, S. (2014). Pat1 contributes to the RNA binding activity of the Lsm1-7-Pat1 complex. RNA N. Y. N *20*, 1465–1475.

Coller, J., and Parker, R. (2005). General translational repression by activators of mRNA decapping. Cell *122*, 875–886.

Coller, J.M., Tucker, M., Sheth, U., Valencia-Sanchez, M.A., and Parker, R. (2001). The DEAD box helicase, Dhh1p, functions in mRNA decapping and interacts with both the decapping and deadenylase complexes. RNA N. Y. N *7*, 1717–1727.

Decker, C.J., Teixeira, D., and Parker, R. (2007). Edc3p and a glutamine/asparagine-rich domain of Lsm4p function in processing body assembly in Saccharomyces cerevisiae. J. Cell Biol. *179*, 437–449.

Ernoult-Lange, M., Baconnais, S., Harper, M., Minshall, N., Souquere, S., Boudier, T., Bénard, M., Andrey, P., Pierron, G., Kress, M., et al. (2012). Multiple binding of repressed mRNAs by the P-body protein Rck/p54. RNA N. Y. N *18*, 1702–1715.

Fischer, N., and Weis, K. (2002). The DEAD box protein Dhh1 stimulates the decapping enzyme Dcp1. EMBO J. *21*, 2788–2797.

Franks, T.M., and Lykke-Andersen, J. (2008). The control of mRNA decapping and P-body formation. Mol. Cell *32*, 605–615.

Fromm, S.A., Truffault, V., Kamenz, J., Braun, J.E., Hoffmann, N.A., Izaurralde, E., and Sprangers, R. (2012). The structural basis of Edc3- and Scd6-mediated activation of the Dcp1:Dcp2 mRNA decapping complex. EMBO J. *31*, 279–290.

Garneau, N.L., Wilusz, J., and Wilusz, C.J. (2007). The highways and byways of mRNA decay. Nat. Rev. Mol. Cell Biol. *8*, 113–126.

Gygi, S.P., Rochon, Y., Franza, B.R., and Aebersold, R. (1999). Correlation between protein and mRNA abundance in yeast. Mol. Cell. Biol. *19*, 1720–1730.

Hata, H., Mitsui, H., Liu, H., Bai, Y., Denis, C.L., Shimizu, Y., and Sakai, A. (1998). Dhh1p, a putative RNA helicase, associates with the general transcription factors Pop2p and Ccr4p from Saccharomyces cerevisiae. Genetics *148*, 571–579.

Hogg, J.R., and Collins, K. (2007). RNA-based affinity purification reveals 7SK RNPs with distinct composition and regulation. RNA N. Y. N *13*, 868–880.

Holstege, F.C., Jennings, E.G., Wyrick, J.J., Lee, T.I., Hengartner, C.J., Green, M.R., Golub, T.R., Lander, E.S., and Young, R.A. (1998). Dissecting the regulatory circuitry of a eukaryotic genome. Cell *95*, 717–728.

Jonas, S., and Izaurralde, E. (2013). The role of disordered protein regions in the assembly of decapping complexes and RNP granules. Genes Dev. *27*, 2628–2641.

Krüger, T., Hofweber, M., and Kramer, S. (2013). SCD6 induces ribonucleoprotein granule formation in trypanosomes in a translation-independent manner, regulated by its Lsm and RGG domains. Mol. Biol. Cell *24*, 2098–2111.

Kshirsagar, M., and Parker, R. (2004). Identification of Edc3p as an enhancer of mRNA decapping in Saccharomyces cerevisiae. Genetics *166*, 729–739.

Lavut, A., and Raveh, D. (2012). Sequestration of highly expressed mRNAs in cytoplasmic granules, P-bodies, and stress granules enhances cell viability. PLoS Genet. *8*, e1002527.

Lim, F., and Peabody, D.S. (2002). RNA recognition site of PP7 coat protein. Nucleic Acids Res. *30*, 4138–4144.

Makino, D.L., Halbach, F., and Conti, E. (2013). The RNA exosome and proteasome: common principles of degradation control. Nat. Rev. Mol. Cell Biol. *14*, 654–660.

Marnef, A., and Standart, N. (2010). Pat1 proteins: a life in translation, translation repression and mRNA decay. Biochem. Soc. Trans. *38*, 1602–1607.

Milac, A.L., Bojarska, E., and Wypijewska del Nogal, A. (2014). Decapping Scavenger (DcpS) enzyme: advances in its structure, activity and roles in the cap-dependent mRNA metabolism. Biochim. Biophys. Acta *1839*, 452–462.

Mitchell, S.F., Jain, S., She, M., and Parker, R. (2013). Global analysis of yeast mRNPs. Nat. Struct. Mol. Biol. *20*, 127–133.

Nissan, T., Rajyaguru, P., She, M., Song, H., and Parker, R. (2010). Decapping activators in Saccharomyces cerevisiae act by multiple mechanisms. Mol. Cell *39*, 773–783.

Parker, R. (2012). RNA degradation in Saccharomyces cerevisae. Genetics *191*, 671–702.

Rajyaguru, P., She, M., and Parker, R. (2012). Scd6 targets eIF4G to repress translation: RGG motif proteins as a class of eIF4G-binding proteins. Mol. Cell *45*, 244–254.

Sharif, H., Ozgur, S., Sharma, K., Basquin, C., Urlaub, H., and Conti, E. (2013). Structural analysis of the yeast Dhh1-Pat1 complex reveals how Dhh1 engages Pat1, Edc3 and RNA in mutually exclusive interactions. Nucleic Acids Res. *41*, 8377–8390.

Sheth, U., and Parker, R. (2003). Decapping and decay of messenger RNA occur in cytoplasmic processing bodies. Science *300*, 805–808.

Sweet, T., Kovalak, C., and Coller, J. (2012). The DEAD-box protein Dhh1 promotes decapping by slowing ribosome movement. PLoS Biol. *10*, e1001342.

Tanaka, K.J., Ogawa, K., Takagi, M., Imamoto, N., Matsumoto, K., and Tsujimoto, M. (2006). RAP55, a cytoplasmic mRNP component, represses translation in Xenopus oocytes. J. Biol. Chem. *281*, 40096–40106.

Tritschler, F., Eulalio, A., Helms, S., Schmidt, S., Coles, M., Weichenrieder, O., Izaurralde, E., and Truffault, V. (2008). Similar modes of interaction enable Trailer Hitch and EDC3 to associate with DCP1 and Me31B in distinct protein complexes. Mol. Cell. Biol. *28*, 6695–6708.

Tritschler, F., Braun, J.E., Eulalio, A., Truffault, V., Izaurralde, E., and Weichenrieder, O. (2009). Structural basis for the mutually exclusive anchoring of P body components EDC3 and Tral to the DEAD box protein DDX6/Me31B. Mol. Cell *33*, 661–668.

Wolf, J., and Passmore, L.A. (2014). mRNA deadenylation by Pan2-Pan3. Biochem. Soc. Trans. *42*, 184–187.

Zid, B.M., and O'Shea, E.K. (2014). Promoter sequences direct cytoplasmic localization and translation of mRNAs during starvation in yeast. Nature *514*, 117–121.

Appendix I: Characterization of the Dhh1 and ATPase-deficient Dhh1^{DQAD} protein interactomes

Introduction

Previously, our lab demonstrated that expression of an ATPase-deficient allele of Dhh1, Dhh1^{DQAD}, leads to the constitutive formation of processing bodies (PBs) in the absence of stress. In addition, we showed that Dhh1^{DQAD} is unable to recycle in and out of PB foci (Carroll et al., 2011). Because Dhh1^{DQAD} is trapped in PB foci, we hypothesized that this mutant protein may show an increase in association with factors that assemble in PBs. The increase in association with certain PB factors may be due to an inability of Dhh1^{DQAD} to recycle off of an ATPase-activating protein or a resident PB protein. In this appendix I assess the interactome of Dhh1 and Dhh1^{DQAD}. In summary, I show that the interacting proteins of affinity purified Dhh1^{DQAD} mRNA-protein (mRNP) complexes does not differ significantly from wild-type Dhh1 mRNPs. Furthermore, I demonstrate that only a fraction of the total Dhh^{DQAD}-GFP protein pool is localized to PBs by fluorescent quantification of Dhh1^{DQAD}-GFP in constitutively forming PBs. This may explain why few differences are observed between Dhh1 and Dhh1^{DQAD} mRNP complex composition.

Results and Discussion

Several mRNA decay factors colocalize in protein foci in Dhh1^{DQAD} cells

Given that Dhh1^{DQAD} constitutively colocalizes with Dcp2 – even in the absence of PB-inducing conditions – we wanted to confirm that the composition of these foci is similar to PBs by testing whether or not other mRNA decay factors also localize to foci in cells expressing Dhh1^{DQAD}. To further investigate the "DQAD bodies" that form in glucose replete conditions, several known decay factors were C-terminally GFP tagged and expressed in the presence of wild-type Dhh1 or Dhh1^{DQAD}. In cells expressing Dhh1, four different mRNA decay factors – Dcp1, Pat1, Xrn1, and Edc3 – localized diffusely throughout the cytoplasm **(Fig 4.1 A)**. However, in cells expressing Dhh1^{DQAD}, all four factors localized in foci **(Fig 4.1 B)**. This observation suggests these factors are present in PBs, however, direct colocalization with Dcp2 and/or Dhh1^{DQAD} is needed to confirm that these foci are in fact *bona fide* PBs.

Fig 4.1

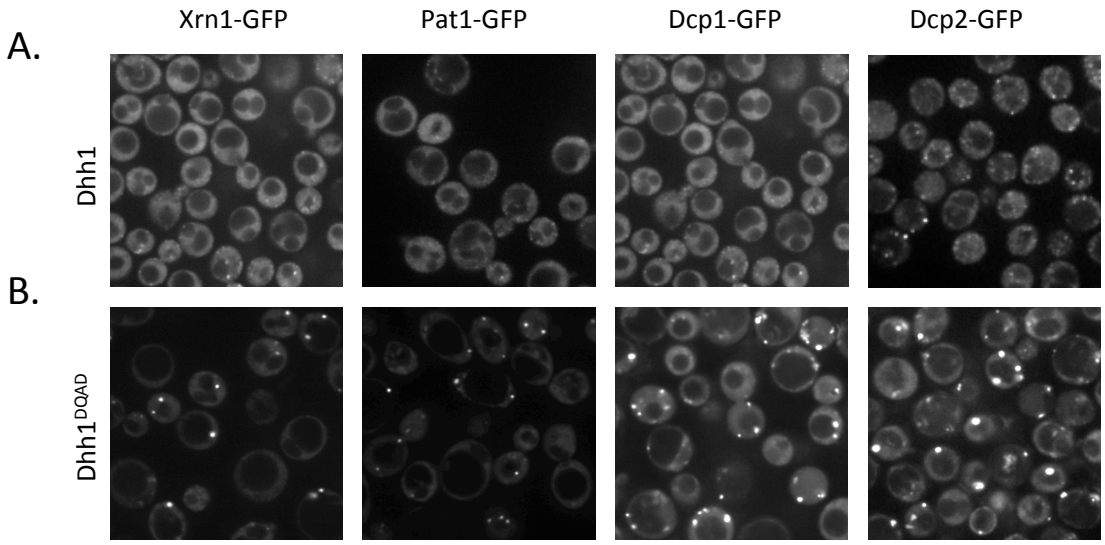

Fig 4.1: Several decay factors localize with Dhh1^{DQAD}
Xrn1, Pat1, Dcp1, and Dcp2 were C-terminally tagged with GFP and expressed in either (A) *DHH1* or (B) *DHH1^{DQAD}* cells. Cells were grown to mid-log phase (OD_{600}=0.3-0.8) and foci formation was assessed by fluorescent microscopy.

Dhh1 and Dhh1^{DQAD} do not show significant differences in their protein interactome

Because the ATPase-deficient Dhh1^{DQAD} mutant shows a significant change in its localization pattern compared to wild-type Dhh1 in logarithmically growing yeast, I wanted to examine whether Dhh1^{DQAD} and wild-type Dhh1 have different interactions mRNA decay factors during vegetative growth. To assess protein-protein interactions of Dhh1 and Dhh1^{DQAD}, the wild-type and mutant proteins were C-terminally tagged with a tandem affinity purification tag (TAP) and expressed in *dhh1Δ* cells. Affinity purifications were performed using IgG-coupled magnetic beads, and co-precipitating factors were identified by mass spectrometry. Consistent with prior observations, Dhh1-TAP interacted with decapping factors, the deadenylation machinery, the 5'-3' exonuclease Xrn1, translational repressors, and other factors with poorly understood function in 5'-3' mRNA turnover during logarithmic growth **(Fig 4.2 A, data not shown)** (Coller et al., 2001; Mitchell et al., 2013; Nissan et al., 2010; Sharif et al., 2013; Tritschler et al., 2009). Interestingly, there were no significant differences in interaction between wild-type Dhh1 and Dhh1^{DQAD}.

One possible explanation for the similar protein interaction network between wild-type and mutant Dhh1 proteins is that there are changes in composition in different Dhh1-containing subcomplexes that are impossible to separate from the total Dhh1-mRNP pool in a large-scale experiment. For example, while Dhh1^{DQAD} forms PBs constitutively, the amount of Dhh1 present in PBs may be only a small fraction of the total pool of Dhh1 protein. To measure the amount of Dhh1 protein present in PB foci, Dhh1-GFP or Dhh1^{DQAD}-GFP were expressed in

dhh1Δ cells. In order to compare PBs between the two conditions, cells were shifted to glucose-free media and the fluorescent intensity of Dhh1 and Dhh1^{DQAD} within foci and in the cytoplasmic pool were quantified. Dhh1-GFP and Dhh1^{DQAD}-GFP localization to PBs was confirmed by colocalization with Dcp2-mCherry (data not shown). Interestingly, the Dhh1-GFP fluorescence within the PB was only around 17% of the total protein **(Fig 4.2 B)**, thus revealing that the vast majority of Dhh1 is localized to the cytoplasm even during glucose starvation. Dhh1^{DQAD}-GFP PB fluorescence was only slightly higher than wild-type Dhh1, with around 21% of the total protein localizing to PBs **(Fig 4.2 B)**. Dhh1^{DQAD}-GFP PB fluorescence in cells grown in the presence of dextrose was also around 20% (data not shown), suggesting the amount of Dhh1^{DQAD} present in PB foci is similar in the presence or absence of dextrose, in agreement with previous results (Dutta et al., 2011). In comparison, Dcp2-mCherry localization in PBs was significantly higher, around 60% **(Fig 4.2 B)**.

Still, TAP-tagged Dhh1 and Dhh1^{DQAD} complexes were purified from cells grown in mid-log phase in the presence of glucose, where Dhh1 and Dhh1^{DQAD} localization patterns should be quite different, even if only a fraction of Dhh1^{DQAD} is present in PB. However, deconvolution microscopy of logarithmically growing yeast cells expressing Dhh1-GFP showed that Dhh1 has a punctate, granular localization even in glucose replete conditions **(Fig 4.2 C)**. While these foci are microscopically visible, they are still smaller than traditional PBs suggesting that Dhh1 may already be found in smaller PB-like foci that may coalesce after glucose starvation or in cells expressing Dhh1^{DQAD}. The observation that Dhh1 forms small granules in the absence of stress is consistent with previous literature, and our own work (Maillet and Collart, 2002; Tseng-Rogenski et al., 2003; data not shown). Furthermore, as suggested by the work in Chapter II, one other explanation for the similarity of Dhh1 and Dhh1^{DQAD} complexes is that Dhh1^{DQAD} is unable to recycle off of RNA in PB foci – rather than a protein factor. In summary, future work is needed to purify, separate, and identify distinct Dhh1-containing protein complexes and to determine whether or not these mRNPs have redundant or independent functions in mRNA turnover.

Fig 4.2

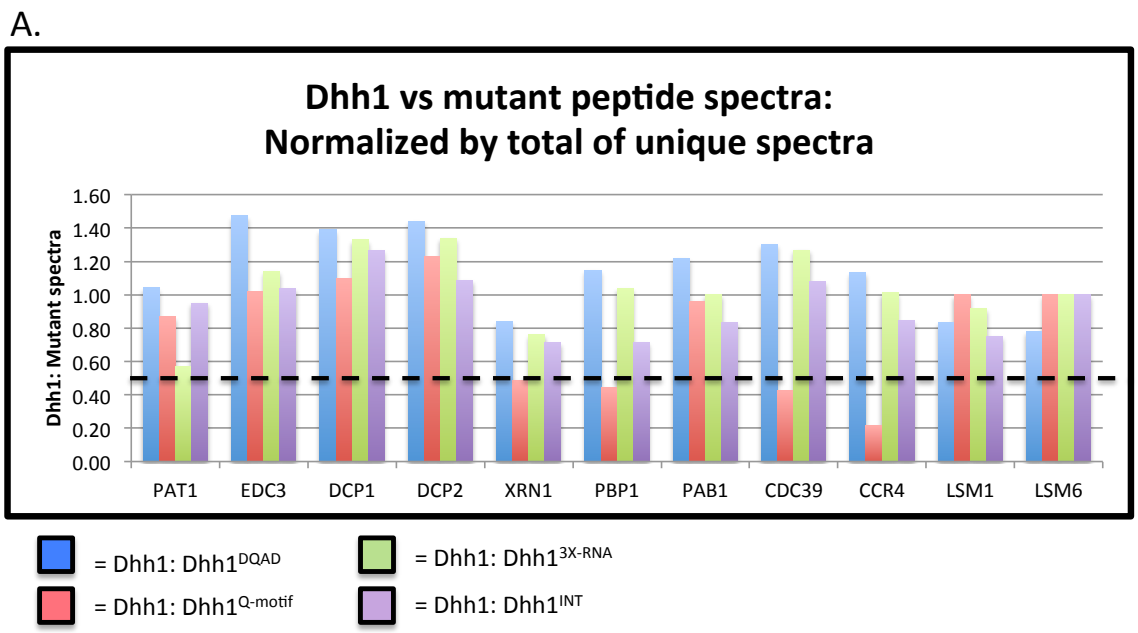

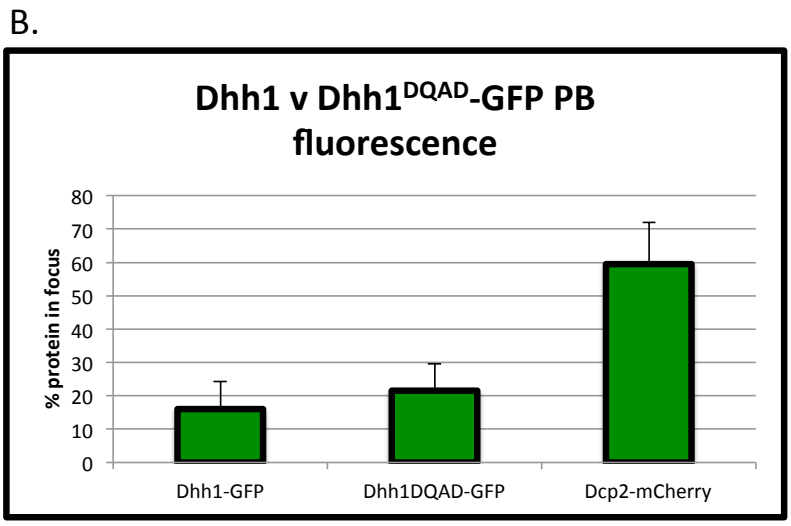

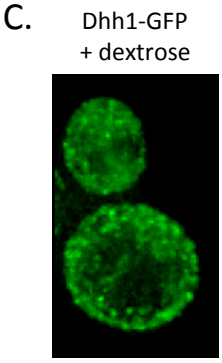

Fig 4.2 Purification of Dhh1 and mutant TAP-tagged complexes shows few differences in protein interactome

Dhh1-TAP (CBP-TEV-ZZ), Dhh1^{DQAD}-TAP, Dhh1$^{Q\text{-}motif}$-TAP, Dhh1$^{3X\text{-}RNA}$-TAP, and Dhh1^{INT}-TAP were grown in dhh1Δ into late log phase (OD^{600} = 1.0) and harvested. Extracts were lysed by cryo-milling and affinity purified using IgG-coupled magnetic beads, with co-eluting proteins identified by LC-MS/MS. (A) Several major mRNA decay protein peptide spectra are shown as a ratio of number of unique peptide spectra found in wild-type Dhh1 versus mutant samples. Black dotted line indicates 2-fold fewer peptide spectra. (B) Dhh1-GFP or Dhh1^{DQAD}-GFP were co-expressed

with Dcp2-mCherry in dhh1Δ yeast grown to mid-log phase, and shifted into glucose-free media as in **Fig 2.1**. The amount of protein found in PB foci was quantified using ImageJ and compared to the total Dhh1-GFP cytoplasmic pool. The graph in B represents the average amount of Dhh1-GFP, Dhh1^{DQAD}-GFP, or Dcp2-mCherry present in at least 20 distinct foci from one independent experiment. (C) dhh1Δ cells expressing Dhh1-GFP were grown into mid-log phase and imaged using a DeltaVision microscope followed by deconvolution. One slice of the image is shown.

Experimental Procedures:

Construction of yeast strains and plasmids:

Construction of yeast strains and plasmids for this study are listed in **Table 4.1-4.2** and were generated using standard molecular cloning techniques. Yeast deletion strains were made by PCR-based homologous recombination transformations, using integration and tagging vectors as previously described (Longtine et al. 1998, Carroll et al 2011). Double knockout strains were made either using the PCR-based transformation method described above, or by mating and dissection of sporulated yeast.

Dhh1 mutagenesis:

Mutations in Dhh1 were generated using a QuikChange II site-directed mutagenesis kit (Agilent Technologies) using PFu Ultra or PFu Turbo. Mutagenic oligonucleotides were designed using the Agilent Technologies primer design platform. Plasmids generated are listed below in **Table 4.2**.

Immunoprecipitation:

Yeast were inoculated in synthetic media containing 2% dextrose and grown overnight to saturation, then backdiluted the following day in 1L synthetic media and grown to OD_{600} = 0.4-1.0. Cells were harvested by centrifugation at 3800 rpm for 10 minutes, resuspended briefly in resuspension buffer (20mM HEPES, 1.2% polyvinylpyrrolidone, 1mM DTT, 1:100 Solution P, 1:1000 Pepstatin A), and spun at 3100 rpm for 15 minutes, then frozen in liquid nitrogen and stored at -80° C. Yeast extracts were prepared as in (Oeffinger et al., 2007). Briefly, cells were lysed with a Retsch planetary ball mill for six cycles of 15 Hz for 3 min with cooling in liquid nitrogen between cycles. 0.25g of lysate was then resuspended in 9mL TBT buffer (20mM HEPES, pH7.4, 110mM KOAc, 2mM MgCl2, 0.5% Triton, 0.1% Tween 20, 1:100 Solution P, 1:1000 DTT, 1:5000 SuperRNasin (Ambion), 1:5000 Antifoam B (Sigma)). The lysate was homogenized and spun briefly for 1 min at 1500 x *g*, followed by clarification of lysate through 2.7µm and 1.6µm GD/X Glass Microfiber syringe filters (25mm, Whatman). The lysates were then incubated with 5mg rabbit IgG (Sigma)-coupled magnetic beads (DynaI) – corresponding to 400ul bead slurry at 20mg/uL slurry) – and were rotated at 4° C for 30 min. The beads were washed three times with 1mL TBT buffer, and a final wash in 1 ml of 100 mM ammonium acetate, pH = 7.4, 0.1 mM MgCl2, 0.2% Tween-20 for 5 min while rotating. Protein complexes were eluted from the beads directly in SDS-PAGE sample buffer (for Western blot) or twice with 500µl of fresh aqueous 500mM NH_4OH, 0.5mM EDTA solution for 20 minutes with rotation (for mass spectrometry). The eluates were then pooled and lyophilized overnight in a SpeedVac (ThermoSavant) and prepared for mass spectrometry.

Microscopy:

Samples were grown overnight in in synthetic media containing 2% dextrose, backdiluted to OD_{600} = 0.05 or 0.1 the following day, and grown to mid-log phase (OD_{600}= 0.3-0.8). Cells were harvested by centrifugation and washed in ¼ volumes of fresh synthetic media +/- 2% dextrose, then harvested again and resuspended in 1 volume of fresh synthetic media +/- 2% dextrose and grown 15 minutes at 30° C. Cells were harvested once more and washed as described above, then plated onto Concavalin A-treated MatTek dishes (MatTek) in induction media and visualized at room temperature by epifluorescent microscopy or by confocal microscopy using an Andor/Nikon Spinning Disk Confocal Microscope. All cells were observed using a 100X-oil immersion objective (NA = 1.49) and images were captured using an iXon Ultra 897 EMCCD camera (Andor) using Metamorph Microscopy Automation & Image Analysis software (Metamorph). All images unless otherwise indicated are collapsed Z-stacks. Unless otherwise indicated, three independent experiments were performed and foci/cell values in the bar graphs representing the mean with standard deviation of the mean (SDM). Quantitation is described below.

Table 4.1: Yeast Strains used in this study

Yeast Strains	Genotype	Source
KWY3264	W303a *dhh1Δ*::KanMX *XRN1-GFP*::*HIS3* *DCP2-mCHERRY*::NatMX	This study
KWY3266	W303a *dhh1Δ*::KanMX *CCR4-GFP*::*HIS3* *DCP2-mCHERRY*::NatMX	This study
KWY3268	W303a *dhh1Δ*::KanMX *PAT1-GFP*::*HIS3* *DCP2-mCHERRY*::NatMX	This study
KWY3270	W303a *dhh1Δ*::KanMX *DCP1-GFP*::*HIS3* *DCP2-mCHERRY*::NatMX	This study
KWY3304	W303a *dhh1Δ*::KanMX *EDC3-GFP*::*HIS3* *DCP2-mCHERRY*::NatMX	This study
KWY3318	W303a *dhh1Δ*::KanMX *DCP2-GFP*::*HIS3*	This study
KWY3278	W303a *CCR4-GFP*::*HIS3*	This study
KWY3280	W303a *PAT1-GFP*::*HIS3*	This study
KWY3282	W303a *EDC3-GFP*::*HIS3*	This study
KWY3284	W303a *DCP1-GFP*::*HIS3*	This study
KWY4448	W303a dhh1Δ::KanMX *P(DHH1)-DHH1-CBP-TEV-ZZ*::*URA3*	This study
KWY4449	W303a dhh1Δ::KanMX *P(DHH1)-DHH1^{DQAD}-CBP-TEV-ZZ*::*URA3*	This study

Table 4.2: Plasmids used in this study

Plasmid	Description	Source
pKW2421	pRS316 P(*DHH1)*-Dhh1-CBP-TEV-ZZ; *URA3* marker	Carroll et al (2011)
pKW2422	pRS316 P(*DHH1*)-Dhh1^{DQAD}-CBP-TEV-ZZ; *URA3* marker	Carroll et al (2011)
pKW3074	pRS316 P(*DHH1)*-Dhh1$^{Q\text{-}motif}$-CBP-TEV-ZZ; *URA3* marker	This study
pKW3126	pRS316 P(*DHH1*)-Dhh1$^{3X\text{-}RNA}$-CBP-TEV-ZZ; *URA3* marker	This study
pKW3127	pRS316 P(*DHH1)*-Dhh1^{INT}-CBP-TEV-ZZ; *URA3* marker	This study

References:

Carroll, J.S., Munchel, S.E., and Weis, K. (2011). The DExD/H box ATPase Dhh1 functions in translational repression, mRNA decay, and processing body dynamics. J. Cell Biol. *194*, 527–537.

Coller, J.M., Tucker, M., Sheth, U., Valencia-Sanchez, M.A., and Parker, R. (2001). The DEAD box helicase, Dhh1p, functions in mRNA decapping and interacts with both the decapping and deadenylase complexes. RNA N. Y. N *7*, 1717–1727.

Dutta, A., Zheng, S., Jain, D., Cameron, C.E., and Reese, J.C. (2011). Intermolecular interactions within the abundant DEAD-box protein Dhh1 regulate its activity in vivo. J. Biol. Chem. *286*, 27454–27470.

Maillet, L., and Collart, M.A. (2002). Interaction between Not1p, a component of the Ccr4-not complex, a global regulator of transcription, and Dhh1p, a putative RNA helicase. J. Biol. Chem. *277*, 2835–2842.

Mitchell, S.F., Jain, S., She, M., and Parker, R. (2013). Global analysis of yeast mRNPs. Nat. Struct. Mol. Biol. *20*, 127–133.

Nissan, T., Rajyaguru, P., She, M., Song, H., and Parker, R. (2010). Decapping activators in Saccharomyces cerevisiae act by multiple mechanisms. Mol. Cell *39*, 773–783.

Sharif, H., Ozgur, S., Sharma, K., Basquin, C., Urlaub, H., and Conti, E. (2013). Structural analysis of the yeast Dhh1-Pat1 complex reveals how Dhh1 engages Pat1, Edc3 and RNA in mutually exclusive interactions. Nucleic Acids Res. *41*, 8377–8390.

Tritschler, F., Braun, J.E., Eulalio, A., Truffault, V., Izaurralde, E., and Weichenrieder, O. (2009). Structural basis for the mutually exclusive anchoring of P body components EDC3 and Tral to the DEAD box protein DDX6/Me31B. Mol. Cell *33*, 661–668.

Tseng-Rogenski, S.S.-I., Chong, J.-L., Thomas, C.B., Enomoto, S., Berman, J., and Chang, T.-H. (2003). Functional conservation of Dhh1p, a cytoplasmic DExD/H-box protein present in large complexes. Nucleic Acids Res. *31*, 4995–5002.